https://ntrs.nasa.gov/search.jsp?R=19770019637 2020-03-22T10:05:02+00:00Z

General Disclaimer

One or more of the Following Statements may affect this Document

- This document has been reproduced from the best copy furnished by the organizational source. It is being released in the interest of making available as much information as possible.

- This document may contain data, which exceeds the sheet parameters. It was furnished in this condition by the organizational source and is the best copy available.

- This document may contain tone-on-tone or color graphs, charts and/or pictures, which have been reproduced in black and white.

- This document is paginated as submitted by the original source.

- Portions of this document are not fully legible due to the historical nature of some of the material. However, it is the best reproduction available from the original submission.

Produced by the NASA Center for Aerospace Information (CASI)

(NASA-CR-150306) REMOTE SENSING OF EFFECTS OF LAND USE PRACTICES ON WATER QUALITY Final Report, 11 Oct. 1974 - 31 May 1977 (Kentucky Univ. Research Foundation, Lexington.) 170 p HC A08/MF A01 CSCL 08H G3/43

N77-26581

Unclas 31859

REMOTE SENSING OF EFFECTS OF LAND USE PRACTICES ON WATER QUALITY

Principal Investigator: Donald H. Graves
Co-Investigator: George B. Coltharp

Contributors: Mahlon C. Hammetter, David C. Jordan, Charles L. Shilling, and Robert F. Wittwer

Contract No. NAS8-31006

Final Report - May 31, 1977
For Period October 11, 1974 - May 31, 1977

Prepared for:
National Aeronautics and Space Administration
George C. Marshall Space Flight Center
Marshall Space Flight Center, Alabama

University of Kentucky Research Foundation
Department of Forestry
Lexington, Kentucky 40506

REMOTE SENSING OF EFFECTS OF LAND USE PRACTICES ON WATER QUALITY

Principal Investigator: Donald H. Graves
Co-Investigator: George B. Coltharp

Contributors: Mahlon C. Hammetter, David C. Jordan, Charles L. Shilling, and Robert F. Wittwer

Contract No. NAS8-31006

Final Report - May 31, 1977
For Period October 11, 1974 - May 31, 1977

Prepared for:
National Aeronautics and Space Administration
George C. Marshall Space Flight Center
Marshall Space Flight Center, Alabama

University of Kentucky Research Foundation
Department of Forestry
Lexington, Kentucky 40506

ACKNOWLEDGMENTS

The authors wish to express their appreciation to Willie R. Curtis and Willis Vogel, Project Leader and Range Scientist, respectively, with the Northeast Forest Experiment Station, Berea, Kentucky. Mr. Curtis made available needed water quality and quantity information without which water quality-land use correlations for three of the study watersheds would have been impossible. Mr. Vogel provided much needed assistance in classification and sampling of vegetation on reclaimed surface mined areas within the study watersheds.

Recognition of project contributions is due the University of Kentucky Robinson Forest staff who ably assisted with field survey efforts, and particularly to Roger Horseman, who actively participated in all ground truth survey efforts.

Ground truth survey of the surface mined study areas would have been impossible without cooperation from Falcon Coal Company. Company officials gave project personnel access to these surface mined areas. Coming at a time of public outcry and debate on environmentally sensitive issues such as surface mining, Falcon's cooperation was courageous and farsighted. This cooperation is gratefully acknowledged.

Recognition is due James Ringe, University of Kentucky forestry student, who completed a special problems course on color additive viewing of multi-date Landsat satellite transparencies. His assistance on color additive analysis is gratefully acknowledged.

The authors also wish to thank all those other individuals, too numerous to mention, whose cooperation and consultation have been of immeasurable benefit to this project and to the authors themselves.

TABLE OF CONTENTS

TABLE OF CONTENTS (cont)

Abstract

An intensive two year study was conducted to determine the utility of manual densitometry and color additive viewing of aircraft and Landsat transparencies for monitoring land use and land use change. The relationship between land use and selected water quality parameters were also evaluated.

Six watersheds located in the Cumberland Plateau region of eastern Kentucky comprised the study area for the project. Land uses present within the study area were reclaimed surface mining and forestry. Fertilization of one of the forested watersheds also occurred during the study period.

Manual photo interpretation techniques were utilized to stratify the study area into vegetative types. An intensive ground truth survey of these types was undertaken to ascertain kind, size, and extent of vegetation present in each type. Values obtained from subsequent densitometric sampling of NASA research aircraft and Landsat imagery were examined for correlation and predictability of corresponding vegetation types. Densitometer filter-aperture combinations were examined for determination of highest vegetation classification success.

Densitometric values were also compared with sample water quality values obtained from the study watersheds. Linear regression equations were derived for water quality-densitometry and water quality-percent disturbed land relationships.

Color additive viewing of seasonal aircraft and Landsat multispectral imagery was also evaluated as a possible land management tool. Particular emphasis was placed on determining utility of Landsat imagery enhancement for land use and land use change detection potential. Land uses or disturbances examined included active and reclaimed surface mining, forest and forest fertilization, forest fire scars, agricultural crops, and apparent suspended sediment in reservoirs.

Manual densitometry of Landsat imagery provided discrimination between wholly forested watersheds and partially surface mined watersheds but little else. Aperture size (1-3 mm) and imprecise placement capabilities limited further discriminative potential.

Manual densitometry of seasonal 1:24,000 color infrared imagery yielded good classification of eight broad vegetation categories of forested and reclaimed surface mines. Species breakdown among hardwood vegetation proved unsatisfactory.

Some correlation between densitometric data and some water quality parameters appears to exist, but ground conditions were not diverse enough to allow meaningful extension of apparent correlations into areas other than the study area.

Color enhancement of medium scale multispectral transparencies with a manual color additive viewer offers some promise, particularly if multi-temporal imagery of varying photo scale can be accommodated by the viewer used. For single date vegetation surveys color infrared imagery offers equal or greater utility.

List of Appendices

PRECEDING PAGE BLANK NOT FILMED

LIST OF FIGURES

LIST OF FIGURES (cont)

LIST OF TABLES

LIST OF TABLES (cont)

INTRODUCTION

History

The Department of Forestry, under the auspices of the University of Kentucky Research Foundation, has completed two years of research designed to assess the capabilities of color infrared and multispectral aircraft photography and multispectral Landsat satellite imagery to detect and monitor land use practices and the resultant effects of these practices on water quality. The project was conducted in the Cumberland Plateau region of eastern Kentucky in cooperation with the National Aeronautics and Space Administration, George C. Marshall Space Flight Center, Huntsville, Alabama.

The Cumberland Plateau of eastern Kentucky serves as a watershed for central and eastern Kentucky and portions of West Virginia, Virginia, Ohio, and Tennessee. Mixed mesophytic forest covers the easily erodable soils of the region (Braun, 1972) and when undisturbed, generally provides excellent protection to these soils even when subjected to characteristically intense storm precipitation.

Prominent land uses in this steep, sparsely-populated region are hillside farming, forest harvesting, and surface mining. While farming and timber harvesting have decreased since the early 1900's, surface mining activity has increased greatly, particularly in the last fifteen years. Approximately 8100 hectares (20,000 acres) of land are currently being surface mined in Kentucky each year. Pressures of the energy

crisis and the fact that almost ninety percent of the area that could be mined economically in Kentucky remains undisturbed indicate a continuation of surface mining for some time in the future.

The Cumberland Plateau region includes the headwaters of the Kentucky, Licking, Big Sandy, and Cumberland rivers which provide water for industrial and domestic use in much of eastern Kentucky. Usable ground water supplies in this region are almost nonexistent. Recent reports indicate that approximately 96 percent of the water used in the Cumberland Plateau of eastern Kentucky and 79 percent of the water used in the Bluegrass region is from surface water supplies. Land use practices in these headwater areas can greatly affect the quality and quantity of flow of this vital resource. With the demonstrated dependency of these regions on surface water supplies, it is likely that the production of high quality water should be the highest and best use of eastern Kentucky watersheds. To achieve a management objective of high quality water production, a system should be devised to equate types and degrees of land use to water quality, based upon remotely sensed imagery.

Users and User Requirements

Remote sensing has potential for providing effective survey techniques to monitor land use at a reasonable cost. Specific capabilities must be determined for various types of remote sensing which seem capable of solving specific local problems. The capabilities and limitations of each sensor or interpretation technique must then be demonstrated

to interested agencies to afford them the opportunity of adoption in day-to-day problem solving situations.

Table 1 lists personnel from various agencies and their respective interests in results and/or information to be gained from this project. Evaluations of the potential use of project equipment, imagery, and interpretive techniques are being conveyed to these and other interested individuals and agencies as results are interpreted.

A seminar involving project personnel and persons from most of the agencies listed in Table 1 was hosted by the Forestry Department in February 1976. The meeting was called to discuss information needs and current projects of these agencies relative to remote sensing. The interagency contacts established at this session have provided the basis for the increased levels of cooperation and communication that presently exist among agencies involved. Improved communications should help provide maximum information return with minimum duplication of effort.

In addition a seminar, to be co-hosted by the University of Kentucky Forestry Department and the SCS, is to be held either prior to or shortly after the termination of this project. These organizations will present results of their separate remote sensing projects. Also anticipated and encouraged will be presentations by other individuals and agencies having present and/or past remote sensing projects applicable to resource management and regulation in Kentucky.

Table 1

CONTACTS

State Agencies

Position/Title/Agency	Area of Application	Possible Utilization
J.R. Farson, Jr./formerly Soil Scientist Div. of Conservation; presently Orphan Mine Reclamation	Surface mine reclamation	Is interested in possible use of equipment and multispectral imagery for detection and evaluation of strip mine revegetation success.
Fred Schuhman/Agronomist Strip Mine Reclamation Larry Springate, formerly Asst.Dir. Strip Mine Reclamation	Surface mining and reclamation activity.	Possible use of Landsat imagery for determinations of acreage reclaimed and success of reclamation practices.
Birney Fish/Exec. Asst. Office of Planning and Research	Effects of mining in Kentucky- also other research areas.	Very interested in water quality modeling, economic effects of mining activity, interagency cooperation and consultation on remote sensing applications within the state.
William Gayle/formerly Director Division of Conservation; presently Exec. Dir. Governor's Council on Agric.	Agricultural applications.	Interested in land use-water quality interactions.
Harry Nadler/formerly Dir. Division of Forestry	Forestry, Forest influences.	Possible monitoring of insect, disease, and forest fire damage in the state forests by satellite and/or low level multispectral imagery.
Jack Rhody/Fire Control Officer Division of Forestry	Forest fire prevention, detection, suppression, and evaluation.	Potential of satellite imagery for use in mapping burned areas and appraisal of damage.

State Agencies (cont)

Position/Title/Agency	Area of Application	Possible Utilization
Walter Martin/formerly Dir./ Div. of Water Quality Planning Section	Water Quality determinations and pollution abatement.	Interested in water quality data which may prove useful with ADAPT system for their modeling and planning efforts.
Mark Matezewski/Forester Div. of Forestry John Dalton/Forester Div. of Forestry	Forest management and forest influences.	Detectability of Southern pine beetle infestations on Pine Mountain from Landsat imagery for mapping and control efforts.
Donald Penegor/Planning Dir./ Div. of Parks	Park layout and design.	Was interested in possibility of using LANDSAT imagery, but Landsat is too small scale-1:24,000 scale smallest scale worked with.
Donald A. Blome/ Inst. of Mining & Min. Research	All facets of mining and minerals research.	Classification of reclaimed and non-reclaimed areas, also interested in reclamation research and ground truth on strip mines.

Federal Agencies

Willie Curtis/Research Forester NE Forest Expt. Station	Strip mine reclamation and water quality.	Working closely with U.K. in ground truth survey and in water quality monitoring on three study watersheds. Is interested in water quality modeling and ground truth data generated from the study.

Position/Title/Agency	Area of Application	Possible Utilization
James W. Kennamer/Watershed Planning Staff Leader/SCS Bob Daniels/retired State Soil Scientist/SCS	Non point source pollution, water quality modeling as affected by land use	Possible use of land use-water quality interactions defined by this study-also cooperation on ground truth for Ky. River drainage basin study.
S.B. McLaughlin/ORNL	Water quality modeling, land use classification, strip mine reclamation.	Interested in ground truth and baseline water quality data, also land use effects on water quality with particular reference to strip mining activities.
Ed Swenson/U.S. Forest Service James McDivott/ Economic Research Service	Land use mapping and change analysis, strip mining effects.	Interested in how Landsat imagery might aid in regional land use studies. Interested in demonstration of study equipment usage and potential in regional studies.
Robert Reynolds/U.S.F.S. Harry Bullock/U.S.F.S.	Land use, water quality, soil classification.	Potential of Landsat and aircraft MSS imagery for use by U.S.F.S. in management activities.
C.T.N. Paludan/COR/NASA Sanford Downs/Alt.COR/NASA	Natural resources applications of MSS imagery.	Interested in the results of project research efforts, also in liaison activities.
C. Al Waters/Photo Interpreter EPA/EPIC	Surface mining-water quality correlation.	Interested in support data for his surface mining study in eastern Kentucky.

University Personnel

Position/Title/Agency	Area of Application	Possible Utilization
Tim Cannon/Research Assoc. Auburn University	Physiographic mapping	Support data for regional physiographic study.
Robert Blevins/Assoc. Prof. University of Kentucky	Soil Mapping	Potential of aircraft MSS and CIR imagery for soil mapping, also of Landsat MSS imagery for soil association mapping.
Gerald Nordin/Asst. Prof. University of Kentucky	Entomology	Potential of Landsat MSS imagery and color additive viewing to show Southern pine beetle and other insect infestations.
Thomas Jackson/Asst. Prof. University of Kentucky	Civil Engineering	Hydrologic modeling, land use-water quality interactions.

Project personnel presented project results to NASA officials in Huntsville on February 17, 1977. Equipment and imagery on loan to the University was returned to NASA at this time.

Individuals from public, private, and academic sectors have visited the Forestry Department for consultation and equipment demonstration. In addition many requests for reprints of presented papers have been received. This information exchange demonstrates increasing interest in the use of remote sensing systems and techniques.

Liaison activity of the Department is aimed toward dissemination of general and project-specific remote sensing information to potential users. Additional liaison information may be found in Appendix D.

Study Objectives

Study objectives can be grouped into four main categories: (1) selection of study watersheds and acquisition of ground truth data; (2) vegetation and land use analysis utilizing remotely-sensed data; (3) relationship of various land use practices, as determined by vegetation analysis, to water quality; and (4) liaison activity with state and federal agencies.

Test sites for comparison of remote and in-situ sensing of land use and water quality were to be selected. Land use practices to be examined in this study were: forest fertilization, logging, and various surface mining techniques and reclamation efforts. Sample land use and water quality information were to be collected within the test sites.

Multi-seasonal multispectral and thermal imagery from aircraft overflights over mutually-agreed upon test sites were to be provided by NASA, subject to availability of equipment. Landsat and Skylab imagery including the test sites were to be acquired by the Department. Multistage sampling techniques were to be utilized in the development of densitometric signatures for the land uses of concern to this project. Color additive viewing of the imagery was to be used to supplement the densitometric analyses.

Multi-seasonal remotely sensed data were to be used to assess whether spectral signatures of vegetation are indicative of water quality values associated with the various land uses under study. Data display format was to be influenced by the requirements of state and federal environmental control agencies.

Project personnel were also to establish and maintain liaison with Kentucky offices and departments concerned with strip mine regulation, water quality, forestry, and land use planning. Advice and cooperation were to be sought from these agencies. Additional liaison efforts were to be made to determine Commonwealth remote sensing requirements. Liaison with the Energy Research and Development Agency (ERDA), specifically the Oak Ridge National Laboratory (ORNL), was to be encouraged. Mutual exchange of data and information on the influence of coal strip mining on other uses of land and on water and other environmental quality parameters was to be pursued. Discussion relative to each of these objectives will be found in appropriate sections in this report.

DATA ACQUISITION

Selection and General Description of Study Watersheds

Six watersheds were selected to comprise the primary study area. Three of these watersheds - Jenny Fork, Miller Branch, and Mullins Fork - are privately owned. The other three watersheds - Little Millseat Branch, Falling Rock Branch, and Field Branch - are owned by the University of Kentucky. Area and land use condition of each watershed is shown in Table 2. The location of these watersheds is shown in Figure 1.

All watersheds were forested, but Miller branch and Mullins Fork had been partially surface mined and were in varying stages of rehabilitation. The third study watershed located in the Bear Branch drainage, Jenny Fork, served as a control.

These watersheds were selected for three main reasons: (1) water quality and quantity data were available for all six watersheds, (2) different forest treatments and surface mining activities were present within these watersheds, and (3) the close proximity of these watersheds permitted field surveying from a central location.

Efforts were made to find a replacement watershed on which to monitor logging activity and also to find an additional watershed on which to monitor a method of surface mining not present in the initially-selected study watersheds. Our efforts were unsuccessful, since water quality and quantity sampling systems were absent from otherwise acceptable watersheds.

Table 2. WATERSHED DESCRIPTION

Watershed	Approximate Size		Land Use Condition
	Hectares	Acres	
Field Branch	40.5	100	Forested
Little Millseat Branch	80.1	198	Forested
Falling Rock Branch	93.1	230	Forested
Jenny Fork	116.1	287	Forested
Miller Branch	76.9	190	Forested & Surface Mined
Mullins Fork	132.3	327	Forested & Surface Mined

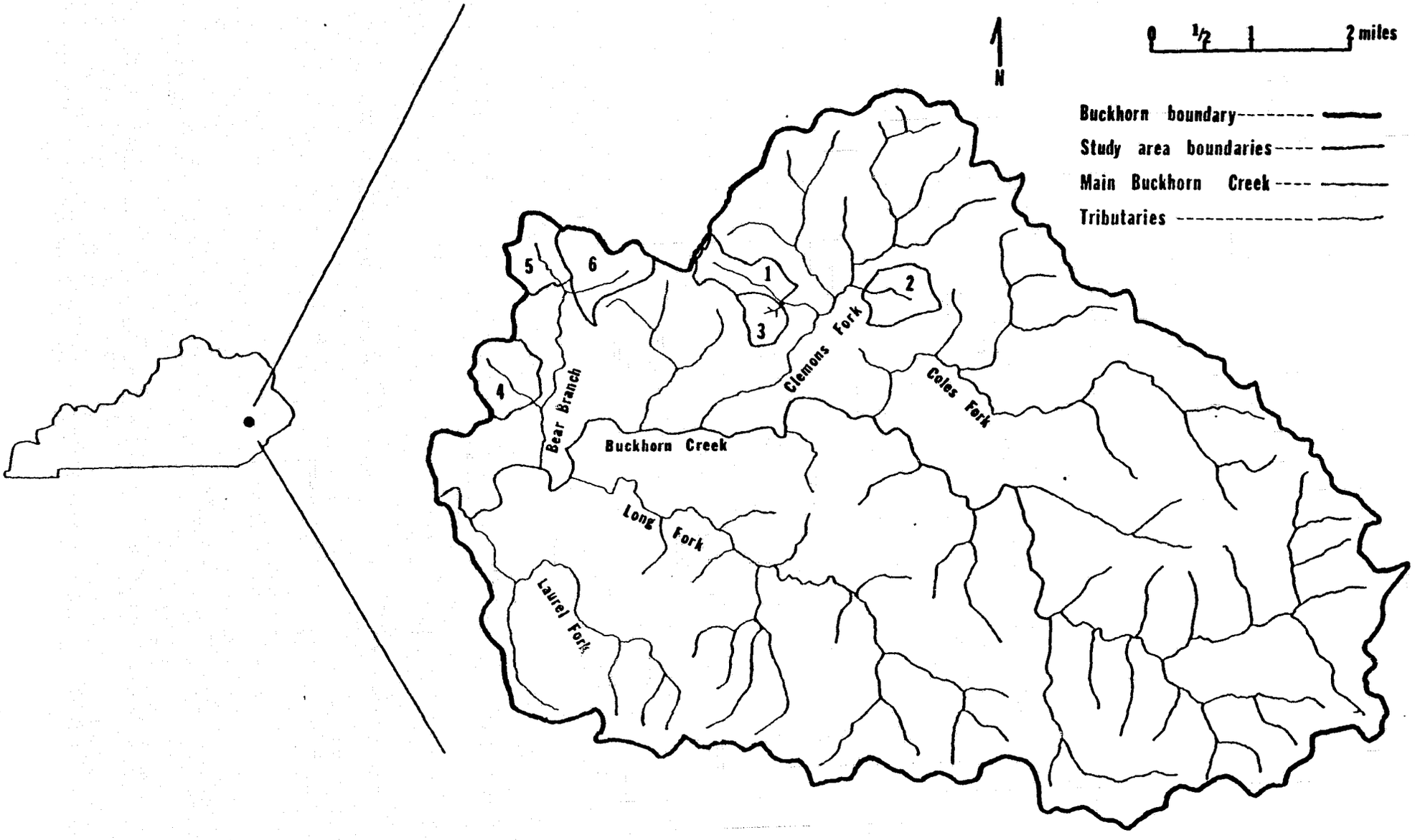

Figure 1. Buckhorn Watershed (Approximately 44 sq. mi.)

A U.S. Forest Service study designed to monitor effects of several mining techniques would have provided the ideal situation for our mining influences evaluation. Unfortunately, core drillings indicated that mining the proposed watersheds would not be economically feasible. The Department was thus unable to secure additional mining systems - water influence data to evaluate. Mining activities monitored in this project were therefore limited to those present within the confines of Miller Branch and Mullins Fork.

Field Survey and Descriptions

Physiography, Geology, and Soils

Kentucky lies within the Appalachian and Interior Low Plateaus physiographic regions of the United States. Physiographic maps place the eastern one-quarter of Kentucky within the Cumberland Plateau province. This plateau is naturally dissected with varying altitude and relief which is an expression of variation in rock outcrop and textures. Elevation ranges generally between 750 and 1500 feet above sea level. The drainage pattern is dendritic and the relief is characterized by irregular, winding, narrow ridges and deep narrow valleys. Flat land is at a minimum, both on ridgetops and in valley bottoms.

The Cumberland Plateau province generally coincides with underlying rocks of the Pennsylvanian geologic period. The Breathitt Formation (middle Pennsylvanian) composed of alternating layers of sandstones, siltstones, and shales dominates the study area.

Geologic field mapping of the Noble quadrangle, within which the study watersheds were located, was completed in June 1976. The geologic map of this quadrangle, contrary to project expectations, will not be published until late 1977. Bedrock geology of adjacent quadrangles (Hazard North, Haddix) has been mapped and published by the U.S. Geological Survey.

Geological information pertinent to the study area is also found in various reports concerning the coal resources of eastern Kentucky. One such report indicates that three-fourths of the rock exposed in the vicinity is sandstone. The remaining one-fourth is carbonaceous shale, calcareous shale, and coal (U.S. Geological Survey Map).

According to the Great Soil Map of Kentucky (April 1975 4-R-34874), soils of the general study area belong to the Jefferson-Shelocta soil association. Soils of this association are deep to moderately deep, well-drained soils formed in residuum or hillside creep material from the parent materials described above on predominantly steep mountain sides. Map scale of 1:750,000 precludes discrimination among various kinds of soils within individual watersheds.

More detailed work on the Robinson Experimental Forest by the Departments of Agronomy and Forestry provides additional soils information pertinent to the area (R.B. Hutchins et al, 1975). Study of selected soil profiles indicates many of the soils on the slopes to be deep (48+ inches to bedrock) and formed from colluvial material that has been transported along

the slopes by gravity. Underlying layers of alternating resistant and nonresistant rocks have created complex, benchy, and often dissected sideslopes.

The latter work has shown that Rigley, not Jefferson, and Shelocta soil series predominate on the slopes. Sandier Rigley soils occur more frequently on south-facing slopes and at upper slope positions on cooler aspects. Finer-textured Shelocta soils occur on north-facing slopes and in concave-shaped "cove" positions. Rigley and Shelocta soils normally occur on sideslopes ranging from 20-60 percent. Side-slopes within the study areas range from 35-60 percent and average about 45 percent.

Other minor soil series present in the study areas include Gilpin, Steinsburg, and Pope. Gilpin soils occur on drier upper slopes. Steinsburg soils occur mostly on upper slopes and ridges with most areas having some rock outcrops. Pope soils are alluvial soils found in wider bottoms of the study watersheds.

Descriptive physical and chemical data (from R.B. Hutchins et al, 1975) are shown in Table 3. Values given are from samples taken from watersheds within Robinson Forest, which includes three of the six watersheds under study. All evidence indicates, however, that soil conditions on the three watersheds outside the boundaries of Robinson Forest are similar except as modified by surface mining activities that occurred on portions of Miller Branch and Mullins Fork.

Table 3. Selected physical and chemical properties of the soils studied (R.B. Hutchins et al, 1975)

Soil Horizon	Depth (cm)	Texture %Sand	%Silt	%Clay	CEC (me/100g)	Exchangeable Ca (me/100g)	pH (1:1 H_2O)	%Base Saturation	%Organic Matter
			Rigley series: Lower third of southwest exposed slope						
A1	0-1	55.9	31.5	12.6	13.07	3.50	5.0	38	8.05
A2	1-20	53.3	32.1	14.6	5.67	0.25	5.0	11	1.68
B21t	20-48	52.8	32.4	14.8	4.86	0.25	5.3	23	0.72
B22t	48-64	51.5	33.7	16.5	5.00	0.25	5.5	35	0.51
B31t	64-94	51.9	30.2	17.9	5.28	0.35	5.7	42	0.28
B32t	94-137	40.7	43.0	16.3	5.96	trace	5.6	36	0.39
			Rigley series: Middle third of southwest exposed slope						
A1	0-2.5	70.5	21.2	8.3	8.99	0.35	5.0	7	4.94
A2	2.5-15	70.1	21.9	8.0	5.14	0.25	5.3	10	2.60
B1	15-28	71.2	20.6	8.2	3.00	trace	5.5	7	0.96
B21t	28-69	69.7	23.3	7.0	2.64	trace	5.6	10	0.32
B22t	69-97	47.8	27.8	14.4	4.00	trace	5.5	10	0.26
B23t	97-124	49.3	30.9	19.8	5.21	trace	5.5	17	0.21
IIB3t	124-145	30.4	43.1	26.5	7.28	trace	5.5	25	0.21
R	145-165	40.1	45.8	14.1	5.38	trace	5.5	23	0.51
			Gilpin series: Upper third of southwest exposed slope						
A1	0-20	35.0	50.5	14.5	6.46	0.25	5.4	9	2.48
B21t	20-36	32.2	50.5	17.3	5.71	trace	5.2	4	1.11
B22t	36-53	35.8	41.3	22.9	5.85	trace	5.3	7	0.55
B23t	53-91	38.0	37.9	24.1	6.17	trace	5.3	14	0.40
			Shelocta* series: Lower third of northeast exposed slope						
A11	0-2.5	37.1	39.2	23.7	15.07	8.25	6.0	77	9.03
A12	2.5-15	32.1	45.5	22.4	11.17	2.75	5.3	34	3.86
B21t	15-30	32.6	43.3	24.1	8.80	1.50	5.2	23	2.36
B22t	30-64	30.0	44.7	25.3	7.88	0.75	5.3	18	0.92
B23t	64-81	42.3	49.1	8.6	6.25	0.35	5.4	19	0.73
B3t	81-102	39.6	48.0	12.4	5.57	1.00	5.8	39	0.92
C	102-127	47.7	39.3	13.0	5.07	1.25	5.8	47	0.94

Table 3. (cont'd)

Soil Horizon	Depth (cm)	Texture %Sand	%Silt	%Clay	CEC (me/100g)	Exchangeable Ca (me/100g)	pH (1:1 H_2O)	%Base Saturation	%Organic Matter
			Shelocta series: Middle third of northeast exposed slope						
A1	0-10	30.0	45.2	24.8	16.42	10.50	6.2	85	7.80
B1	10-30	29.4	45.9	24.7	9.75	4.50	5.2	61	3.34
B21t	30-58	29.3	43.7	27.0	8.32	2.00	5.8	36	1.56
B22t	58-99	28.2	39.2	32.6	6.99	1.00	5.7	30	0.82
B3t	99-119	33.4	45.7	20.9	6.75	0.75	5.6	28	0.86
C	119-152	41.5	39.1	19.4	6.85	1.25	5.7	38	1.27
			Rigley series: Upper third of northeast exposed slope						
A1	0-2.5	55.4	31.8	12.8	23.50	16.00	6.6	88	11.28
A2	2.5-15	57.2	28.5	14.3	9.47	5.75	6.3	79	3.47
B1	15-28	57.4	27.8	14.8	6.66	3.00	6.2	60	2.59
B21t	28-46	56.5	28.2	15.3	4.96	0.35	5.5	14	1.15
B22t	46-71	54.0	29.1	16.9	4.25	0.25	5.5	24	0.47
IIB23t	71-130	10.6	60.3	28.9	7.71	trace	5.2	22	0.27
IIB24t	130-170	8.8	64.7	26.5	9.71	trace	5.0	25	0.32

*This soil is a taxadjunct of Shelocta series.

No generally accepted system exists for classification of mine spoils. Consequently the approach used in this study consisted of collecting soil samples that were representative of the area. Samples were collected from study areas based on the stratification (mapping units) developed in the vegetative mapping phase of the study. Composite spoil samples for each type were collected from the top six inches of spoil material utilizing a soil auger. Additional composite samples were collected from large types to provide more representative spoil information for these types.

This stratification system appeared to have disadvantages, however, since soil samples taken within a type were found to be quite heterogeneous. For example, pH values of samples taken within type 27 in Mullins Fork (see Table 4) ranged from 4.8 to 8.0. Soil pH values from all surface mined types ranged from 4.3 to 8.4, with averages of surface-mined types in Miller Branch and Mullins Fork being 6.6 and 6.3, respectively. These averages indicate spoil pH should not be an inhibiting factor to plant growth on these sites.

As of September 1975, land disturbance due to surface mining accounted for 49 percent and 44 percent of the acreage in Miller Branch and Mullins Fork, respectively. Significant plant cover had been established on all but two of the surface mined types by this date. Wide variations of pH values among samples are thus expected to diminish over time, due to ameliorating influences of this vegetation.

Table 4. pH Values of Mine Spoil Samples

Miller Branch

Type	Range	Average
4	4.3	4.3
5	4.8-6.5	5.7
7	6.5	6.5
8	6.6	6.6
12	7.6	7.6
13	8.4	8.4
15	7.5	7.5

Mullins Fork

Type	Range	Average
8	5.3	5.3
10	6.5-7.2	6.8
12	4.3-6.8	5.6
19	4.6-7.0	5.7
24	6.9	6.9
25	8.1-8.2	8.2
26	5.5-7.5	6.8
27	4.8-8.0	6.4

Additional soil analyses were not undertaken. Wide variations of pH values within types indicated that further soil analyses would not offer meaningful, type-specific data.

Vegetation

Detailed vegetative ground truth information is available from a system of permanent inventory plots on the Robinson Forest study watersheds. In addition, all study watersheds were stratified by species, size, and density classes through stereoscopic examination and interpretation of 1:20,000 ASCS panchromatic photographs (Figures 2 and 3). Types were assigned numbers for reference, but no attempt was made to assign identical numbers to similar types in the other study watersheds. Watersheds were then randomly sampled within strata, utilizing a one-time, one plot per 0.4 hectare variable plot inventory of forested plots. Data collected included species, diameter, merchantable height, total height, and crown closure percent.

Trees one inch and greater in diameter were tallied in two inch diameter classes, except for one and two inch classes. The one inch class includes all trees less than 1.5 inches dbh and the two inch class includes those trees from 1.6 inches to 2.9 inches dbh.

Variables measured in non-forest types were ground cover percent, crown closure percent, species, and species percent. Species percent refers to the percentage of ground cover for each species present.

REPRODUCIBILITY OF THE
ORIGINAL PAGE IS POOR

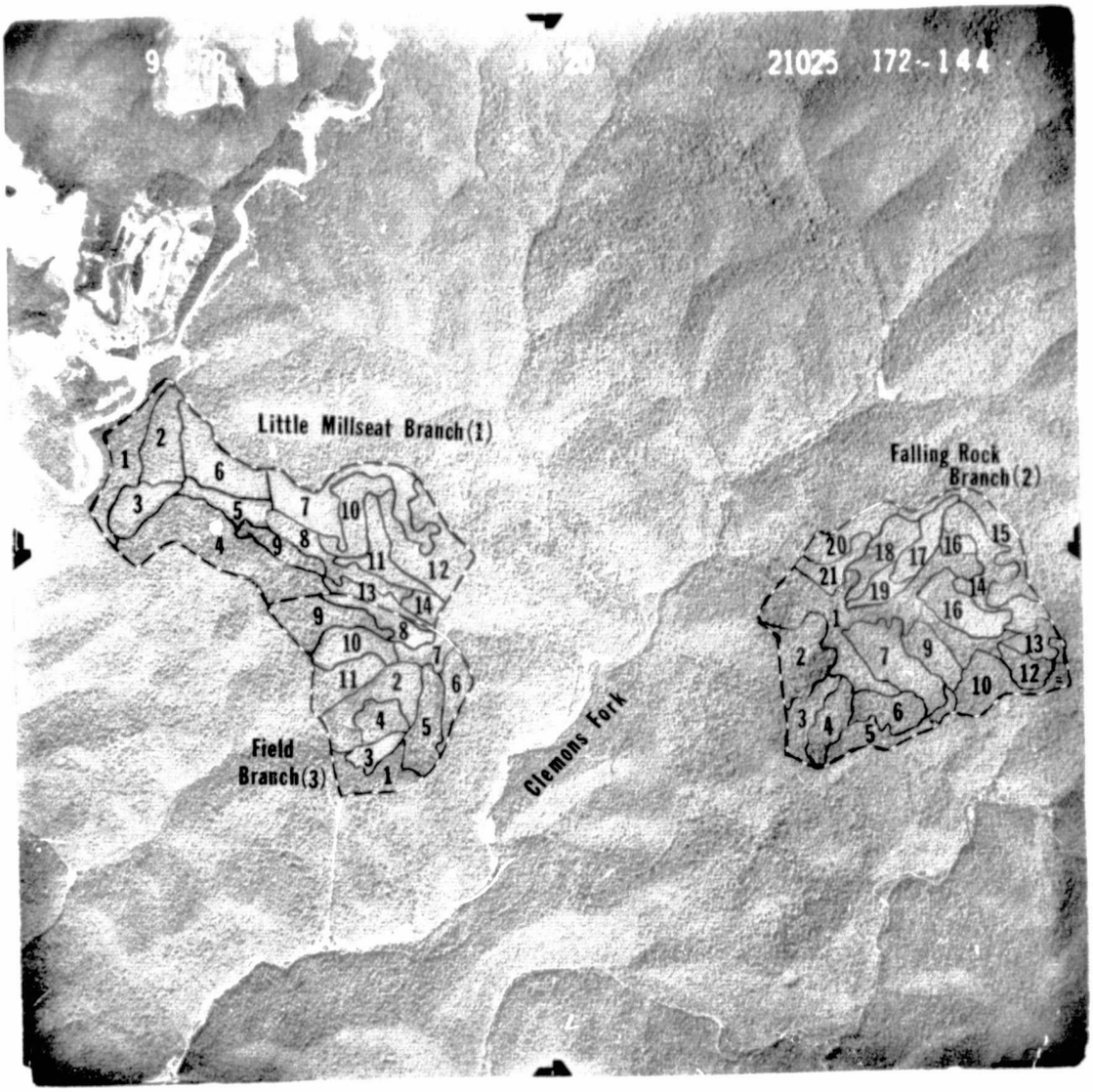

Figure 2. Study watersheds with vegetation types delineated.

REPRODUCIBILITY OF THE
ORIGINAL PAGE IS POOR

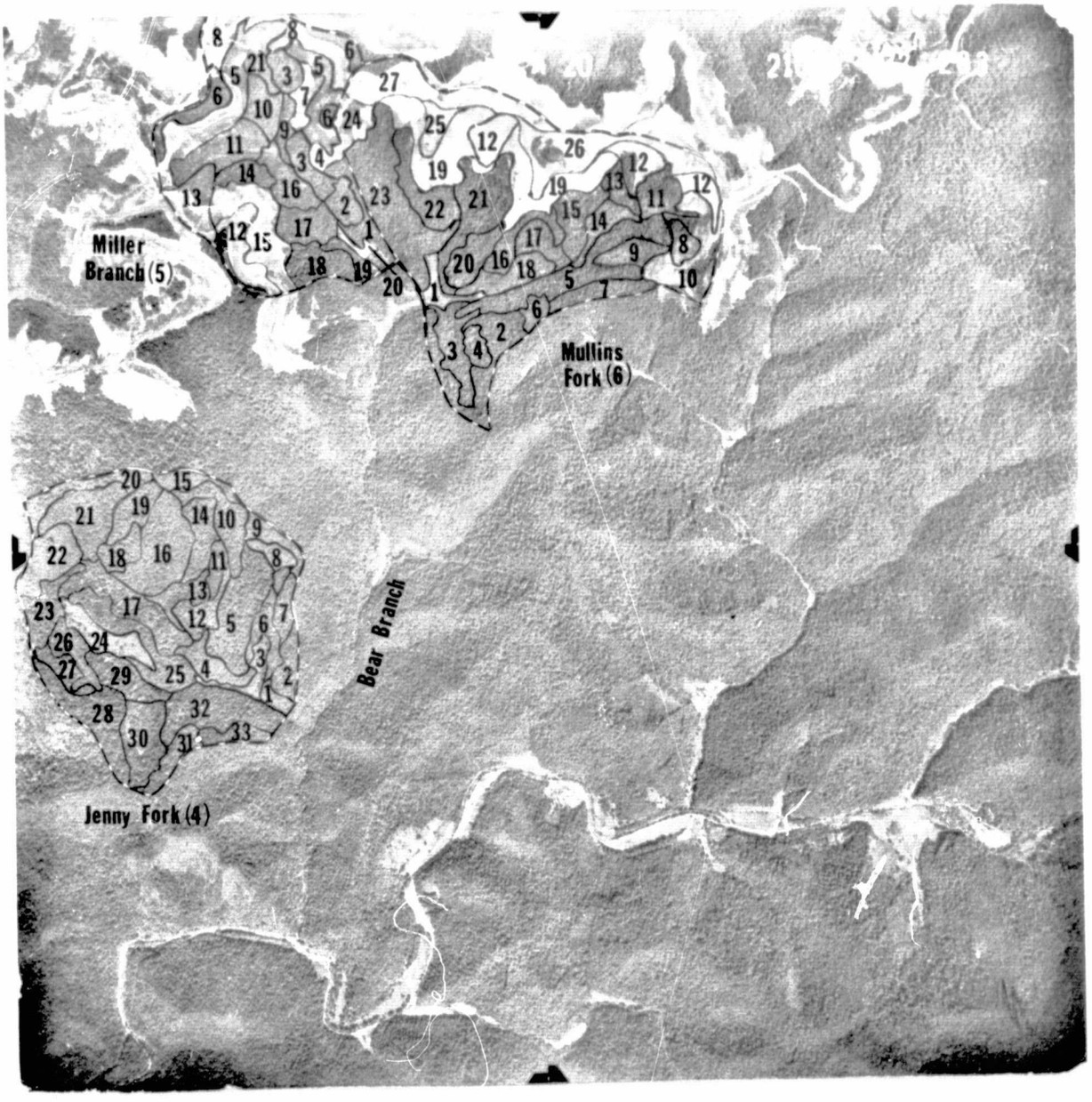

Figure 3. Study watersheds with vegetation types delineated.

Table 5 presents species groupings used in Tables 6-11. Tables 6-11 include vegetation summary data for the study watersheds. Up to three species groups were included in the name for each type, dependent on the percentage of basal area occupied by each group in the sample population. When one or two species groups comprised over eighty percent of the basal area within a type, no additional species groups were included in the type name. As a result, types are categorized in Tables 6-11 by type names composed of one, two, or three species groups.

Information for surface mined and other grass types is displayed separately in Tables 12 and 13, except for reclaimed types in which both trees and heavy grass cover are present. These types appear in both forest and surface mine vegetation summaries. Additional information on each timber type delineated is included in Appendix A.

Water Quality

Several years of water quality and quantity information are available for each study watershed. Broad-crested (120^{o} V-notch) weirs were constructed and instrumented by the U.S. Forest service in 1967 on the three privately-owned watersheds. These watersheds include the two surface mined areas. Similar weirs and instrumentation were established by the University in 1971 on the three watersheds located in Robinson Forest. Instrumentation on each watershed includes a water stage recorder at each weir and an eight-inch weighing-type recording precipitation guage.

Table 5 Species Groupings for Tables 6-11

Scientific Name	Common Name
	Oak
Quercus alba	white oak
Quercus stellata	post oak
Quercus velutina	black oak
Quercus prinus	chestnut oak
Quercus rubra	northern red oak
Quercus coccinea	scarlet oak
Quercus falcata	southern red oak
	Hick
Carya ovata	shagbark hickory
Carya laciniosa	shellbark hickory
Carya tomentosa	mockernut hickory
Carya ovalis	red hickory
Carya glabra	pignut hickory
	YP
Liriodendron tulipifera	yellow-poplar
Magnolia acuminata	cucumber magnolia
Tilia americana	American basswood
	Beech
Fagus grandifolia	American beech
	Maple
Acer saccharum	sugar maple
Acer rubrum	red maple

Table 5 (continued)

Scientific Name	Common Name
	B.Gum
Nyssa sylvatica	blackgum
	Hem
Tsuga canadensis	eastern hemlock
	Pine
Pinus echinata	shortleaf pine
Pinus virginiana	Virginia pine
Pinus rigida	pitch pine
	Sass
Sassafras albidum	sassafras
	Birch
Betula lenta	sweet birch
	W.Ash
Fraxinus americana	white ash
	B.Locust
Robinia pseudoacacia	black locust
	Misc. Hdwd
	Includes miscellaneous hardwoods in which no particular species group constitutes an appreciable amount of basal area in the type.

Table 6 Vegetation Summary by Type, based on basal area

Little Millseat Branch

Type No.	Type Name	Spec.-Comp.%	Total %	Avg. Crown Closure %			Cover Type Code
				Overstory	Understory	Grass & Bare	
1	Oak-Hick-Maple	56-20-11	87	44	49	7	3
2	YP-Oak-Hick	34-27-12	73	79	17	4	3
3	YP-Oak	69-22	91	79	16	5	3
4	Oak-YP-Hick	37-27-13	77	62	33	5	3
5	YP-Beech-Birch	38-33-17	88	63	19	18	3
6	Oak-Pine	50-32	82	34	55	11	U*
7	Pine-Oak	50-45	95	72	25	3	U
8	Oak-Beech-Hick	48-19-13	80	49	42	9	3
9	YP-Beech	42-28	70	42	54	4	3
10	Oak-Hick-YP	49-18-13	80	81	19	0	3
11	YP-Beech-Oak	35-27-14	76	62	31	7	3
12	Oak	80	80	54	37	9	3
13	Oak-Pine	61-20	81	61	36	3	3
14	Oak-YP-Beech	46-20-17	83	84	11	5	3

*U = unclassified

Table 7 Vegetation Summary by Type, Based on basal area

Falling Rock Branch

Type No.	Type Name	Spec.-Comp.%	Total %	Avg. Crown Closure %			Cover Type Code
				Overstory	Understory	Grass & Bare	
1	YP-Beech-Oak	26-23-16	65	73	24	3	2
2	Oak-YP-Hick	42-22-10	74	67	31	2	3
3	Oak-Misc.Hdwd	70	70	74	24	2	3
4	YP-Misc.Hdwd	63	63	88	12	0	3
5	Oak	83	83	60	32	8	3
6	YP-Oak	48-28	76	78	21	1	3
7	Oak	79	79	79	20	1	3
9	Oak-Hick-YP	27-19-18	64	84	15	1	3
10	Oak-YP-Maple	49-19-12	80	70	29	1	3
12	Oak-YP	43-36	79	71	25	4	3
13	Oak-Maple	68-18	86	88	12	0	3
14	Oak-Maple	71-13	84	42	55	3	3
15	Oak	82	82	85	15	0	3
16	Oak	81	81	84	16	0	3
17	Oak	80	80	82	18	0	3
18	Oak	81	81	56	38	6	3
19	Oak	90	90	95	5	0	3
20	Oak	80	80	51	46	3	3
21	Oak	82	82	73	27	0	3

Table 8 Vegetation Summary by Type, based on basal area

Field Branch

Type No.	Type Name	Spec.-Comp.%	Total %	Avg. Crown Closure %			Cover Type Code
				Overstory	Understory	Grass & Bare	
1	YP-Hick-Oak	64-14-12	90	45	50	5	3
2	Oak-YP-Misc.Hdwd	47-16-37	63	72	24	4	3
3	YP	91	91	79	21	0	3
4	Oak-Maple	75-12	87	40	43	17	3
5	Oak-Maple	66-11	77	26	64	10	3
6	Oak-Pine-B.Gum	53-16-10	79	25	51	24	U*
7	Oak-Beech-YP	30-23-21	74	80	17	3	2
8	Pine-Oak	55-34	89	47	49	4	1
9	Oak-Hick-YP	34-29-21	84	54	44	2	3
10	YP-Oak-Maple	32-22-15	69	75	20	5	3
11	Oak-Hick	48-32	80	47	48	5	3

*U = unclassified

Table 9 Vegetation Summary by Type, based on basal area

Jenny Fork

Type No.	Type Name	Spec.-Comp.%	Total %	Avg. Crown Closure %			Cover Type Code
				Overstory	Understory	Grass & Bare	
1	Oak-Beech-YP	62-20-13	95	76	24	0	3
2	Oak-Beech	54-22	76	82	18	0	3
3	YP-W.Ash-Sass	35-20-15	70	63	16	21	3
4	Oak-Beech	60-21	81	75	25	0	3
5	Oak-Hick	56-26	82	76	24	0	3
6	Oak-Beech-YP	43-31-13	87	84	16	0	3
7	Pine-Oak	72-25	97	50	32	18	1
8	Oak-Hick-YP	36-29-20	85	89	10	1	3
9	Oak-Maple	71-11	82	74	25	1	3
10	Oak-Hick	58-24	82	82	18	0	3
11	Oak-Maple	74-13	87	100	0	0	3
12	Oak-Pine	47-47	94	71	25	4	1
13	Beech-YP-Oak	54-16-14	84	93	7	0	3
14	Oak-YP-Hick	35-21-20	76	91	9	0	3
15	Oak-Hick	77-11	88	74	18	8	3
16	Oak-Hick	67-21	88	87	12	1	3
17	Beech-YP	49-20	69	87	13	0	3

Table 9 (continued)

Type No.	Type Name	Spec.-Comp.%	Total %	Avg. Crown Closure %			Cover Type Code
				Overstory	Understory	Grass & Bare	
18	Oak-Beech	72-16	88	47	53	0	3
19	Oak	80	80	80	20	0	3
20	Oak-Hick	49-40	89	62	38	0	3
21	Oak-Hick-YP	67-17-10	94	71	28	1	3
22	YP-Hick	46-19	65	17	80	3	3
23	YP-Hick-Oak	40-39-13	92	74	20	6	3
24	Pine-YP-Sass	44-22-11	77	2	85	13	U*
25	Oak-Hick-Beech	44-19-15	78	85	15	0	3
26	YP-B.Locust	61-15	76	93	6	1	3
27	YP-Oak-Hick	44-33-15	92	96	4	0	3
28	Oak-YP-Hick	35-31-15	81	79	19	2	3
29	Beech-YP	63-19	82	94	6	0	3
30	YP-Hick	56-12	68	90	8	2	3
31	Oak-Maple	66-11	77	93	6	1	3
32	Beech-YP-Hem	54-14-11	79	93	6	1	2
33	Oak-Birch-Hick	26-22-15	63	94	5	1	3

*U = unclassified

Table 10 Vegetation Summary by Type, based on basal area

Miller Branch

Type No.	Type Name	Spec.-Comp.%	Total %	Avg. Crown Closure %			Cover Type Code
				Overstory	Understory	Grass & Bare	
1	Oak	96	96	64	22	14	3
2	Oak-Hick	72-11	83	6	94	0	3
3	Oak-Hick	79-13	92	38	61	1	3
5	B.Locust	97	97	72	0	28	8
6	Oak-Maple	58-19	77	38	61	1	3
9	Ham-Oak	61-29	90	68	30	2	U*
10	YP-Oak	49-32	81	75	21	4	3
11	Oak-YP-Hick	54-18-15	87	68	31	1	3
14	Oak-Beech-YP	32-30-19	81	88	11	1	3
16	YP-Pine-Hick	36-19-11	66	7	22	1	3
17	Oak-Beech-YP	34-33-15	82	91	8	1	3
18	Beech-YP-Oak	32-18-16	66	78	21	1	3
19	YP-Hick	47-42	89	90	10	0	3
21	YP	90	90	12	85	3	3

*U = unclassified

Table 11 Vegetation Summary by Type, based on basal area

Mullins Fork

Type No.	Type Name	Spec.-Comp.%	Total %	Avg. Crown Closure %			Cover Type Code
				Overstory	Understory	Grass & Bare	
2	Oak-Hick	63-14	77	69	31	0	3
3	YP	82	82	55	42	3	3
4	Oak	68	68	19	81	0	3
5	Beech-Oak	57-13	70	89	10	1	3
6	Oak	78	78	1	99	0	3
7	Oak-Maple-Hick	51-18-16	85	46	54	0	3
9	Oak-Beech	69-12	81	32	58	10	3
11	Oak	90	90	12	88	0	3
13	Oak	86	86	62	38	0	3
14	Beech-YP-Hick	26-22-13	61	18	61	21	3
15	Oak	78	78	42	48	10	3
16	Oak	78	78	40	60	0	3
17	Oak	82	82	58	38	4	3
18	Oak-Hick	66-16	82	83	14	3	3
19	B.Locust	100	100	36	0	64	8
20	Oak-Pine	68-29	97	44	47	9	U*

*U = unclassified

Table 11 (continued)

Type No.	Type Name	Spec.-Comp.%	Total %	Avg. Crown Closure %			Cover Type Code
				Overstory	Understory	Grass & Bare	
21	Oak-Beech	61-20	81	78	21	1	3
22	Oak-Hick	65-21	86	68	31	1	3
23	Oak-Beech-YP	38-26-18	82	83	15	2	3
24	B.Locust	100	100	45	0	55	8

Table 12 Vegetation Summary by Type

Miller Branch

Type No	Type Name[ǂ]	Spec. Comp.%[*]	GC %	Bare Ground %	Cover Type Code
4	Misc. Grasses	100	50	50	6
5	Fescue-Lesp.	55-36	79.6	21.4	8
7	Lesp-Fescue	66-34	68.3	31.7	5
8	Fescue-Lesp.	52-40	92.8	7.2	4
12	Lesp-Fescue	73-17	92.5	7.5	4
13	Fescue-S.Clover	80-16	23.8	76.2	7
15	Fescue-Lesp.	57-28	70.8	29.2	5
20	Bare-Pond	50-50	0	100	7

* Represents percent of ground cover percent occupied by a species.

ǂ Type Abbreviations: Fescue = Kentucky 31 Fescue; Rye = Rye Grass; B.Rye = Balboa Rye; Lesp. = Serecea Lespedeza; Vetch = Crown Vetch; Bare = Bare Ground; S. Clover = Sweet Clover; A.Lesp. = Annual Lespedeza; Pond = Sediment Pond

Table 13 Vegetation Summary by Type

Mullins Fork

Type No	Type Name†	Spec. Comp.%*	GC %	Bare Ground %	Cover Type Code
1	Misc.Grass-forbs	100	85.0	15.0	4
8	Rye	90	95.0	5.0	4
10	Rye-S.Clover	72-25	56.0	44.0	6
12	Fescue	90	77.7	22.3	5
19	Fescue-Vetch	52-35	95.5	4.5	8
24	Lesp-Fescue	57-43	85.0	15.0	8
25	S.Clover-Fescue	49-36	42.5	57.5	6
26	Rye-A.Lesp.-Fescue	44-22-22	73.6	26.4	5
27	B.Rye	95.0	50.0	50.0	6

* Represents percent of ground cover percent occupied by a species.

† Type Abbreviations: Fescue = Kentucky 31 Fescue; Lesp. = Serecea Lespedeza; S.Clover = Sweet Clover; Rye = Rye Grass; Vetch = Crown Vetch; A.Lesp. = Annual Lespedeza; B.Rye = Balboa Rye; Bare = Bare Ground; Pond = Sediment Pond

Table 14 Cover Type Coding Used in Tables 6-13

Cover Type Code	Name
1	Coniferous-Deciduous
2	Deciduous-Hemlock
3	Deciduous
4	Dense Grass 1
5	Dense Grass 2
6	Sparse Grass 1
7	Sparse Grass 2
8	Black Locust-Grass

Weekly grab samples of water are taken at each weir and analyzed for several water parameters. Physical parameters measured include turbidity, temperature, and suspended sediment. Chemical parameters analyzed are dissolved oxygen, alkalinity, pH, conductivity, calcium, magnesium, sodium, potassium, sulfates, and nitrates. Recent analyses also include determinations of total coliform, fecal coliform, and fecal streptococcus.

Only eight water quality parameters monitored on study watersheds are common to all six watersheds; these are: turbidity, pH, conductivity, calcium, magnesium, sodium, potassium, and sulfates. Correlation efforts have been limited to these common parameters.

Imagery and Descriptions

Overflights

Multispectral imagery from 1972 and 1973 aircraft overflights of portions of Robinson Forest was made available to the Department by NASA personnel at Marshall Space Flight Center. This imagery did not provide complete coverage in each overflight of all the current project's study watersheds. The imagery that was provided, however, was particularly valuable in recording changes within surface mined areas.

All-season, multispecral aircraft imagery of study areas was to have been provided during the current contract period. Actually furnished were multispectral and color infrared transparencies from April 7, 1975 and September 3, 1975 NASA aircraft overflights (Figures 4 and 5). These flights did provide nonfoliated and foliated ground cover conditions for

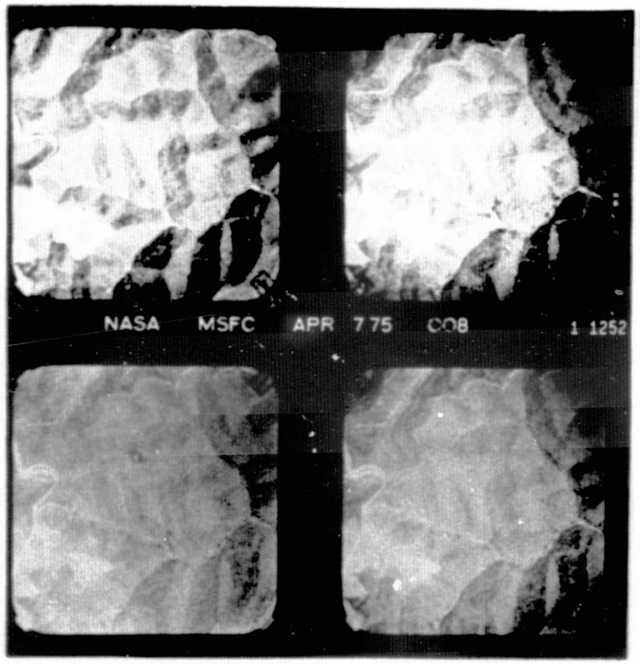

(a) Spring

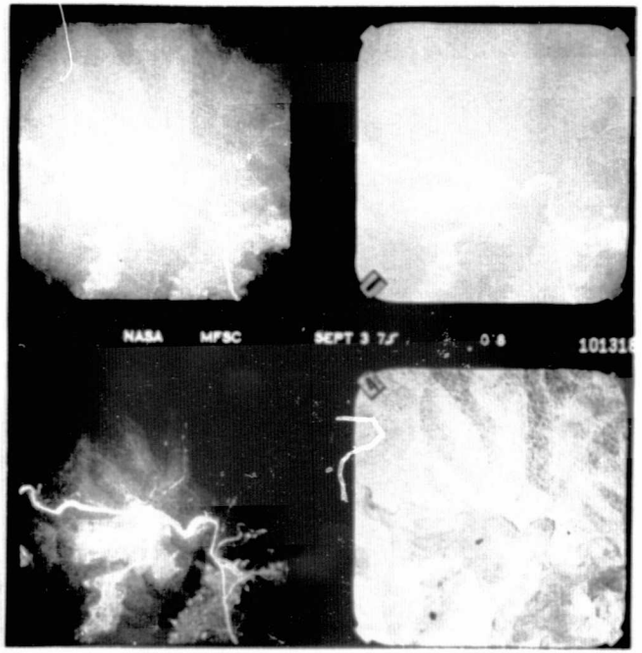

(b) Fall

REPRODUCIBILITY OF THE ORIGINAL PAGE IS POOR

Figure 4

Multispectral imagery from (a) April 7, 1975 and (b) September 3, 1975 NASA research aircraft overflights over the study watersheds. April imagery provides prefoliar coverage of deciduous vegetation; September imagery portrays fully foliated forest vegetation.

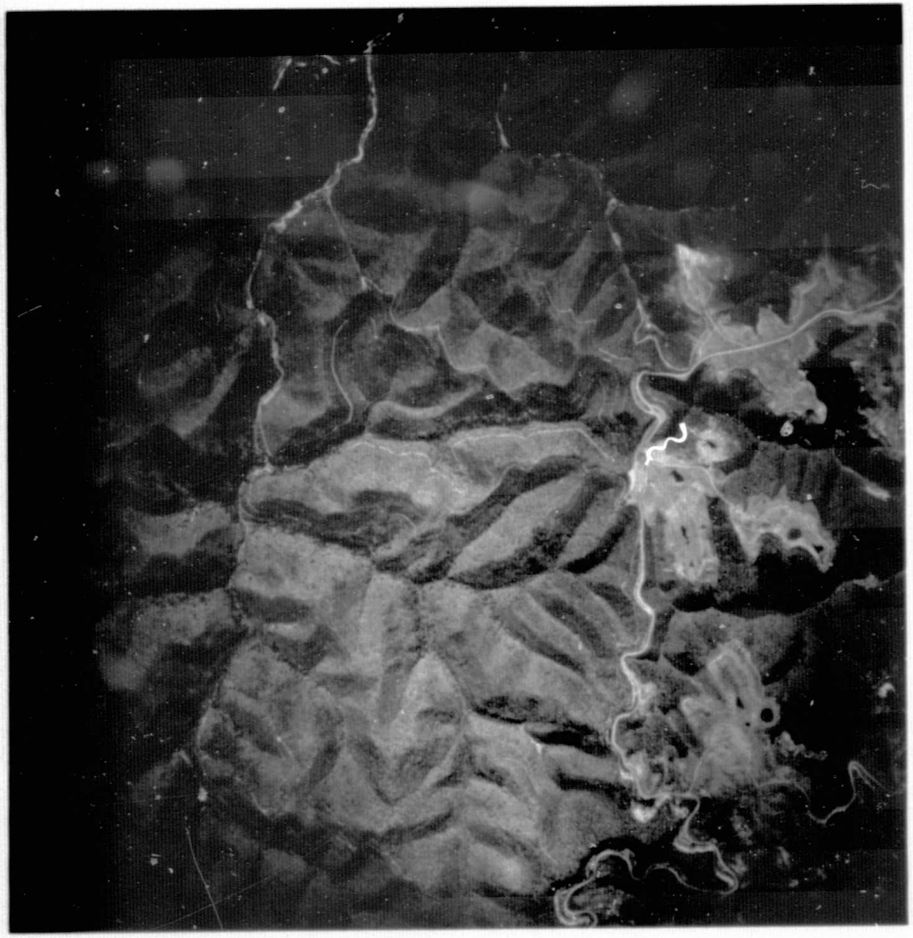

(a) Spring

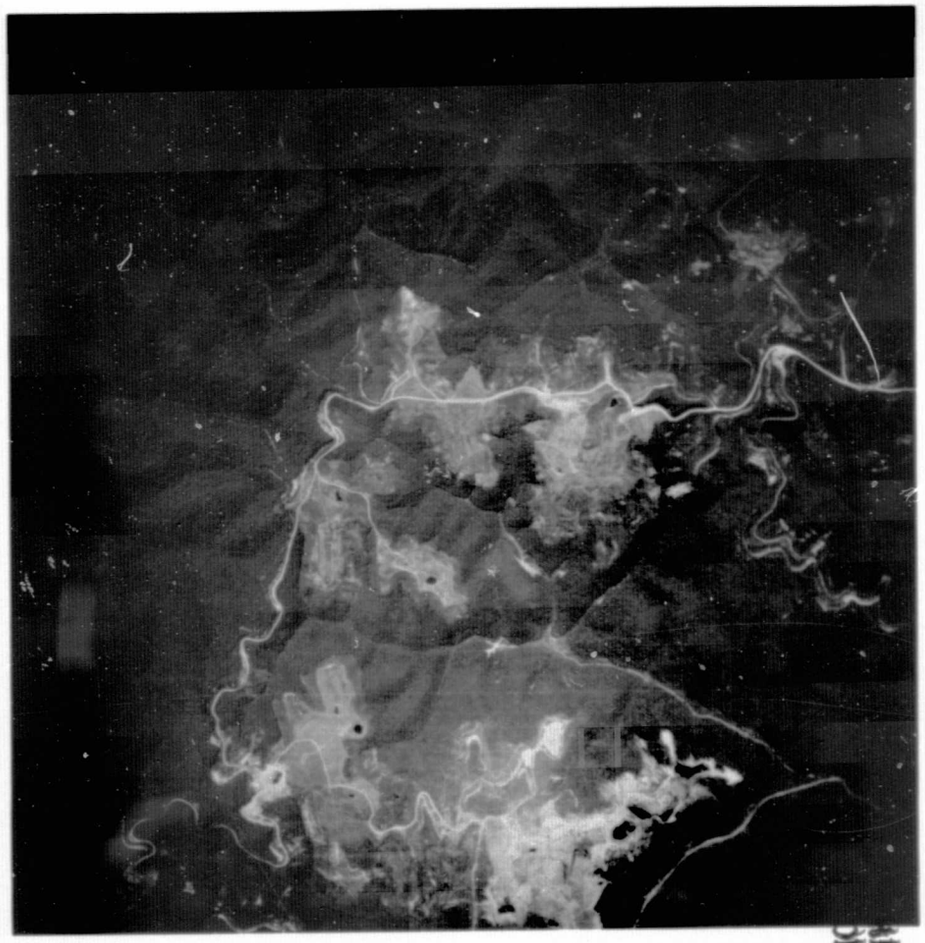

(b) Fall

REPRODUCIBILITY OF THE
ORIGINAL PAGE IS POOR

Figure 5

Color infrared imagery from (a) April 7, 1975 and (b) September 3, 1975 NASA research aircraft overflights over the study watersheds. April imagery provides prefoliar coverage of deciduous vegetation; September imagery portrays fully foliated forest vegetation.

imagery analysis, and the addition of the color infrared coverage to the overflights was certainly welcome and, as will be discussed in the evaluation section, quite useful. The resultant imagery was not without problems, however. These problems are discussed in the evaluation section of this report.

Thermal imagery coverage of the study areas was to have been provided under this contract, subject to availability of equipment. The scheduled flight was never completed, however, because time constraints of the project left insufficient time for both analysis of this imagery and completion of other project objectives.

Side Looking Airborne Radar imagery of the study areas was also investigated for use in project correlation efforts. This imagery proved more expensive than expected, and acquisition plans were dropped.

Satellite

Landsat imagery for use in color additive viewing and densitometry was purchased from the EROS Data Center in Sioux Falls, South Dakota. Landsat 1:3,369,000 and 1:1,000,000 positive and negative multispectral transparencies having ten percent or less cloud cover and a five or better quality rating were acquired for analysis. Landsat imagery was obtained for the years 1972-1976. Of greatest value to the project were April 12, 1975 and September 3, 1975 Landsat scenes, which most closely coincided with aircraft overflights.

Reference files available at Marshall Space Flight Center were examined to determine the availability of usable Skylab imagery coverage of the study areas. Our search of NASA imagery files indicated that no cloud-free Skylab imagery of the study areas was available.

Color Additive Viewing

An International Imaging Systems manual color additive viewer on loan to the University by NASA, Marshall Space Flight Center, was utilized in the color additive analysis portion of the study. A Super D Beseler Topcon camera equipped with a 58 millimeter lens was used to photograph selected composites off the color additive viewer screen. Close-ups of the composites were taken utilizing a Topcon Extension Tube Set.

Color composites of the April and September, 1975 multispectral overflight imagery were examined for potential to reveal additional information about the study watersheds. Color composites of positive and negative Landsat multispectral transparencies were analyzed for study area differences and also for significant phenomena outside the study areas. Single date-multiband, multidate-single band, and multidate-multiband combinations were examined to determine optimum land use-color additive combinations for several land uses and land use changes. Band-filter combinations that appeared to have potential utility were indexed for future replication and evaluation. Particular emphasis was given to satellite imagery taken closest to the dates of the study overflights, namely the April 12, 1975 and September 2, 1975 Landsat scenes.

Densitometry

Manual spot transmission densitometers were used to examine all available imagery-wavelength bands of aircraft and satellite transparencies to determine ground cover signatures. One densitometer utilized was a Macbeth TD-528 equipped with interchangeable one and three millimeter opal glass diffuse and one millimeter F/4.5 projection apertures. The TD-528 offered additional response functions through use of the visual, Wratten 93, Wratten 18A, and Wratten 96 filters that were incorporated into this digital display densitometer.

The other densitometer utilized in this study was a Macbeth TD-500 equipped with interchangeable one and two millimeter opal glass diffuse apertures. The fixed Wratten 106 gelatin-Corning 9788 glass filter combination did not provide for any other analysis variations with this meter display densitometer.

Neither densitometer was equipped with attachments necessary to allow precise geographical positioning and referencing of imagery utilized. Exact relocation and remeasurement of sampling points was thus virtually impossible, even with the use of templets. The error associated with this lack of measurement precision became particularly important in satellite imagery analysis.

Data were collected on aircraft overflight imagery at the rate of one reading per 0.4 hectare (1 acre) per type utilizing all combinations of the above apertures and filters. Densitometry samples were taken randomly

within the delineated types. The four filters available on the TD-528 densitometer allowed each sample point to in turn be sampled four times for each aperture. The fixed filter combination on the TD-500 densitometer permitted only one reading per sample location. Available aperture-filter combinations are identified in Table 15.

Assuming the aircraft overflight imagery had an exact RF of 1:24,000, sample sizes corresponding to one, two, and three millimeter apertures were 0.04 hectares (0.11 acres), 0.18 hectares (0.45 acres), and 0.41 hectares (1.01 acres), respectively. These figures are directly related to the areas of the respective apertures.

Data were collected on the available Landsat satellite multispectral transparencies at the rate of one reading per watershed on 1:1,000,000 imagery and one reading per general study area on 1:3,369,000 imagery. The smallest aperture available on the densitometers is one millimeter in diameter. The ground surface area represented by this circular aperture is 79 hectares (194 acres) on the 1:1,000,000 imagery and 892 hectares (2203 acres) on 1:3,369,000 imagery. Quite obviously one reading per 0.4 hectare per type was impossible. Some overlap of readings from adjacent watersheds occurred even with one reading per watershed samples taken on 1:1,000,000 imagery. This overlap occurred both because the study watersheds vary in size from 40 to 131 hectares and because the watersheds are not circular in shape.

Late densitometer delivery by Macbeth delayed densitometric analysis of the April overflight imagery. This delay, coupled with lag time

Table 15.

Densitometer-Aperture-Filter Combinations

CODE	DESCRIPTION
1d-XX	TD-500 Densitometer with 1 mm diffuse aperture-fixed filter combination
2d-XX	TD-500 Densitometer with 2 mm diffuse aperture-fixed filter combination
1d-OR	TD-528 Densitometer with 1 mm diffuse aperture-visual (orange)
1d-BL	TD-528 Densitometer with 1 mm diffuse aperture-Wratten #18A (black)
1d-GR	TD-528 Densitometer with 1 mm diffuse aperture-Wratten #93 (green)
1d-GY	TD-528 Densitometer with 1 mm diffuse aperture-Wratten #96 (gray)
3d-OR	TD-528 Densitometer with 3 mm diffuse aperture-visual (orange)
3d-BL	TD-528 Densitometer with 3 mm diffuse aperture-Wratten #18A (black)
3d-GR	TD-528 Densitometer with 3 mm diffuse aperture-Wratten #93 (green)
3d-GY	TD-528 Densitometer with 3 mm diffuse aperture-Wratten #96 (gray)
1p-OR	TD-528 Densitometer with 1 mm projection aperture-visual (orange)
1p-BL	TD-528 Densitometer with 1 mm projection aperture-Wratten #18A (black)
1p-GR	TD-528 Densitometer with 1 mm projection aperture-Wratten #93 (green)
1p-GY	TD-528 Densitometer with 1 mm projection aperture-Wratten #96 (gray)

associated with the transformation of densitometric information into data processing format, resulted in the elimination of some of the densitometer replications on the September overflight imagery. Implications of these eliminations are discussed in the evaluation section of this report.

EVALUATION

Imagery Interpretive Utility

Aircraft

All overflight imagery appears to suffer somewhat from the effects of vignetting. Careful selection of individual transparencies that were analyzed helped minimize and in most cases eliminate apparent adverse effects of this vignetting.

Large scale multispectral imagery from aircraft overflights has potential to provide valuable information for photographic analysis. Red and infrared bands appear to have the greatest general utility of the four bands present in the normal four band format. Blue and green bands, particularly the blue, tend to be washed out due to haze effects.

The April overflight produced acceptable multispectral imagery of three of the six study watersheds. Double exposures and one missed watershed accounted for the missing coverage. Band 1 was hazy but still showed adequate ground detail for densitometer sampling. Bare areas were distinct in this band, but forest-surface mine boundaries were not readily discernible. Band 2 was similar to band 1 but details in band 2 were perhaps slightly less obscurred by the effects of haze. Bare areas showed up best on band 3, but ground details on this imagery appeared to be somewhat blurred. Band 3 showed the best surface mine detail of the four bands, and pines and hemlocks stood out well. Band 4 had the greatest vegetative interpretive utility of the four bands. This band also yielded the most distinct photographic image of the four bands. Forest types were most easily identified in this band, as were water resources and forest-surface mine boundaries.

The September overflight yielded complete multispectral imagery coverage of the study watersheds. Unfortunately the high haze conditions that prevailed on the day of the overflight resulted in the complete washout of band 1. Band 2 imagery, although hazy, was sufficiently clear to define the forest type boundaries and to be sampled densitometrically. As was the case with the April band 2 imagery, September band 2 imagery showed bare areas well but forest-surface mine interfaces poorly. Band 3 displayed bare soil areas the best of the four bands, but again the forest-surface mine boundaries appeared poorly defined. Band 3 imagery exhibited the most contrast of the four bands, which tended to limit its utility somewhat. The best discrimination of forest types, forest-surface mine interfaces, and water details was provided by band 4. Although this band did not show bare soil well, it was rated the best of the four bands.

Large scale color infrared imagery has considerable potential for use in land analyses. CIR imagery is particularly well suited for vegetative surveys, such as forest typing, damage appraisal, and reclamation revegetation success. Just as with other films, date of imaging has a major effect on the utility of the imagery for different interpretation objectives.

The April 1975 overflight produced excellent color infrared imagery of all study watersheds. Ground details shown by this imagery were extraordinary - even long overgrown logging roads stood out well. Coniferous vegetation was very prominent, and surface mine details were very apparent. While much of the interpretative utility of this imagery was related to time of year and phenological development of the dominant hardwood vegetation, a good portion of this utility was attributable to the inherent capacity of color infrared film to cut haze and to portray vegetative phenomena.

The September 1975 overflight yielded complete color infrared imagery coverage of the study watersheds. This imagery appeared to suffer significantly from the effects of vignetting and was not as clear as the April overflight imagery. The high haze conditions prevailing on the day of the overflight undoubtedly contributed to the general haziness of this imagery. As mentioned previously in this report, careful selection of individual transparencies used in densitometric analysis helped minimize the adverse effects of haze and vignetting.

Satellite

Landsat satellite multispectral imagery offers a unique perspective to users of earth resources. Changing patterns of land use, previously unrecognized, are now detectable with the advent of repetitive Landsat imagery coverage of the whole planet. Landsat imagery furnishes the regional resource planner with a new tool and a new information base. This new tool is not without limitations, however.

Tonal and quality variations among transparencies from different dates can be considerable. Bands 6 and 7 occasionally are exceedingly light and washed out. On the other hand, band 4 often appears quite dark and somewhat indistinct. Imagery from dates having low sun elevations often appears dark, and land uses do not contrast well. Transparencies, though good for regional and/or large-area analyses, do not allow identification or quantification of smaller land use features. Excessive degradation of image quality occurs when transparency enlargement is attempted.

Greatest utilization of this imagery lies in applications or studies that are state-wide or regional in scope. Broad geographically-based efforts to utilize this newest informational tool will have different objectives

and focuses. Some comments on the apparent utility of the different Landsat multispectral bands would appear in order.

Some land uses are usually apparent on band 4 transparencies. Surface mines and roads usually stand out, and agricultural areas also separate from forests. Topographic detail is often obscure on band 4 and water bodies are usually indistinct. Fire scars may be apparent on spring or winter imagery but not to the same degree as in the near infrared landsat bands. Band 4 positive transparencies often appear quite dark, and potential use of th se transparencies is restricted. Usage of the corresponding negative transparencies is similarly restricted by excessively light tones instead of dark tones.

Band 5 transparencies generally portray land use details better than band 4. Band 5 also appears clearer than band 4 and less subject to haze effects. Surface mines and roads are usually distinguishable on band 5, particularly when sun angles are large. Water bodies are generally discernible on band 5, depending somewhat on the predominant land uses surrounding them. Topographic features are more in evidence on band 5 than band 4. Suspended sediment in water bodies is sometimes apparent on band 5. Fire scars are more apparent on band 5 than on band 4 and more apparent on positive than on negative transparencies. Agriculture-forest interfaces are usually distinguishable on band 5 and are perhaps more apparent on negative transparencies than on positives.

Band 6 imagery portrays topographic features better than either band 4 or band 5. Water resources stand out on band 6 and, although band 6 is near infrared, heavy suspended sediment loads in reservoirs and rivers may show up. Roads and surface mines may be indistinct on band 6, particularly with

low sun angles. Agriculture-forest discrimination is fair to good, dependent upon the sun angle. Fire scars are very apparent on imagery taken during winter or early spring. Positive and negative transparencies yield similar results, with the exception that fire scars may be more easily recognized on positive transparencies.

Band 7 characteristics are similar to band 6, except that topography and water resources are slightly more apparent on band 7. The normal infrared signature response of water usually overrides the influence of suspended sediment on the signature, thus water appears black on positive and white on negative transparencies. Band 7 usually fails to show roads, and, to a lesser extent, surface mines.

Color Additive Viewing

General Comments

Three films were evaluated for use in color additive analysis. Test composites were photographed with Ektachrome EH-ASA 160, Ektachrome EHB-ASA 160, and Kodachrome Professional II-ASA 40. The latter film gave the most accurate reproduction of test composite colors. Kodachrome Professional II-ASA 40 film was subsequently used for all additional color additive photography.

Some experimentation was also conducted with f/stops and shutter speeds to be used in composite photography. A test set of composites was photographed in triplicate by bracketing the light meter-indicated f/stop - shutter speed setting indicated by the camera light meter. Over and underexposures were made by holding f/stop constant and varying shutter

speed and by holding shutter speed constant while varying f/stop by one-half stop.

Varying shutter speed while holding f/stop constant produced bracketed images that were too dark or too light for interpretation. Bracketed images produced through f/stop variation did not present the extremes of the former method. Dependent on the colors generated on the viewer screen, darker and/or lighter exposures than indicated as optimum had potential utility. When dark shades of green or blue predominated in composites, underexposures were generally too dark but overexposures were often useful. When brighter shades of green and red predominated, overexposures were often faded but underexposures were sometimes useful. When portions of composites were photographed, underexposures often were too dark to interpret, regardless of the colors predominant in the composites.

Lower f/stops and longer shutter speeds were generally required for close-ups of particular areas on the composite compared to settings for full-chip composite pictures. F/stops for close-ups typically ranged 1/2 to 1 full f/stop lower and shutter speeds 0 to 2 times slower than for full chip composites. F/stops utilized in composite photography predominated in the 5.6 and lower range. F/stops of 4 and lower were typical for close-up photography. Shutter speeds of 1/8 to 1 second were utilized exclusively in later portions of composite photography.

Figure 6a was imaged using an f/stop of 4 and a shutter speed of 1 second, Figure 6b using an f/stop of 2.8 and a shutter speed of 1 second, and

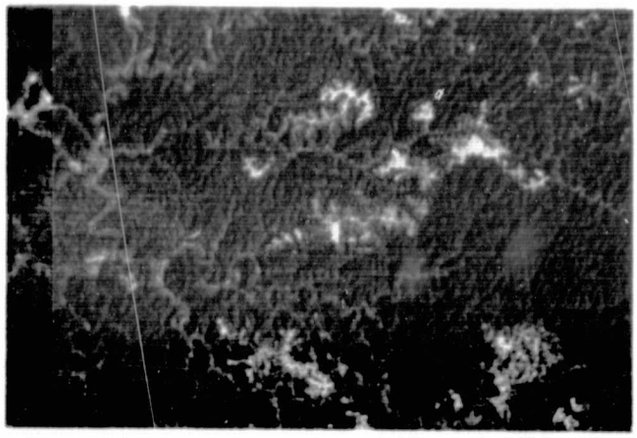

(a)

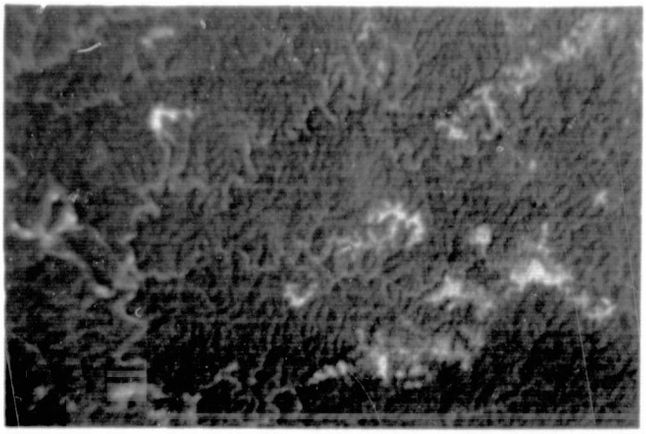

(b)

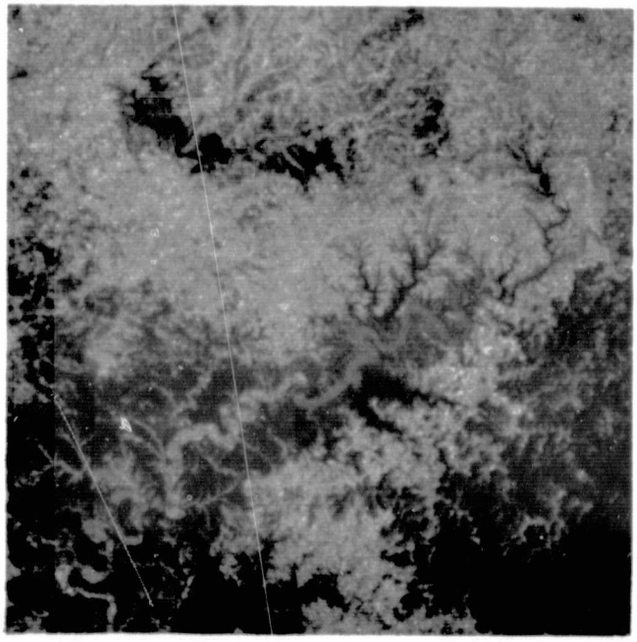

(c)

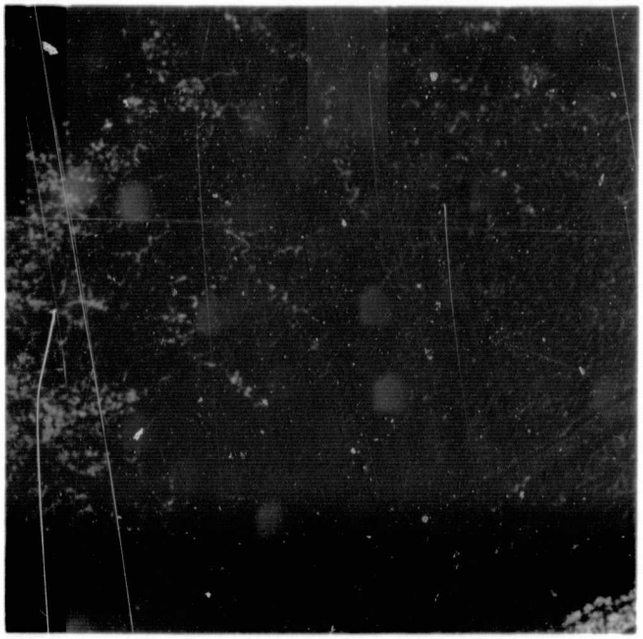

(d)

Figure 6

Color composites showing: (a) active and reclaimed mining; (b) active, recent active, and reclaimed mining; (c) agricultural-forest boundaries and water resources; (d) fire scars and water resources; and (e) spring forest vegetation.

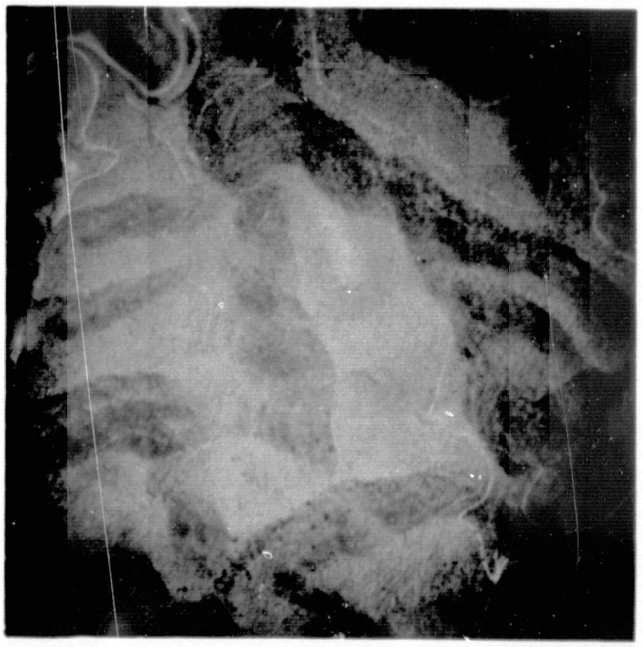

(e)

REPRODUCIBILITY OF THE
ORIGINAL PAGE IS POOR

Figure 6d using an f/stop of 9.5 and a shutter speed of 1 second. Figures 6c and 6e were taken early in the study by University of Kentucky Photographic Services personnel. No f/stop and shutter speed information is available for these figures.

Color composite feature resolution and delineation potential was not quantifiable when viewed on the color additive viewer screen. Such characteristics were qualifiable, however, by subjective visual ratings.

Aircraft

Color additive analysis of aircraft imagery included only single date-multiband combinations. Multidate color additive analyses were not feasible as scale differences between the April and September overflight imagery prevented multidate combinations.

April and September composites were examined for utility in land use classification and/or land use change analyses. Variations due to band-filter combinations produced the greatest differences between the various composites examined, but light intensity was also important. Excessive light intensities focused on various bands or on the composite as a whole often resulted in images in which detail colors bled into surrounding areas. Bleeding became a greater problem as the number of bands included in the composite increased.

Imagery vignetting and color additive viewer focusing appeared to combine to cause another problem in aircraft composite evaluation. In Figure 6e,

the edges of the composite are darker than the center, even though the picture has been cropped to eliminate most of the edge effect. Besides limiting the interpretation of the darker areas, these factors caused problems which were compounded when composites were photographed for later evaluation. The camera was usually set up to focus on the middle of the image (and viewer screen), where image light intensity was maximum. Resultant photographs were invariably under or overexposed in portions of the image.

Figure 6e is a 2-band April color composite made with a red filter on band 2 (green) and a green filter on band 4 (infrared). Light intensity was kept below maximum on both bands, because combining high light intensities with these bands caused severe bleeding of ground detail. The April composite was selected because (1) hardwoods distinguish well from conifers, and (2) ground details such as roads and mined areas also discriminate well. The green and red color filters used tend to complement each other, particularly if light intensities used with both are fairly equal.

September aircraft composites provide vegetation details such as hardwood densities and size classes that were not generally visible on April composites. September composites did not delineate roads, strip mine reclamation areas, and coniferous vegetation as well as the April composites.

Satellite

There are many published reports dealing with color additive viewing of Landsat multispectral transparencies (Jones, 1976; Nichols et al, 1974;

Welby, 1976; Graves and Hammetter, 1975). Many others have used Landsat computer compatible tapes and computers in combination with various image display devices to create color composite images (Todd, Mausel, and Wenner, 1973; Lawrence and Herzog, 1975; Siegal and Abrams, 1976).

This study dealt only with the use of Landsat positive and negative transparencies in color composite generation.

Two types of color composites are generated from Landsat multispectral positive and negative transparencies; these are (1) color composites generated on manual color additive viewers and (2) color composites created from superimposing diazochrome transparencies. Both methods of composite generation can be used in single date and multi-date analysis of land use and land use change (Nichols et al., 1974). Although both systems of composite generation can be used for such analyses, project investigators worked only with color additive viewer image generation.

Color additive research efforts using satellite imagery have focused on single date-multiband, multidate-single band, and multidate-multiband combinations of both positive and negative transparencies. Land uses and land use changes studied for potential monitoring through color additive analyses included forests, forest fertilization, and forest fire scars; agricultural fields; active and reclaimed surface mines; and water resources.

Several general comments about color additive viewing of satellite transparencies can be made. Two-chip combinations may display ground details

as well as or better than three or four chip combinations, particularly if similarity to color infrared response is not a goal. Resolution possible with composites is directly related to the quality of the bands utilized to produce the composite. The inclusion of a poor quality band into a composite image may reduce the overall utility of the composite. The usual inclusion of bands 4, 5, and 7 in EROS-generated composites, which produces a "classic" infrared composite, may not result in the most useful composite.

Multidate combinations composed of two chips appear to give best feature resolution if both chips are either positive or negative. Positive-negative combinations tend to cancel out all details that remained unchanged over the time period. Such combinations may be usable for change analysis, since they readily delineate such areas.

Fire scars are most apparent on composites which emphasize the input of near infrared bands. This is illustrated in the multidate-single band composite of Figure 6d. This composite includes an April 12, 1975 band 6 positive transparency with a clear filter and a light intensity setting of 9, a September 3, 1975 band 6 positive transparency with a green filter and a light intensity setting of 9, and a September 3, 1975 band 6 negative transparency with a red filter and a light intensity setting of 7. Fire scars stand out in very dark green, reservoirs in red, surface mines and agricultural areas in white, and forests in medium green. The main reason for the prominence of the fire scars is the clear filter and high light intensity used with the April band 6, since the fire scars were not apparent on the September imagery.

An equivalent light intensity with a clear filter overrides similar light intensities used with red, green, and blue filters. Red and green filters with identical light intensity settings appear about equal in effect, while a blue filter with identical light intensity influences color composite generation the least.

Figure 6c is a single date-multiband composite generated by combining April 13, 1975 positive transparencies of band 5 with a green filter and a light intensity setting of 9, band 6 with a red filter and a light intensity setting of 4, and band 7 with a red filter and a light intensity setting of 4. In this composite relatively clear water appears deep blue and sediment-laden water in light blue. Forest-agriculture boundaries are distinct, with forest appearing dark green and agricultural fields showing up in shades of orange and white. Distinction of differences in the water is possible because sediment-laden water is visibly lighter in band 5, and is also evident in the near infrared band 6 image. Band 7 portrays the water as black, the characteristic infrared response of water. The distinct agriculture-forest boundaries are quite prominent in bands 6 and band 7 and are apparently emphasized in the composite by the slight overbalance of the red light intensities used with bands 6 and 7 opposed by the higher light intensity used with the green filter on band 5.

Similar apparent water quality differences can be portrayed using multi-date-single band and multidate-multiband combinations. In these the overall input of bands 4 and 5, and perhaps 6, should be increased by weighting the light intensity-filter combinations more heavily. Negative

transparencies could also be used, resulting in clear water appearing lighter instead of darker than sediment-laden water.

Figure 6a is a multidate-multiband combination. To create this composite, an April 12, 1975 band 7 negative transparency with a blue filter and a light intensity setting of 5, an April 12, 1975 band 7 positive transparency with red filter and a light intensity setting of 7, and a September 3, 1975 band 5 positive transparency with clear filter and a light intensity setting of 9 were superimposed. Forest areas appear deep auburn, reclaimed mine areas appear pinkish, and active mining and other bare or highly disturbed areas appear white.

The dominance of the combination of the clear filter and high light intensity is apparent in the white color of the surface mined areas where mining was active and/or poorly reclaimed in September. The red-band 5 combination interacted with the less intensive white found in the reclaimed and partially reclaimed areas to produce the pink tones of these areas. The greater ability of band 5 to portray land uses and cultural features also assisted in discriminating these areas. Forest areas which appear dark on positive transparencies were less affected by the high intensity-clear combination and took the red color of the red filter. The blue filter-negative transparency combination had greatest influence on water body coloration, as the reversed band 7 infrared response allowed the blue to overpower the other colors in the reservoirs.

Figure 6b is a multidate-single band composite produced from combining an April 12, 1975 band 5 positive transparency with red filter and a light intensity setting of 9 with a September 3, 1975 band 5 positive transparency

with a green filter and a light intensity setting of 9. Areas that were not mined in April but disturbed in September are green in color. Other active mining, which was disturbed in both April and in September appear pink to very light green. Reclaimed mine areas are pinkish to auburn, and forest areas appear a dark orange.

The areas of mine change stand out green because the green light transmitted through the white mine area in the September imagery overbalanced the red light that was transmitted through the darker forest that was present in the area in the April imagery.

The differences portrayed in the mined areas would not be as great if multidate combinations of band 6 or band 7 were used, due to the lower land use discrimination potential of these bands as compared to bands 4 and 5. Multidate-band 4 combinations might discriminate as well as or better than band 5 combinations, but most available band 4 imagery is dark with very low contrast.

The composites selected for inclusion in this report were chosen from an extensive number of composites which themselves were selected for further analysis from extensive band-filter-light intensity combinations. These composites were included because they appeared to portray certain land uses and/or environmental phenomena better than the other composites generated. Researchers or other users of color composites would do well to keep the indicated interrelationships of the various factors involved in color composite generation in mind.

The Relation Between Land Cover and Aircraft Imagery Densitometry

A number of research projects have been concerned with the development of the technology and/or methodology for automated land use classification, forest cover mapping, crop surveys, and soil surveys using remotely sensed data. Highly accurate classifications have been achieved using data obtained with an airborne multispectral scanner (Coggeshall and Hoffer, 1973; Todd, Mausel and Baumgardner, 1973; Cipra, et.al., 1972). These efforts have used data collected at one given time. Steiner and Maurer (1968) and Steiner (1970) have studied the use of densitometric measurements made at sample points on multitype photography at several different times with regard to crop classification. They have found, using linear discriminant analysis, that a combination of densitometric variables measured at two or more points in time is more likely to produce correct classifications than such a combination measured at one given time.

The primary objective of this study was to determine the feasibility of classifying land cover using manually operated spot densitometer data gathered from color infrared and multispectral imagery from April and September, 1975, NASA aircraft overflights. Other related objectives included: 1) determining the relative utility of the April, September and combined data sets for land cover classification; 2) determining the "best" aperture to use from the viewpoint of terrain cover classification; and 3) determining the capability to distinguish between undisturbed forested areas and strip-mined areas in various stages of reclamation.

Before proceeding to a discussion of the data processing, some comment relevant to the application of linear discriminant analysis in automated classification procedures is needed. Discriminant analysis is a multivariate statistical method that calculates functions which discriminate between groups in an optimal manner. The discriminant functions calculated by the analysis determine boundaries which produce a set of subspaces, one subspace for each group. The location of the boundaries is such that a minimum number of misclassifications (i.e., individual points lying in the incorrect subspace) occurs. A detailed discussion of the mathematics is given by Rao (1973). A major factor involved in assessing the usefulness of the sample linear discriminant functions developed, namely the accurate estimation of the probabilities of misclassification (error rates) when using the functions to classify new samples, has been neglected by some studies (Steiner, 1970).

Steiner's only estimates of the error rates were obtained by observing the performance of his sample discriminant functions when applied to the set of data from which his discriminant functions were calculated. Lachenbruch (1968) has observed that when applied to a new sample, the observed probabilities of misclassification are usually greater than those computed from the initial sample. He proceeds to show that this increase in the error rates is related to the "shrinkage" of the multiple correlation coefficient, R^2, in new samples. This phenomenon occurs when using a set of regression coefficients computed from a sample for prediction purposes. In this case it is found that the correlation between predicted and observed values in a new sample is less than R. Thus Steiner's estimates of the error rates may be overly optimistic.

Possibly the most widely used method of estimating the misclassification probabilities can be described as follows: If the initial samples are sufficiently large, choose a subset of observations from each group; compute discriminant functions using this subset; and then use the classification results for all or part of the remaining observations to estimate error rates. See Cipra, et.al. (1972), Coggeshall and Hoffer (1973), Todd, Mausel and Baumgardner (1973), and Baumgardner and Henderson (1973) for examples using this method. This method of evaluating the performance of the sample discriminant functions developed in this project was eliminated because very few (< 5) observations were present for seven of the eight terrain cover groups associated with the project (Table 16).

A procedure which has the advantages of the above method but which uses all observations without introducing serious bias in the estimates of error rates has been proposed by Lachenbruch (1965). Lachenbruch's procedure, sometimes referred to as the jackknife method, can be described as follows: Take all possible splits of size 1 in one subset (test set) and the remainder in the other subset (training set). This has the effect of successively omitting one observation from the computation of the discriminant functions. The estimates of the misclassification probabilities are then computed by summing the number of cases that were misclassified from each group and dividing by the number in each group. Lachenbruch and Mickey (1968) compare several methods of estimating error rates and recommend the use of this method especially when normality is questionable and the sample size is small relative to the number of variables. This method seemed reasonable to use with

the project data set considering the number of groups containing fewer than 5 observations.

A stepwise discriminant analysis program, BMDP7M, employing the jackknife procedure has been written as part of the BMDP (Biomedical Computer Programs) package developed at UCLA's Health Sciences Computing Facility. BMDP7M performs a multiple group linear discriminant analysis as described in Dixon (1975) and Jennrich (1976). The variables used in computing the linear discriminant functions are chosen in a stepwise manner. At each step the variable that adds most to the separation of the groups (largest F value) is entered or the variable with the smallest F value is removed. By specifying contrasts, the user can state which group differences are of interest and thus influence the selection of the variables. Prior probabilities may be assigned to the groups. A limiting value of F-to-enter may be specified. A variable with an F-to-enter value less than this value cannot be entered into the set of discriminating variables. Similarly a limiting F-to-remove value may be specified and an entered variable having an F-to-remove value less than this value may be removed from the set of discriminating variables. Levels (one for each variable) directing the choice of variables in the stepping procedure may be assigned. Variables with lower level numbers are entered first unless their F-to-enter values are less than the threshhold value.

At this stage it was necessary to make somewhat arbitrary decisions concerning the use of the options described above since an infinite number of options was faced. It was decided that separation of each pair of

groups was of equal importance; so, no special contrasts of groups were used. Limiting F-to-enter and F-to-remove values of 2.00 and 1.75 respectively were specified.

Eight terrain cover types of interest appear in the ground truth data and are summarized in Table 16. Other cover types such as Hemlock-Deciduous (55%-45%) and Pine-Deciduous-Grass (25%-65%-10%) are represented by only one field type each. Since an absolute minimum of two samples in each group is required to use the program, these types could not be included in the analysis. Prior probabilities were assigned to the groups for computational purposes as shown in Table 16.

Many possible functions of the data presented themselves for possible inclusion in the set of discriminating variables. Wiegand, et.al. (1975) has found that the density units have no effect on the classification results. Therefore, arbitrary digital counts from the two Macbeth spot densitometers were used. To eliminate any possible effect of field type size in the discrimination program, each field type was represented in part by a vector of averages of density readings where each average was obtained using a different aperture-filter-machine-film combination. Also, the coefficients of variation associated with these means were included as suggested by Driscoll, et.al. (1972). Additionally, percentage increases were included for the 8 available aperture-filter combinations on the color infrared imagery. Finally, ratios of certain values were included in the list of variables (Table 17). The sample mean and standard deviation of each variable for each of the eight land cover groups is given in Appendix C.

It is well known that stepwise procedures for variable selection usually do not lead to the "optimal" subset of variables. Hence, various large subsets of the variables were entered into the program in an effort to see whether a very few variables might, from these analyses, appear to be of large importance irrespective of the subset entered. When the 14 April density variables and their coefficients of variation were entered, an overall error rate of 11.9 percent was estimated when using CIR-1d-BL, CIR-1d-GR and CIR-1d-GY densities for the discriminant analysis (Table 18). When the 8 percentage increases were also allowed to enter, the program obtained an estimated 8.5 percent overall error rate when using CIR-1d-BL, CIR-1d-GY, CIR-1d-OR, INC-1d-GR and INC-1d-OR variables (Table 19). Next, the ratios for the April color infrared imagery data were also permitted to enter the set of discriminating variables. The CIR-1d-OR, INC-1d-BL, INC-1d-GR and R-CIR-1d-BL/GY variables were chosen and an estimated overall error rate of 11.0 percent was obtained (Table 20).

A similar series of analyses beginning with the 20 September densities and their coefficients of variation gave estimated overall error rates of 15.3 percent, 13.6 percent and 11.0 percent. The five variables used to obtain the 11.0 percent error rate included: INC-1d-GR, INC-1d-OR, R-CIR-1d-BL/GY, R-CIR-3d-BL/GY and R-CIR-3d-GR/OR (Table 21).

When considering these error rates, it must be noted that if all observations were simply classified as Deciduous, an estimated overall error rate of only 18.6 percent would be obtained. Hence, overall error rates that exceeded 10 percent were considered unsatisfactory.

At this stage the decision was made to assign a few of the variables to level one, the remainder to level two, and then to repeat runs as described above. Of the numerous attempts made, the best results produced gave an overall estimated error rate of 5.9 percent (Table 22). This occurred when CIR-1d-BL, CIR-1d-GR and CIR-1d-GY were assigned to level one while the remaining 11 April density variables, the 14 associated coefficients of variation, the 8 percentage increases and the 6 ratios for the April color infrared imagery data were assigned to level two. In addition to the three level one variables, INC-1d-GR and INC-1d-OR were included in the set of discriminating variables. This set of five variables also proved superior, with respect to estimated overall error rate, to any other set found when all variables from Table 17 were allowed to enter.

While this classification may not be the best result achievable if all possible combinations of the variables were to be examined or other program options chosen, it gives an indication of what might be achieved. Except for the Dense Grass 1 group, no more than one observation in any group was misclassified when using the jackknife method.

Our next consideration was to compare the relative utility, to terrain cover classification, of the April, September and combined data sets. When only variables constructed wholly from the April data were permitted to enter into the set of discriminating variables, the lowest estimated overall error rate found was 11.9 percent as previously noted in Table 18. Meanwhile, when using only the September data, an estimated overall error

rate of 12.7 percent using variables R-CIR-1d-BL/GY and R-CIR-3d-BL/GY was the best attained (Table 23).

By examining Tables 18, 22 and 23 one can note the following: 1) The September data gave no separation of the mixed forest types from the deciduous type. 2) None of the sets was able to classify Dense Grass 1 areas correctly. 3) The combined data set offered much higher accuracy in classifying Coniferous-Deciduous, Deciduous-Hemlock and Deciduous areas than did the April or September set alone. 4) The estimated overall error rate, when either set alone was used, was at least double that obtained when using the combined data set. Multi-temporal data analysis would thus appear better for classification efforts than single-date data analysis.

In order to choose the "best" aperture size, several runs were made in which only those variables associated with a certain aperture were included. The results for the best of these analyses are summarized in Table 24.

The 1 mm diffuse aperture gave the lowest estimated overall error rate when either the April data set or the combined data set was considered. The 3 mm diffuse aperture was best when the September data set was considered; but since only 3 mm diffuse aperture (no 1 mm) readings were available for the September multispectral imagery, the latter conclusion may prove biased. It was observed that the lowest estimated overall

error rate of 5.9 percent was obtained with data collected using a 1 mm diffuse aperture. Results thus indicate the 1 mm diffuse aperture to be superior for this type of vegetative classification.

If classification of areas as either forested under multiple use management or surface mined forested under reclamation was the goal, the estimated probabilities of misclassification were quite small, as shown in Table 21. Table 21 shows that all 102 forested areas were classified, using the jackknife procedure, into one of the three forest types, while 15 of 16 strip-mined areas were classified into one of the five associated types. Thus, the estimated probabilities of misclassification for forested and strip-mined areas were 0.0 and 0.063 respectively. Again, additional searching might have produced completely accurate classifications if the program were directed to emphasize this separation when choosing the discriminating variables.

It is noteworthy to observe that by using 10 variables and all 118 observations for each classification, 117 of the 118 field types were correctly classified. Yet the jackknife estimated overall error rate was 10.2 percent. This indicates the circumstances which could cause Steiner's estimated error rate to be overly optimistic since he had only 9 observations in each group and used 13 variables when estimating the discriminant functions.

Table 16. Description of the 8 Cover Types Used in the Analyses

Name	Description	# of areas so classified from ground survey	prior probability used in BMDP7M
Coniferous - Deciduous	(approximately a 50-50 mix)	3	.03
Deciduous - Hemlock	(10-15% Hemlock, 80+% Hardwoods)	3	.03
Deciduous	(80+% Hardwoods, < 5% Hemlock)	96	.79
Dense Grass 1	(85+% Grass or non-woody vegetation)	4	.03
Dense Grass 2	(65-80% Grass)	4	.03
Sparse Grass 1	(40-60% Grass)	3	.03
Sparse Grass 2	(< 25% Grass)	2	.03
Black Locust-Grass	(Black Locust overstory with mixed grass understory)	3	.03

Table 17. List of Variables Used in the Analyses.

Type of Variable	Time	Type of Imagery	Variable Label [a/]
Average Density	April	Color Infrared	CIR-1d-XX
Average Density	April	Color Infrared	CIR-2d-XX
Average Density	April	Color Infrared	CIR-1d-BL
Average Density	April	Color Infrared	CIR-1d-GR
Average Density	April	Color Infrared	CIR-1d-GY
Average Density	April	Color Infrared	CIR-1d-OR
Average Density	April	Color Infrared	CIR-1p-BL
Average Density	April	Color Infrared	CIR-1p-GR
Average Density	April	Color Infrared	CIR-1p-GY
Average Density	April	Color Infrared	CIR-1p-OR
Average Density	April	Color Infrared	CIR-3d-BL
Average Density	April	Color Infrared	CIR-3d-GR
Average Density	April	Color Infrared	CIR-3d-GY
Average Density	April	Color Infrared	CIR-3d-OR
Coeff. Variation	April	Color Infrared	CV-CIR-1d-XX
Coeff. Variation	April	Color Infrared	CV-CIR-2d-XX
Coeff. Variation	April	Color Infrared	CV-CIR-1d-BL
Coeff. Variation	April	Color Infrared	CV-CIR-1d-GR
Coeff. Variation	April	Color Infrared	CV-CIR-1d-GY
Coeff. Variation	April	Color Infrared	CV-CIR-1d-OR
Coeff. Variation	April	Color Infrared	CV-CIR-1p-BL
Coeff. Variation	April	Color Infrared	CV-CIR-1p-GR
Coeff. Variation	April	Color Infrared	CV-CIR-1p-GY
Coeff. Variation	April	Color Infrared	CV-CIR-1p-OR
Coeff. Variation	April	Color Infrared	CV-CIR-3d-BL
Coeff. Variation	April	Color Infrared	CV-CIR-3d-GR
Coeff. Variation	April	Color Infrared	CV-CIR-3d-GY
Coeff. Variation	April	Color Infrared	CV-CIR-3d-OR
2 Filters - Ratio	April	Color Infrared	R-CIR-1d-BL/GY
2 Filters - Ratio	April	Color Infrared	R-CIR-1d-GR/OR
2 Filters - Ratio	April	Color Infrared	R-CIR-1p-BL/GY
2 Filters - Ratio	April	Color Infrared	R-CIR-1p-GR/OR
2 Filters - Ratio	April	Color Infrared	R-CIR-3d-BL/GY
2 Filters - Ratio	April	Color Infrared	R-CIR-3d-GR/OR

Table 17. continued

Type of Variable	Time	Type of Imagery	Variable Label [a/]
Average Density	Sept.	Color Infrared	CIR-1d-BL
Average Density	Sept.	Color Infrared	CIR-1d-GR
Average Density	Sept.	Color Infrared	CIR-1d-GY
Average Density	Sept.	Color Infrared	CIR-1d-OR
Average Density	Sept.	Color Infrared	CIR-3d-BL
Average Density	Sept.	Color Infrared	CIR-3d-GR
Average Density	Sept.	Color Infrared	CIR-3d-GY
Average Density	Sept.	Color Infrared	CIR-3d-OR
Average Density	Sept.	Multispectral - 2	MS2-3d-BL
Average Density	Sept.	Multispectral - 2	MS2-3d-GR
Average Density	Sept.	Multispectral - 2	MS2-3d-GY
Average Density	Sept.	Multispectral - 2	MS2-3d-OR
Average Density	Sept.	Multispectral - 3	MS3-3d-BL
Average Density	Sept.	Multispectral - 3	MS3-3d-GR
Average Density	Sept.	Multispectral - 3	MS3-3d-GY
Average Density	Sept.	Multispectral - 3	MS3-3d-OR
Average Density	Sept.	Multispectral - 4	MS4-3d-BL
Average Density	Sept.	Multispectral - 4	MS4-3d-GR
Average Density	Sept.	Multispectral - 4	MS4-3d-GY
Average Density	Sept.	Multispectral - 4	MS4-3d-OR
Coeff. Variation	Sept.	Color Infrared	CV-CIR-1d-BL
Coeff. Variation	Sept.	Color Infrared	CV-CIR-1d-GR
Coeff. Variation	Sept.	Color Infrared	CV-CIR-1d-GY
Coeff. Variation	Sept.	Color Infrared	CV-CIR-1d-OR
Coeff. Variation	Sept.	Color Infrared	CV-CIR-3d-BL
Coeff. Variation	Sept.	Color Infrared	CV-CIR-3d-GR
Coeff. Variation	Sept.	Color Infrared	CV-CIR-3d-GY
Coeff. Variation	Sept.	Color Infrared	CV-CIR-3d-OR
Coeff. Variation	Sept.	Multispectral - 2	CV-MS2-3d-BL
Coeff. Variation	Sept.	Multispectral - 2	CV-MS2-3d-GR
Coeff. Variation	Sept.	Multispectral - 2	CV-MS2-3d-GY
Coeff. Variation	Sept.	Multispectral - 2	CV-MS2-3d-OR
Coeff. Variation	Sept.	Multispectral - 3	CV-MS3-3d-BL
Coeff. Variation	Sept.	Multispectral - 3	CV-MS3-3d-GR

Table 17. continued

Type of Variable	Time	Type of Imagery	Variable Label [a]
Coeff. Variation	Sept.	Multispectral - 3	CV-MS3-3d-GY
Coeff. Variation	Sept.	Multispectral - 3	CV-MS3-3d-OR
Coeff. Variation	Sept.	Multispectral - 4	CV-MS4-3d-BL
Coeff. Variation	Sept.	Multispectral - 4	CV-MS4-3d-GR
Coeff. Variation	Sept.	Multispectral - 4	CV-MS4-3d-GY
Coeff. Variation	Sept.	Multispectral - 4	CV-MS4-3d-OR
2 Filters - Ratio	Sept.	Color Infrared	R-CIR-1d-BL/GY
2 Filters - Ratio	Sept.	Color Infrared	R-CIR-1d-GR/OR
2 Filters - Ratio	Sept.	Color Infrared	R-CIR-3d-BL/GY
2 Filters - Ratio	Sept.	Color Infrared	R-CIR-3d-GR/OR
Ratio of 2 Bands	Sept.	Multispectral - 2,3	R-MS2/3-3d-BL
Ratio of 2 Bands	Sept.	Multispectral - 2,3	R-MS2/3-3d-GR
Ratio of 2 Bands	Sept.	Multispectral - 2,3	R-MS2/3-3d-GY
Ratio of 2 Bands	Sept.	Multispectral - 2,3	R-MS2/3-3d-OR
Ratio of 2 Bands	Sept.	Multispectral - 2,4	R-MS2/4-3d-BL
Ratio of 2 Bands	Sept.	Multispectral - 2,4	R-MS2/4-3d-GR
Ratio of 2 Bands	Sept.	Multispectral - 2,4	R-MS2/4-3d-GY
Ratio of 2 Bands	Sept.	Multispectral - 2,4	R-MS2/4-3d-OR
Ratio of 2 Bands	Sept.	Multispectral - 3,4	R-MS3/4-3d-BL
Ratio of 2 Bands	Sept.	Multispectral - 3,4	R-MS3/4-3d-GR
Ratio of 2 Bands	Sept.	Multispectral - 3,4	R-MS3/4-3d-GY
Ratio of 2 Bands	Sept.	Multispectral - 3,4	R-MS3/4-3d-OR
Percent Increase [b]	Both	Color Infrared	Inc-1d-BL
Percent Increase	Both	Color Infrared	Inc-1d-GR
Percent Increase	Both	Color Infrared	Inc-1d-GY
Percent Increase	Both	Color Infrared	Inc-1d-OR
Percent Increase	Both	Color Infrared	Inc-3d-BL
Percent Increase	Both	Color Infrared	Inc-3d-GR
Percent Increase	Both	Color Infrared	Inc-3d-GY
Percent Increase	Both	Color Infrared	Inc-3d-OR

[a] Aperture, instrument and filter codes are given in Table 5.

[b] Percent Increase Inc-1d-BL is defined as: $\frac{(\text{Sept.-CIR-1d-BL})-(\text{April-CIR-1d-BL})}{(\text{April-CIR-1d-BL})} * 100\%$

Table 18. Jackknifed Classification Results Using Three April Densities.

Group	No. of Areas	Pct. CORCT	Number of Areas Classified into C-D	D-H	DEC	DG1	DG2	SG1	SG2	BLG
C-D	3	33.3	1	1	1	0	0	0	0	0
D-H	3	100.0	0	3	0	0	0	0	0	0
DEC	96	97.9	0	0	94	1	0	0	0	1
DG1	4	0.0	0	1	2	0	0	1	0	0
DG2	4	50.0	0	0	1	0	2	1	0	0
SG1	3	66.7	0	0	1	0	0	2	0	0
SG2	2	50.0	0	0	0	0	1	0	1	0
BLG	3	33.3	0	0	0	0	1	1	0	1
TOTAL	118		1	5	99	1	4	5	1	2

Overall Error Rate (14/118) = 11.9%
Variables used: April - CIR-1d-BL, CIR-1d-GY, CIR-1d-GR
Tables 18-23 use the following abbreviations for the groups:
C-D = Coniferous-Deciduous, D-H = Deciduous-Hemlock,
DEC = Deciduous, DG1 = Dense Grass 1, DG2 = Dense Grass 2,
SG1 = Sparse Grass 1, SG2 = Sparse Grass 2,
BLG = Black Locust-Grass.

Table 19. Jackknifed Classification Results Using Three Densities and Two Percent Increases.

Group	No. of Areas	Pct. CORCT	Number of Areas Classified into C-D	D-H	DEC	DG1	DG2	SG1	SG2	BLG
C-D	3	33.3	1	0	2	0	0	0	0	0
D-H	3	100.0	0	3	0	0	0	0	0	0
DEC	96	99.9	0	1	95	0	0	0	0	0
DG1	4	0.0	0	1	1	0	0	1	0	1
DG2	4	50.0	0	0	0	0	2	1	0	1
SG1	3	66.7	0	0	0	0	1	2	0	0
SG2	2	100.0	0	0	0	0	0	0	2	0
BLG	3	100.0	0	0	0	0	0	0	0	3
TOTAL	118		1	5	98	0	3	4	2	5

Overall Error Rate (10/118) = 8.5%
Variables Used: April - CIR-1d-BL, CIR-1d-GY, CIR-1d-OR, INC-1d-GR, INC-1d-OR

Table 20. Jackknifed Classification Results Using an April Density, A Ratio of April Densities and Two Percent Increases.

Group	No. of Areas	Pct. CORCT	Number of Areas Classified into C-D	D-H	DEC	DG1	DG2	SG1	SG2	BLG
C-D	3	66.7	2	1	0	0	0	0	0	0
D-H	3	33.3	1	1	1	0	0	0	0	0
DEC	96	99.0	1	0	95	0	0	0	0	0
DG1	4	0.0	1	0	1	0	0	1	0	1
DG2	4	25.0	0	0	0	0	1	1	0	2
SG1	3	33.3	0	0	0	1	0	1	1	0
SG2	2	100.0	0	0	0	0	0	0	2	0
BLG	3	100.0	0	0	0	0	0	0	0	3
TOTAL	118		5	2	97	1	1	3	3	6

Overall Error Rate (13/118) = 11.0%
Variables Used: April-CIR-1d-OR, R-CIR-1d-BL/GY, INC-1d-BL, INC-1d-GR
See Table 18 for a list of GROUP codes

Table 21. Jackknifed Classification Results Using Three Ratios of September Densities and Two Percent Increases.

Group	No. of Areas	Pct. CORCT	Number of Areas Classified into C-D	D-H	DEC	DG1	DG2	SG1	SG2	BLG
C-D	3	33.3	1	0	2	0	0	0	0	0
D-H	3	66.7	0	2	1	0	0	0	0	0
DEC	96	99.0	0	1	95	0	0	0	0	0
DG1	4	0.0	0	0	1	0	0	1	0	2
DG2	4	25.0	0	0	0	3	1	0	0	0
SG1	3	66.7	0	0	0	0	1	2	0	0
SG2	2	50.0	0	0	0	0	1	0	1	0
BLG	3	100.0	0	0	0	0	0	0	0	3
TOTAL	118		1	3	99	3	3	3	1	5

Overall Error Rate (13/118) = 11.0%
Variables Used: Sept-R-CIR-1d-BL/GY, R-CIR-3d-BL/GY, R-CIR-3d-GR/OR; INC-1d-GR, INC-1d-OR
See Table 18 for a list of GROUP codes

Table 22. Jackknifed Classification Results for the "Best" Set of Discriminating Variables.

Group	No. of Areas	Pct. CORCT	Number of Areas Classified into C-D	D-H	DEC	DG1	DG2	SG1	SG2	BLG
C-D	3	100.0	3	0	0	0	0	0	0	0
D-H	3	100.0	0	3	0	0	0	0	0	0
DEC	96	100.0	0	0	96	0	0	0	0	0
DG1	4	0.0	0	1	1	0	0	1	0	1
DG2	4	75.0	0	0	0	0	3	1	0	0
SG1	3	66.7	0	0	0	0	1	2	0	0
SG2	2	50.0	0	0	0	0	1	0	1	0
BLG	3	100.0	0	0	0	0	0	0	0	3
TOTAL	118		3	4	97	0	5	4	1	4

Overall Error Rate (7/118) = 5.9%
Variables Used: April - CIR-1d-BL, CIR-1d-GR, CIR-1d-GY; INC-1d-GR, INC-1d-OR
See Table 18 for a list of GROUP codes

Table 23. Jackknifed Classification Results Using Two Ratios of September Densities.

Group	No. of Areas	Pct. CORCT	Number of Areas Classified into C-D	D-H	DEC	DG1	DG2	SG1	SG2	BLG
C-D	3	0.0	0	0	3	0	0	0	0	0
D-H	3	0.0	0	0	3	0	0	0	0	0
DEC	96	100.0	0	0	96	0	0	0	0	0
DG1	4	0.0	0	0	1	0	0	1	1	1
DG2	4	25.0	0	0	1	0	1	0	1	1
SG1	3	100.0	0	0	0	0	0	3	0	0
SG2	2	50.0	0	0	0	0	0	1	1	0
BLG	3	66.7	0	0	0	0	1	0	0	2
TOTAL	118		0	0	104	0	2	5	3	4

Overall Error Rate (15/118) = 12.7%
Variables Used: Sept-R-CIR-1d-BL/GY, R-CIR-3d-BL/GY
See Table 18 for a list of GROUP codes

Table 24. Jackknife Estimates of Overall Error Rates by Date and Aperture.

Data Set	Aperture	Variables Used	Overall Error Rate (%)
April	1 mm diffuse - TD500	CIR-1d-XX	18.6
April	1 mm diffuse - TD528	CIR-1d-BL, GR, GY	11.9
April	1 mm projection	CIR-1p-BL, GR; CV-CIR-1p-GR; R-CIR-1p-BL/GY, R-CIR-1p-GR/OR	13.6
April	2 mm diffuse	CIR-2d-XX	18.6
April	3 mm diffuse	CIR-3d-GR, GY; R-CIR-3d-BL/GY, R-CIR-3d-GR/OR	15.3
Sept.	1 mm diffuse - TD528	R-CIR-1d-BL/GY	16.9
Sept.	3 mm diffuse	CIR-3d-BL, GR; R-CIR-3d-BL/GY	12.7
Combined	1 mm diffuse - TD528	April-CIR-1d-BL, GR, GY; INC-1d-GR, OR	5.9
Combined	3 mm diffuse	Sept.-CIR-3d-BL, GR; Sept.-R-CIR-3d-BL/GY	12.7

Landsat Imagery for Classifying Forested and Surface Mined Areas

Since a 1 mm aperture covers an area of 79 hectares when viewing the Landsat 1:1,000,000 imagery, density readings for the individual project field types could not be made. Instead density readings for each project watershed were obtained using eight aperture-filter combinations with each type of imagery (Appendix B).

The objective of this study was to determine the capability to distinguish between forested watersheds under multiple use management and surface mined forested watersheds under reclamation using manually operated spot densitometer data gathered from April 12 and September 3, 1975, Landsat multispectral imagery.

From ground survey observations, Little Millseat, Falling Rock, Field Branch and Jenny Fork were classified as forested land while Miller Branch and Mullins Fork watersheds were classified as approximately 50 percent surface mined areas. Each watershed was represented by a vector of 128 density readings where each reading was obtained using a different aperture-filter-film-date combination.

The sample mean and standard deviation of each variable for the two groups of watersheds is given in Appendix B.

The stepwise linear discriminant analysis program, BMDP7M, was again used in the data analysis. Equal prior probabilities of .5 were assigned to both watershed groups. As a first step, only those variables

obtained from the April 12, 1975, Landsat imagery were allowed to enter. A 100 percent accurate jackknife classification of the six watersheds was obtained using the density obtained with multispectral negative, band 4, 1 mm projection aperture and visual filter (N-MS4-1p-OR). It was then of interest to find that the N-MS4-1p-OR densities obtained from the September 3, 1975, Landsat imagery gave the same results. Subsequent investigation showed that any one of several other variables, such as densities obtained with multispectral positive or negative, band 4 or 5, 1 mm projection or diffuse aperture and visual, Wratten #18A, Wratten #93 or Wratten #96 filter, produced the same classification results as found above. These results indicate that separation of forested from 50 percent strip mined areas is easily accomplished using manually operated spot densitometer data gathered from Landsat multispectral imagery.

Meanwhile little or no separation of the groups was found when using data obtained either from April Landsat multispectral band 7 negative transparencies or from September Landsat multispectral band 6 positive or negative imagery.

Densitometry-Water Quality Correlations

April and September, 1975 Landsat 1:1,000,000 transparencies were sampled densitometrically and the results compared with water quality data from the six watersheds. Only water quality data from samples taken close to the April and September satellite imaging dates were used in correlation efforts, since evaluation of water quality estimates are only relevant at a given point in time.

Water quality samples included in correlation efforts were not collected at the same time on all six watersheds, because of sampling schedule differences between the U.S. Forest Service and the University of Kentucky. Results from water quality samples taken from Little Millseat Branch, Falling Rock Branch, and Field Branch watersheds on April 11 and April 18, 1975 were averaged, as were August 22 and September 9, 1975. Resultant averages were plotted against April and September Landsat densitometric values. Water quality sample results taken from Jenny Fork, Miller Branch, and Mullins Fork on April 8 and April 15, 1975 and on August 25 and September 9, 1975 were averaged and plotted against the April and September densitometric values.

Figures 7-14 show the relationship of the eight water quality parameters and April densitometric values which appeared to correlate best. Densitometry of the April 12, 1975 Landsat band 4 negative transparency obtained with the TD-528, one millimeter diffuse aperture, and green spectral response filter produced values most closely fitting the April water quality parameter averages. Some water quality parameters appear to correlate with densitometry better than others.

Figure 7

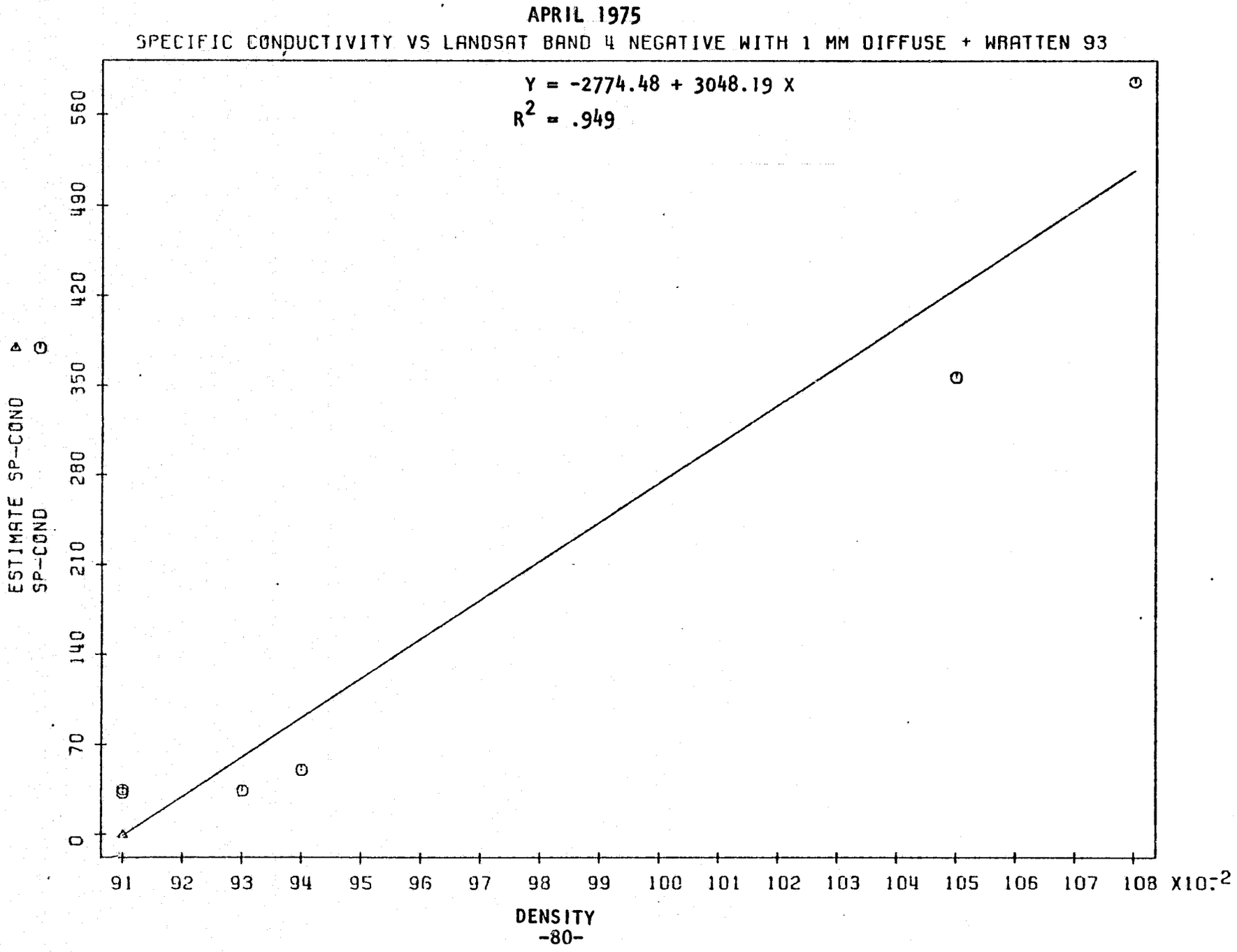
APRIL 1975
SPECIFIC CONDUCTIVITY VS LANDSAT BAND 4 NEGATIVE WITH 1 MM DIFFUSE + WRATTEN 93
Y = -2774.48 + 3048.19 X
R2 = .949
ESTIMATE SP-COND
SP-COND
0
70
140
210
280
350
420
490
560
91
92
93
94
95
96
97
98
99
100
101
102
103
104
105
106
107
108
X10-2
DENSITY
-80-

Figure 8

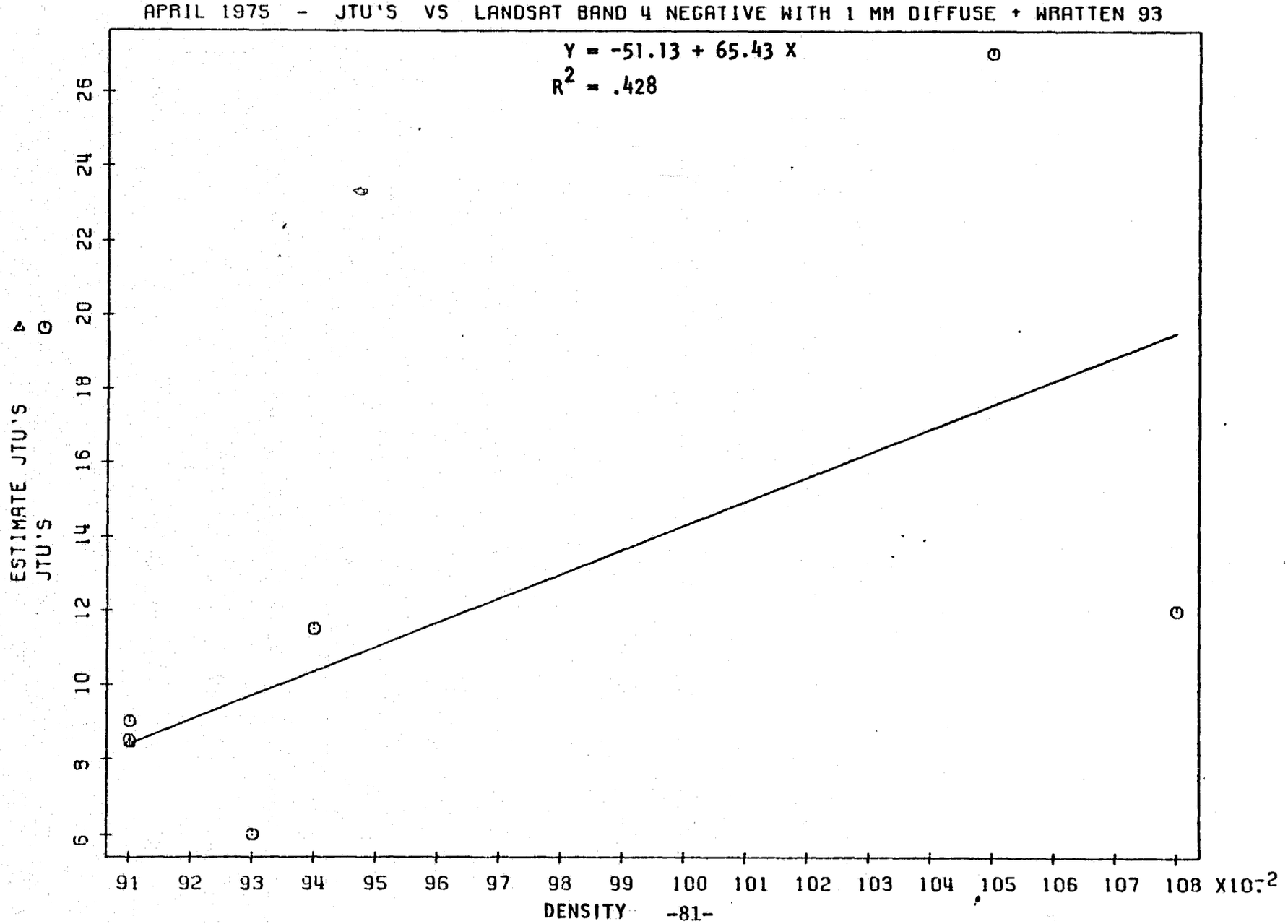
APRIL 1975 - JTU'S VS LANDSAT BAND 4 NEGATIVE WITH 1 MM DIFFUSE + WRATTEN 93
Y = -51.13 + 65.43 X
R2 = .428
ESTIMATE JTU'S
JTU'S
6
8
10
12
14
16
18
20
22
24
26
91
92
93
94
95
96
97
98
99
100
101
102
103
104
105
106
107
108
X10-2
DENSITY

Figure 9

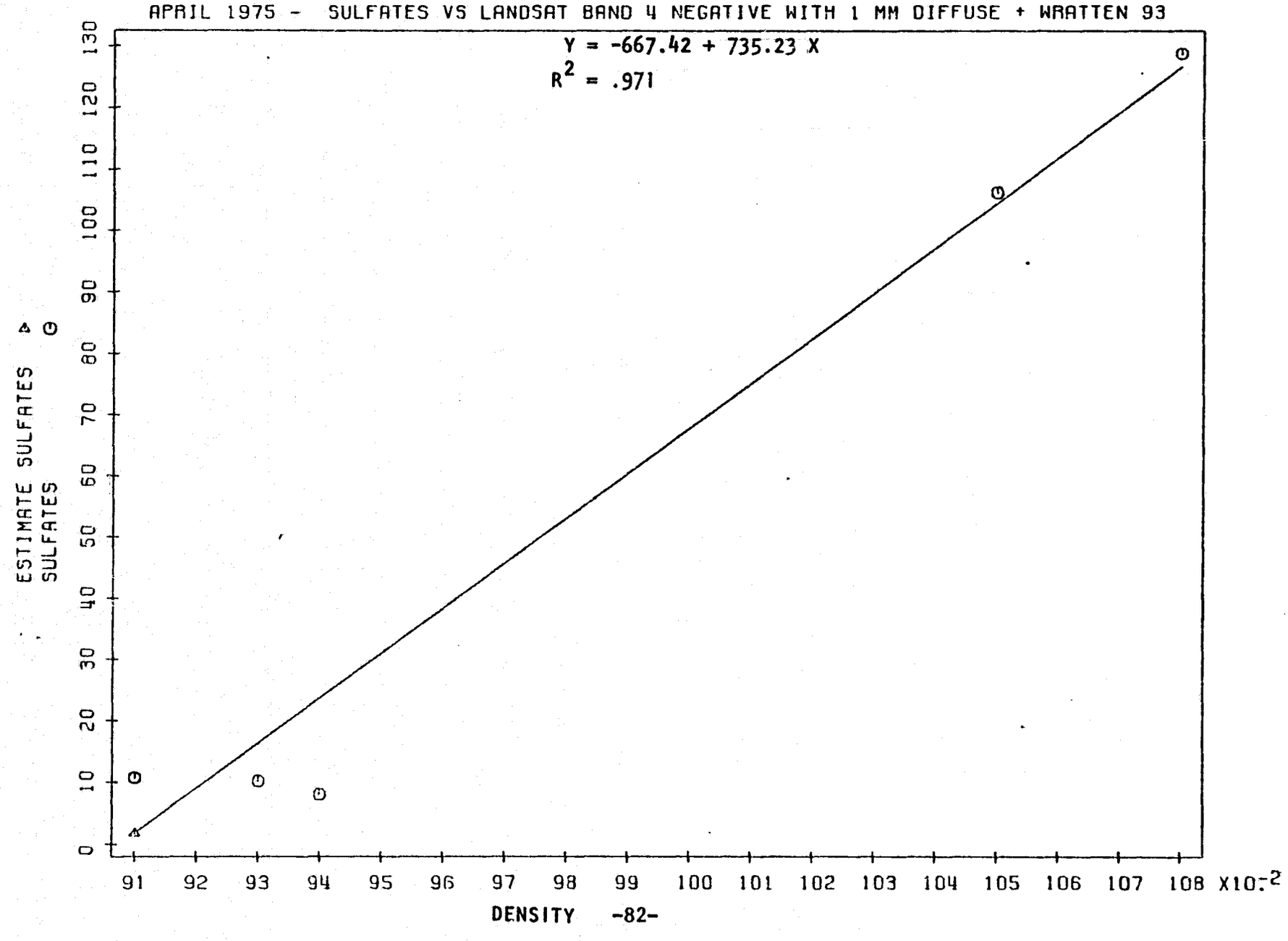
APRIL 1975 - SULFATES VS LANDSAT BAND 4 NEGATIVE WITH 1 MM DIFFUSE + WRATTEN 93
Y = -667.42 + 735.23 X
R2 = .971
ESTIMATE SULFATES
SULFATES
0 10 20 30 40 50 60 70 80 90 100 110 120 130
91 92 93 94 95 96 97 98 99 100 101 102 103 104 105 106 107 108 X10-2
DENSITY -82-

Figure 10

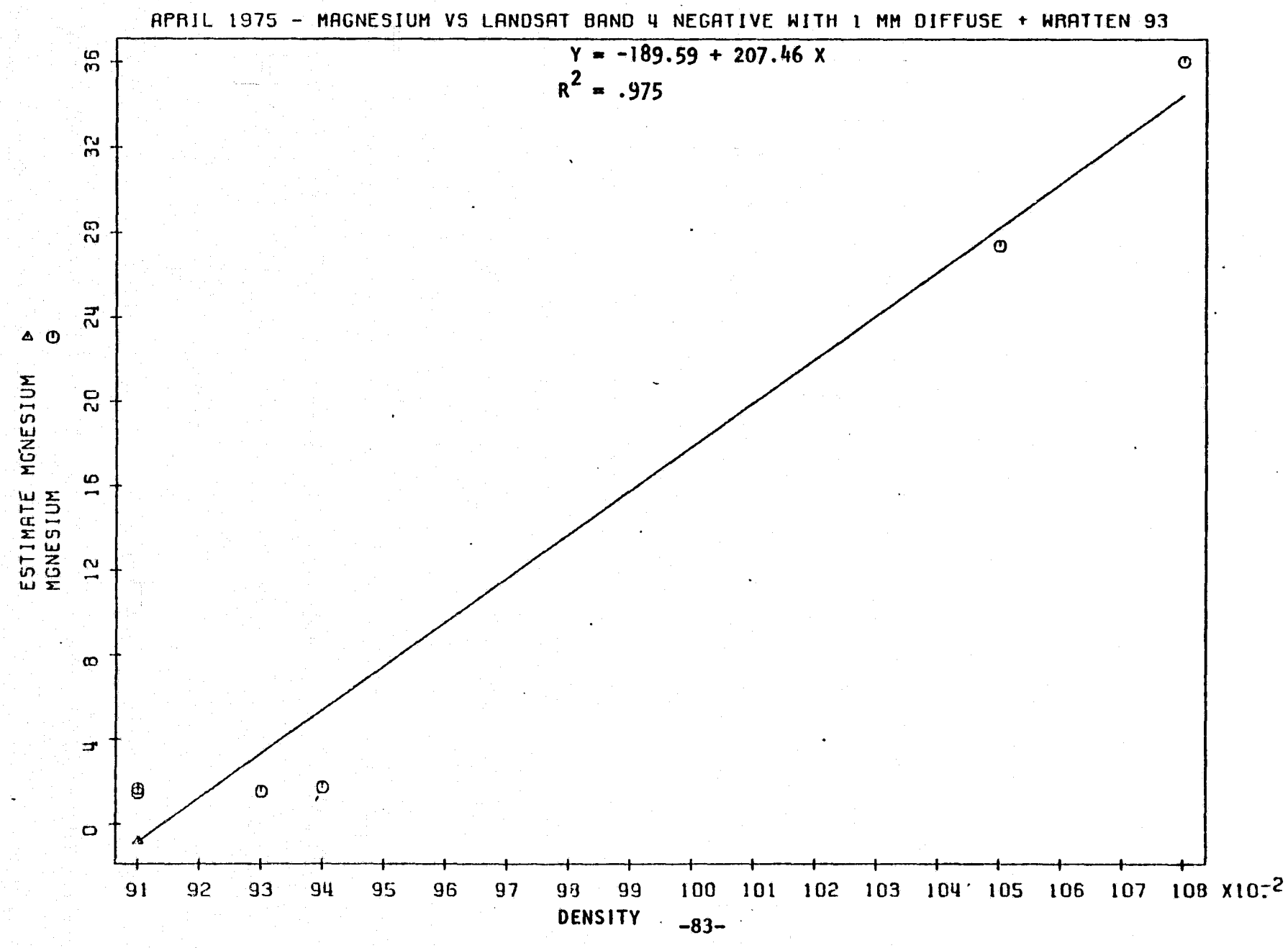
APRIL 1975 - MAGNESIUM VS LANDSAT BAND 4 NEGATIVE WITH 1 MM DIFFUSE + WRATTEN 93
Y = -189.59 + 207.46 X
R2 = .975
ESTIMATE MGNESIUM
MGNESIUM
0
4
8
12
16
20
24
28
32
36
91
92
93
94
95
96
97
98
99
100
101
102
103
104
105
106
107
108
X10-2
DENSITY

Figure 11

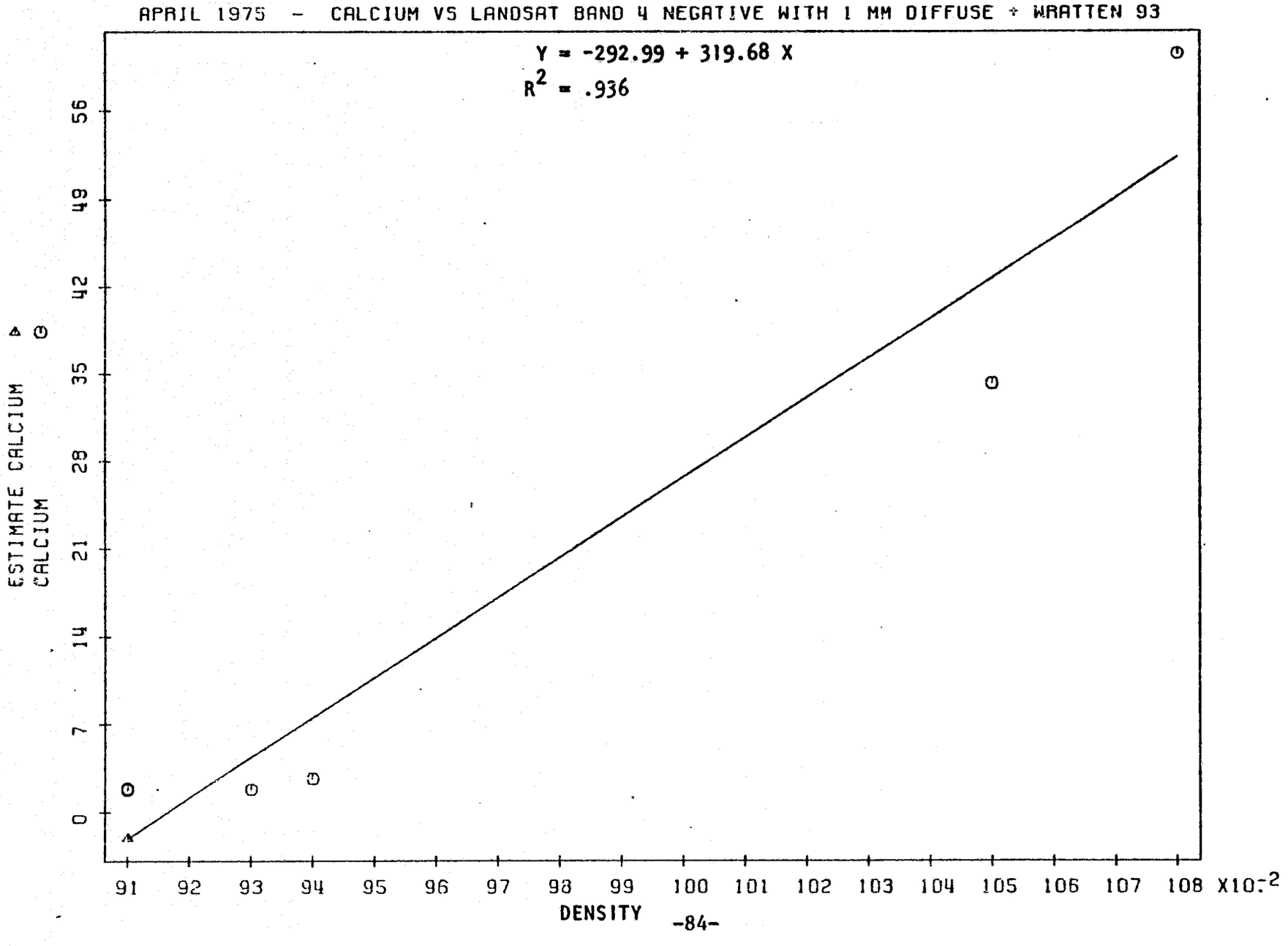
APRIL 1975 - CALCIUM VS LANDSAT BAND 4 NEGATIVE WITH 1 MM DIFFUSE * WRATTEN 93
Y = -292.99 + 319.68 X
R2 = .936
ESTIMATE CALCIUM
CALCIUM
0
7
14
21
28
35
42
49
56
91
92
93
94
95
96
97
98
99
100
101
102
103
104
105
106
107
108
X10-2
DENSITY

C-2

Figure 12

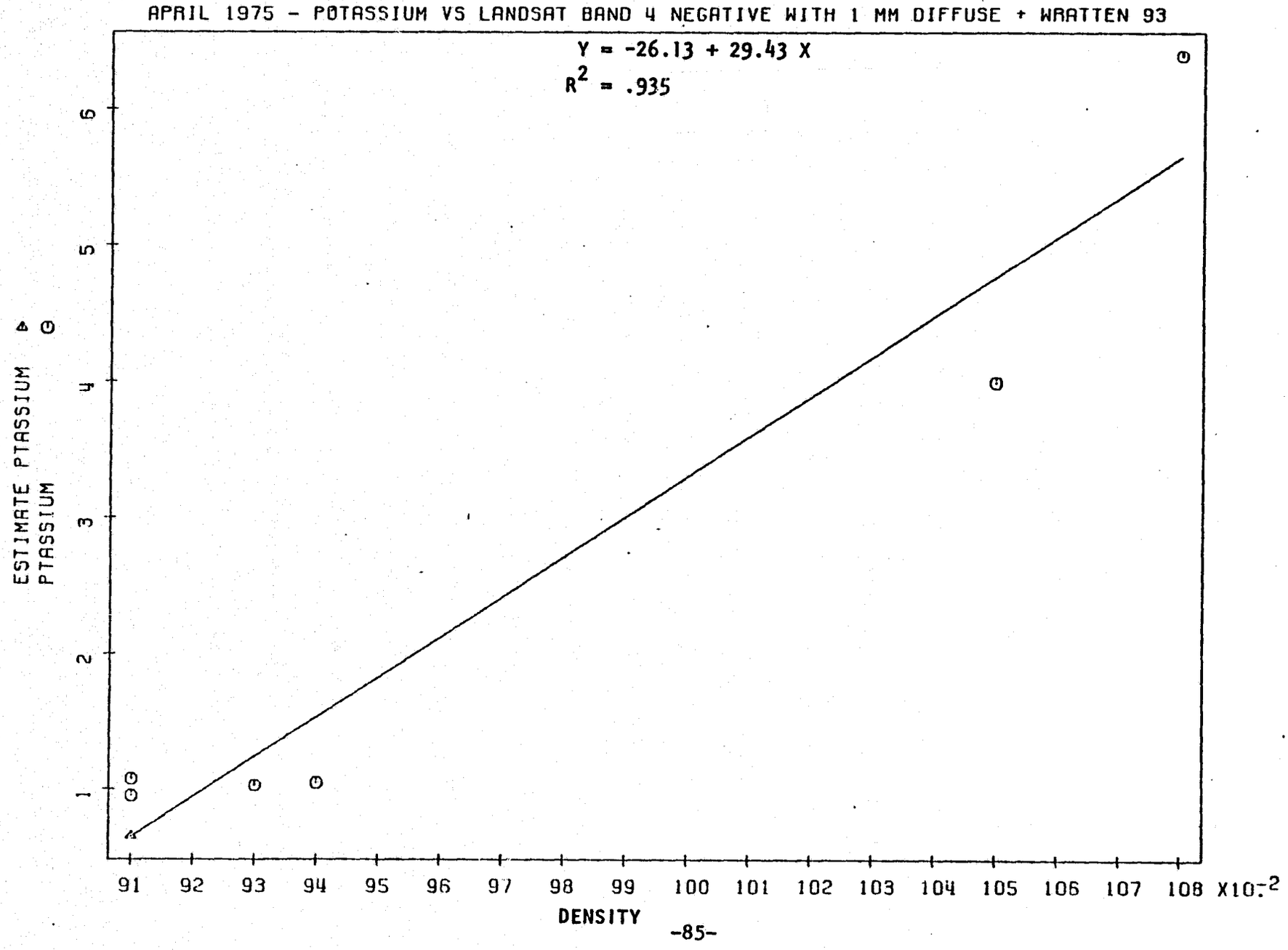
APRIL 1975 - POTASSIUM VS LANDSAT BAND 4 NEGATIVE WITH 1 MM DIFFUSE + WRATTEN 93
Y = -26.13 + 29.43 X
R2 = .935
ESTIMATE PTASSIUM
PTASSIUM
1
2
3
4
5
6
91
92
93
94
95
96
97
98
99
100
101
102
103
104
105
106
107
108
X10-2
DENSITY

Figure 13

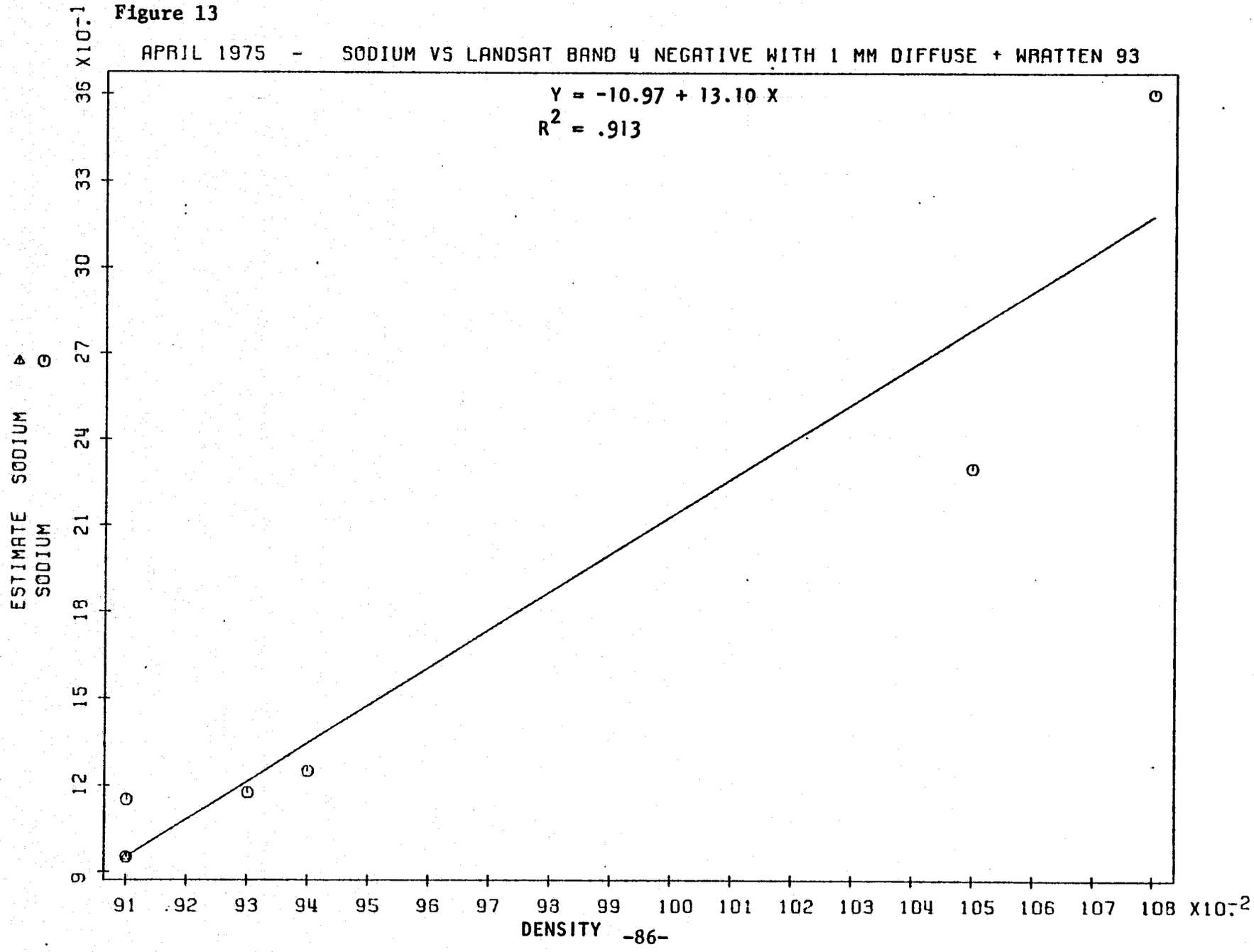
APRIL 1975 - SODIUM VS LANDSAT BAND 4 NEGATIVE WITH 1 MM DIFFUSE + WRATTEN 93
Y = -10.97 + 13.10 X
R2 = .913
ESTIMATE SODIUM
SODIUM
36 X10-1
33
30
27
24
21
18
15
12
9
91 92 93 94 95 96 97 98 99 100 101 102 103 104 105 106 107 108 X10-2
DENSITY

Figure 14

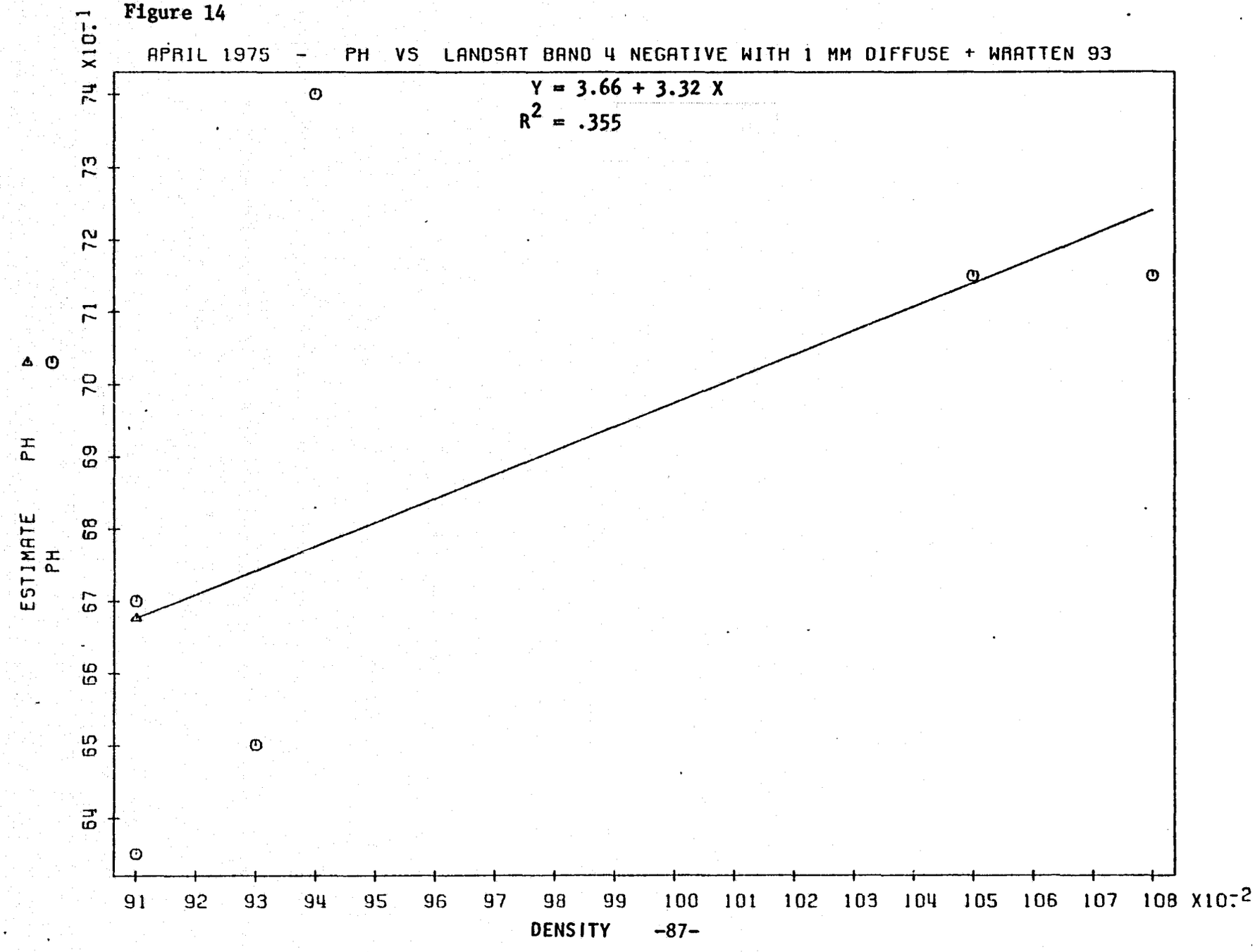
APRIL 1975 - PH VS LANDSAT BAND 4 NEGATIVE WITH 1 MM DIFFUSE + WRATTEN 93
Y = 3.66 + 3.32 X
R2 = .355
ESTIMATE PH
74 X10-1
73
72
71
70
69
68
67
66
65
64
91 92 93 94 95 96 97 98 99 100 101 102 103 104 105 106 107 108 X10-2
DENSITY -87-

Fully forested watersheds segregate into the lower left and partially surface mined watersheds into the upper right portion of these figures. The surface mined watersheds recorded a higher density signature since negative transparencies yield reverse values. On negative transparencies surface mines appear darker than surrounding forest areas, causing higher density signature values for mined watersheds.

Sulfate and magnesium appear to exhibit the highest degree of correlation with densitometry values of the eight water quality parameters investigated. Increases in density values appear related to increases in sulfate and magnesium concentrations. Similar correlations appear for the other water quality parameters, only not with the degree of fit of sulfate and magnesium. Hydrogen ion concentration (pH) evidence a significantly poorer regression fit to densitometric values (R^2=0.355) than the other parameters.

Figures 15-22 show densitometric-water quality correlations for the September values. Best regression fit was obtained through densitometry of a September 3, 1975 band 5 positive transparency with the TD-528 densitometer when equipped with a one millimeter diffuse aperture and green spectral response filter.

Since a positive transparency was utilized, densitometric values for fully forested watersheds are darker than for partially surface mined watersheds. Water quality values for wholly forested watersheds are found at the higher end of the densitometer scale and those for partially mined watersheds at the lower end.

Figure 15

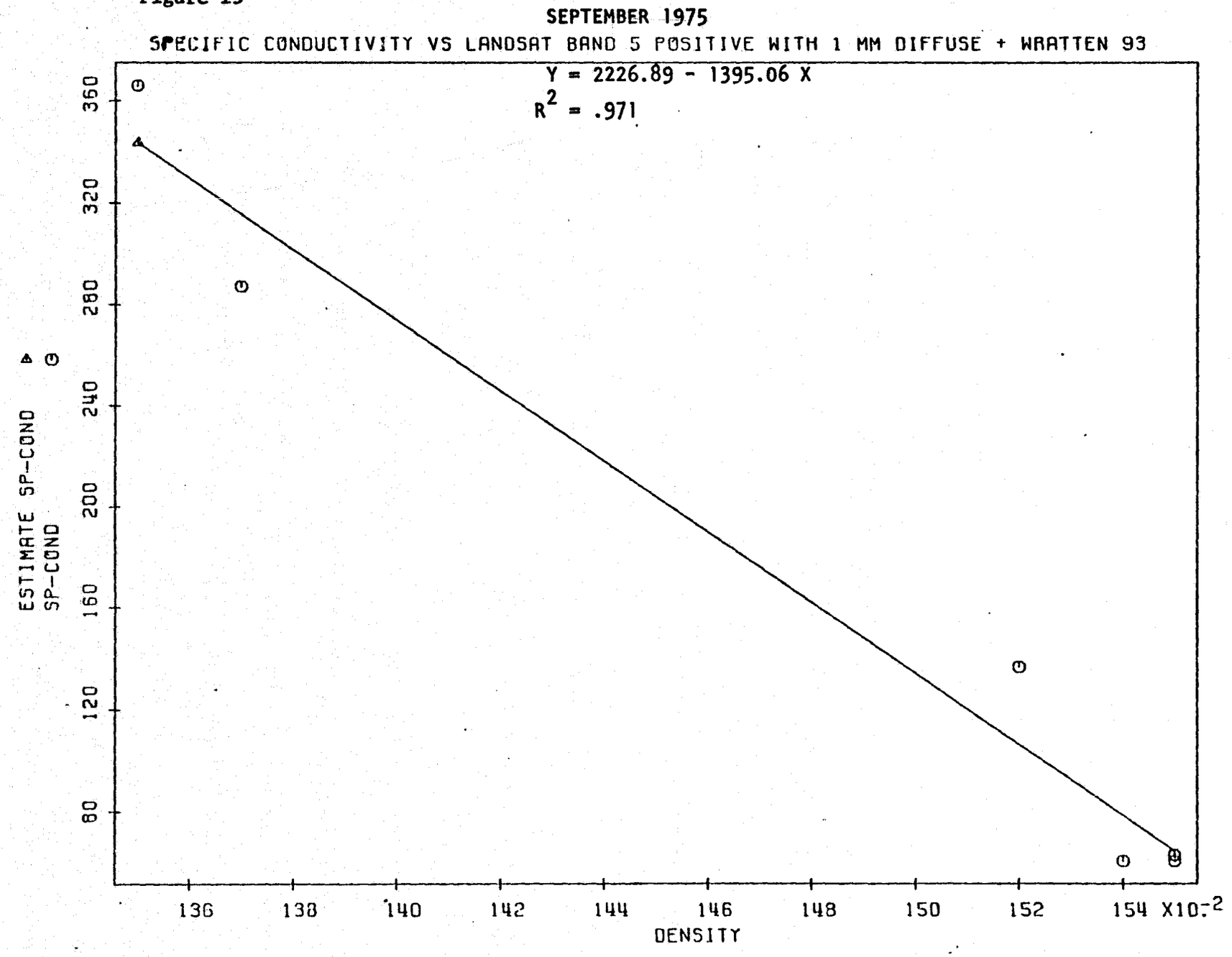
SEPTEMBER 1975
SPECIFIC CONDUCTIVITY VS LANDSAT BAND 5 POSITIVE WITH 1 MM DIFFUSE + WRATTEN 93
Y = 2226.89 - 1395.06 X
R2 = .971
ESTIMATE SP-COND
SP-COND
360
320
280
240
200
160
120
80
136
138
140
142
144
146
148
150
152
154 X10-2
DENSITY

Figure 16

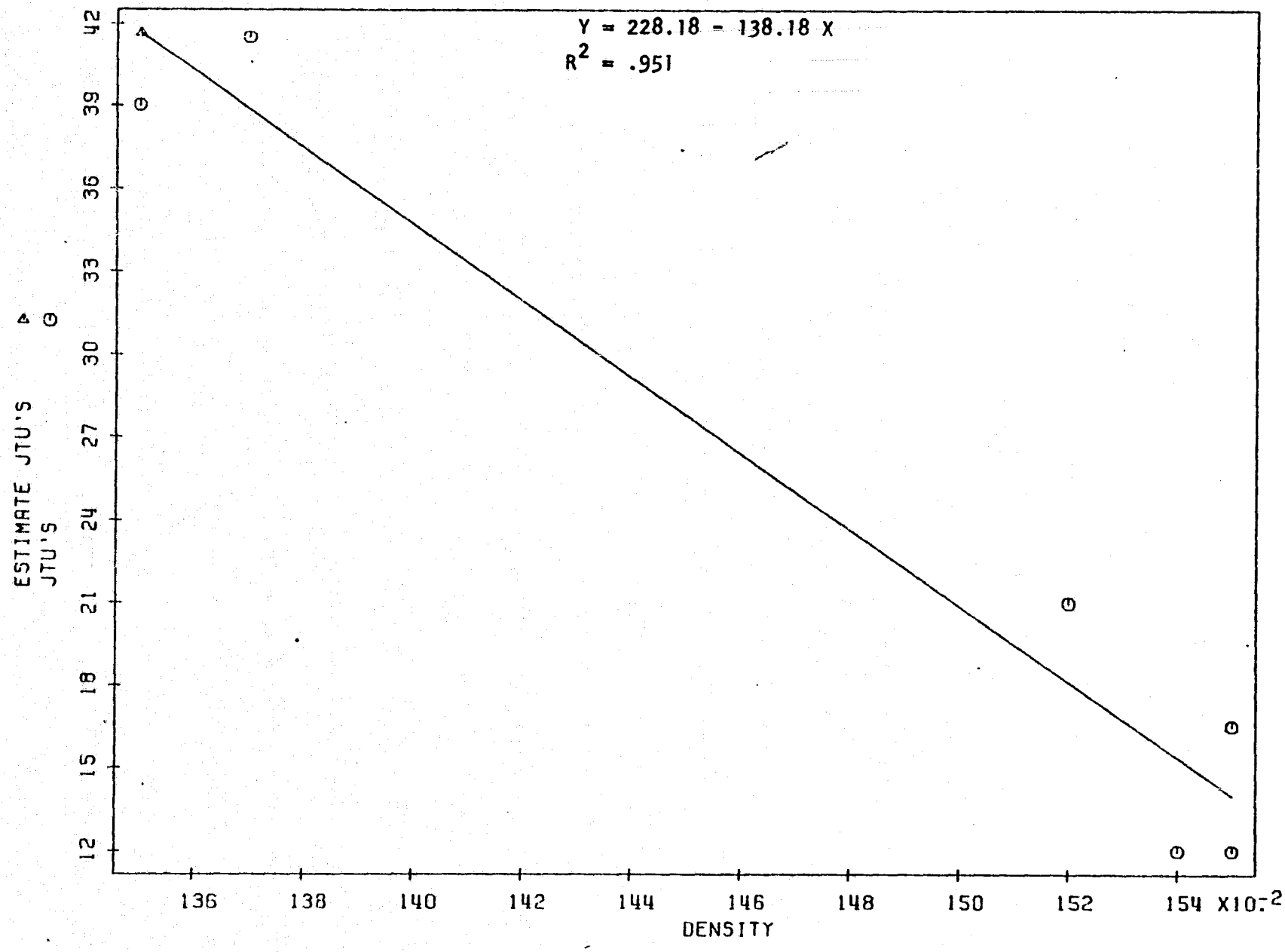
SEPT. 1975 - JTU'S VS LANDSAT BAND 5 POSITIVE WITH 1 MM DIFFUSE + WRATTEN 93
Y = 228.18 - 138.18 X
R2 = .951
ESTIMATE JTU'S
JTU'S
42
39
36
33
30
27
24
21
18
15
12
136
138
140
142
144
146
148
150
152
154 X10-2
DENSITY

Figure 17

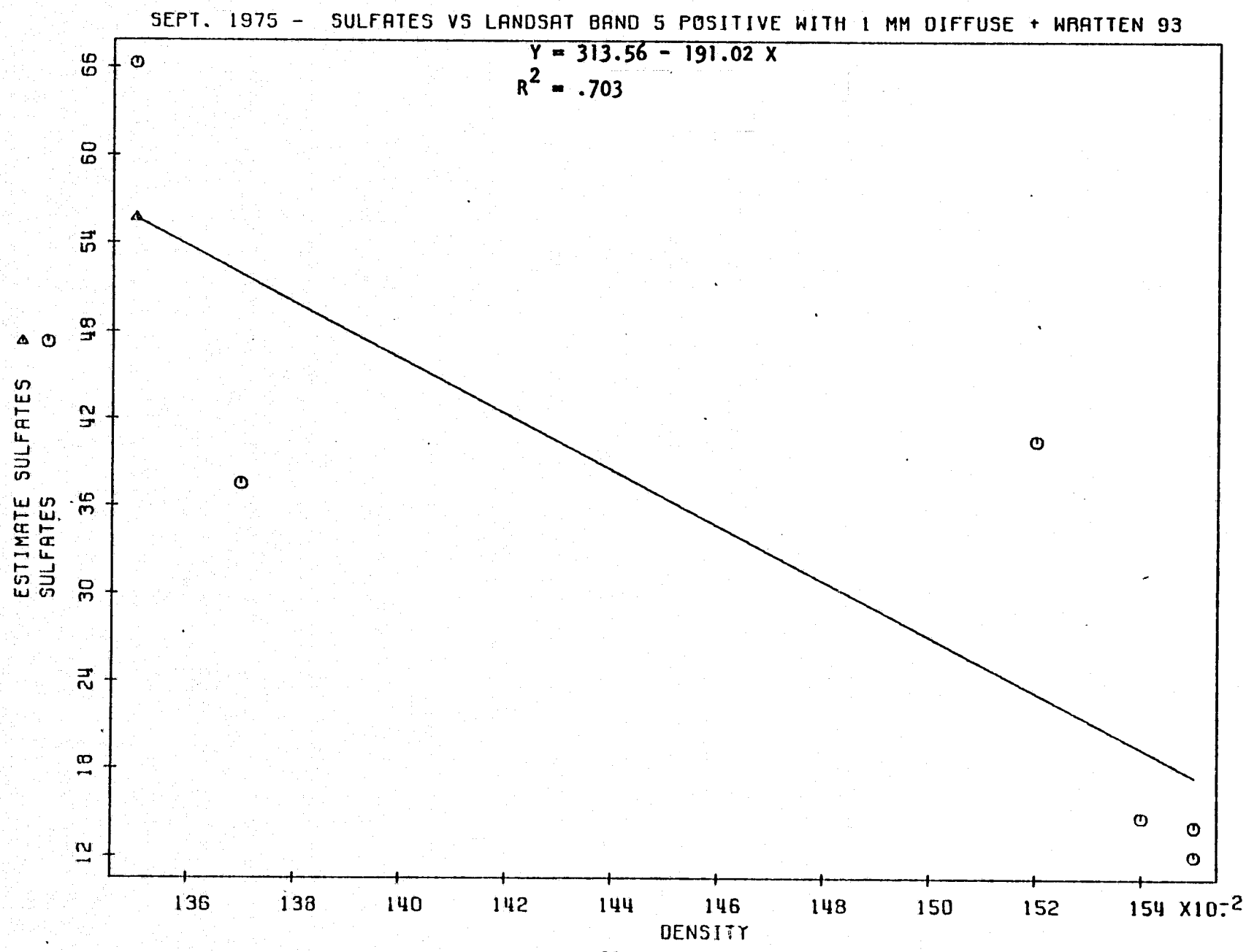
SEPT. 1975 - SULFATES VS LANDSAT BAND 5 POSITIVE WITH 1 MM DIFFUSE + WRATTEN 93
Y = 313.56 - 191.02 X
R2 = .703
ESTIMATE SULFATES
SULFATES
66
60
54
48
42
36
30
24
18
12
136
138
140
142
144
146
148
150
152
154 X10-2
DENSITY

Figure 18

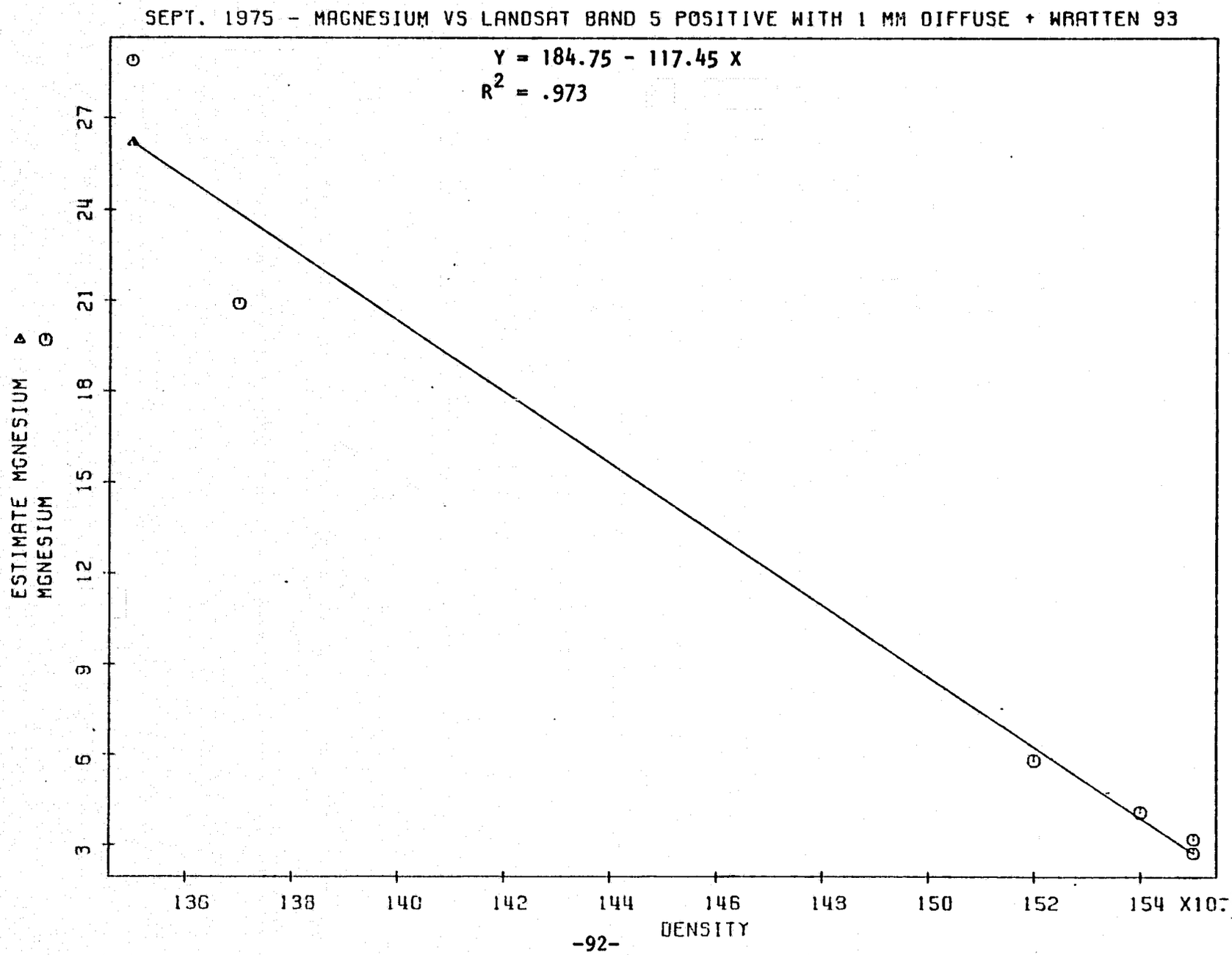
SEPT. 1975 - MAGNESIUM VS LANDSAT BAND 5 POSITIVE WITH 1 MM DIFFUSE + WRATTEN 93
Y = 184.75 - 117.45 X
R2 = .973
ESTIMATE MGNESIUM
MGNESIUM
3
6
9
12
15
18
21
24
27
136
138
140
142
144
146
148
150
152
154 X10-2
DENSITY

Figure 19

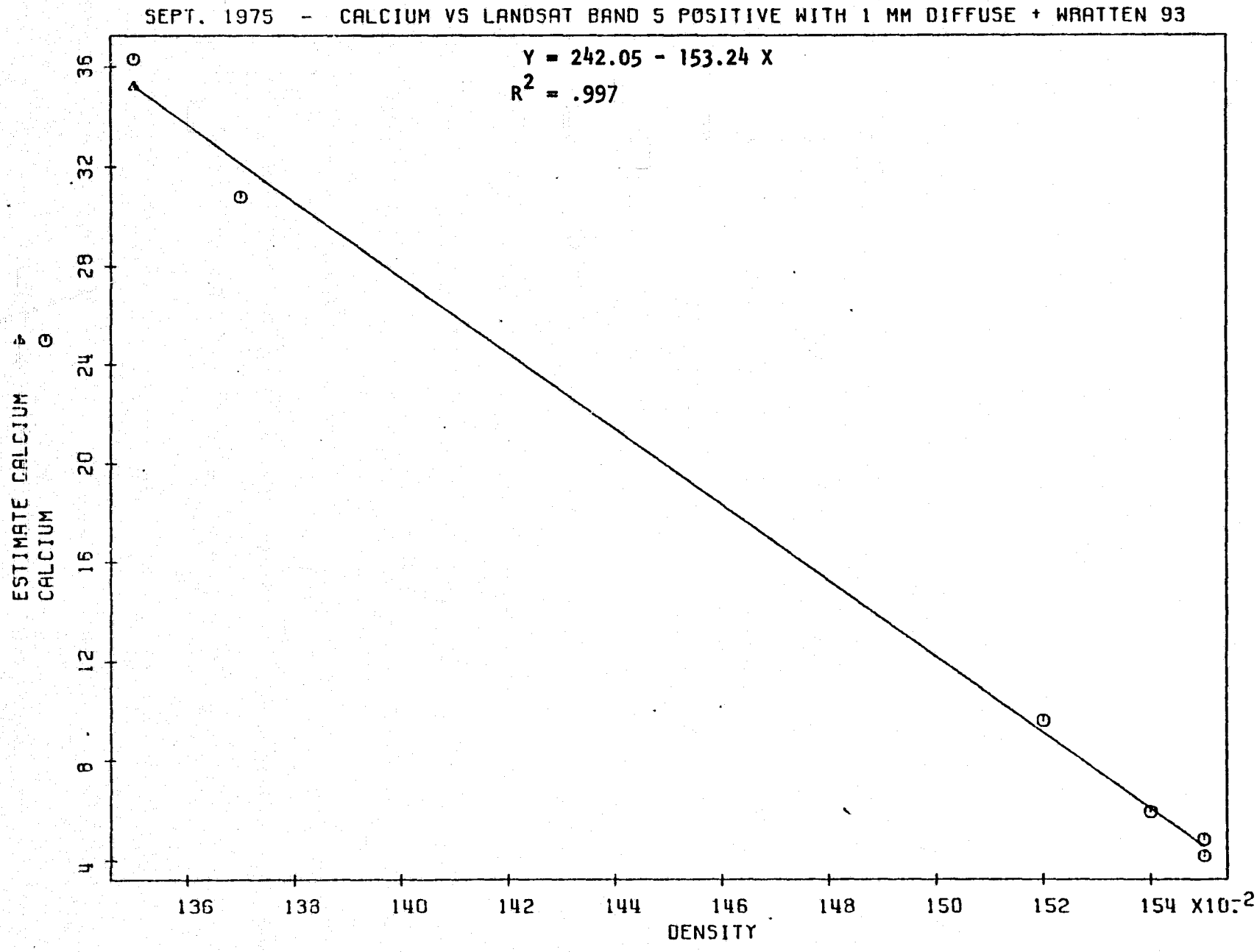
SEPT. 1975 - CALCIUM VS LANDSAT BAND 5 POSITIVE WITH 1 MM DIFFUSE + WRATTEN 93
Y = 242.05 - 153.24 X
R2 = .997
ESTIMATE CALCIUM
CALCIUM
4
8
12
16
20
24
28
32
36
136
138
140
142
144
146
148
150
152
154 X10-2
DENSITY

Figure 20

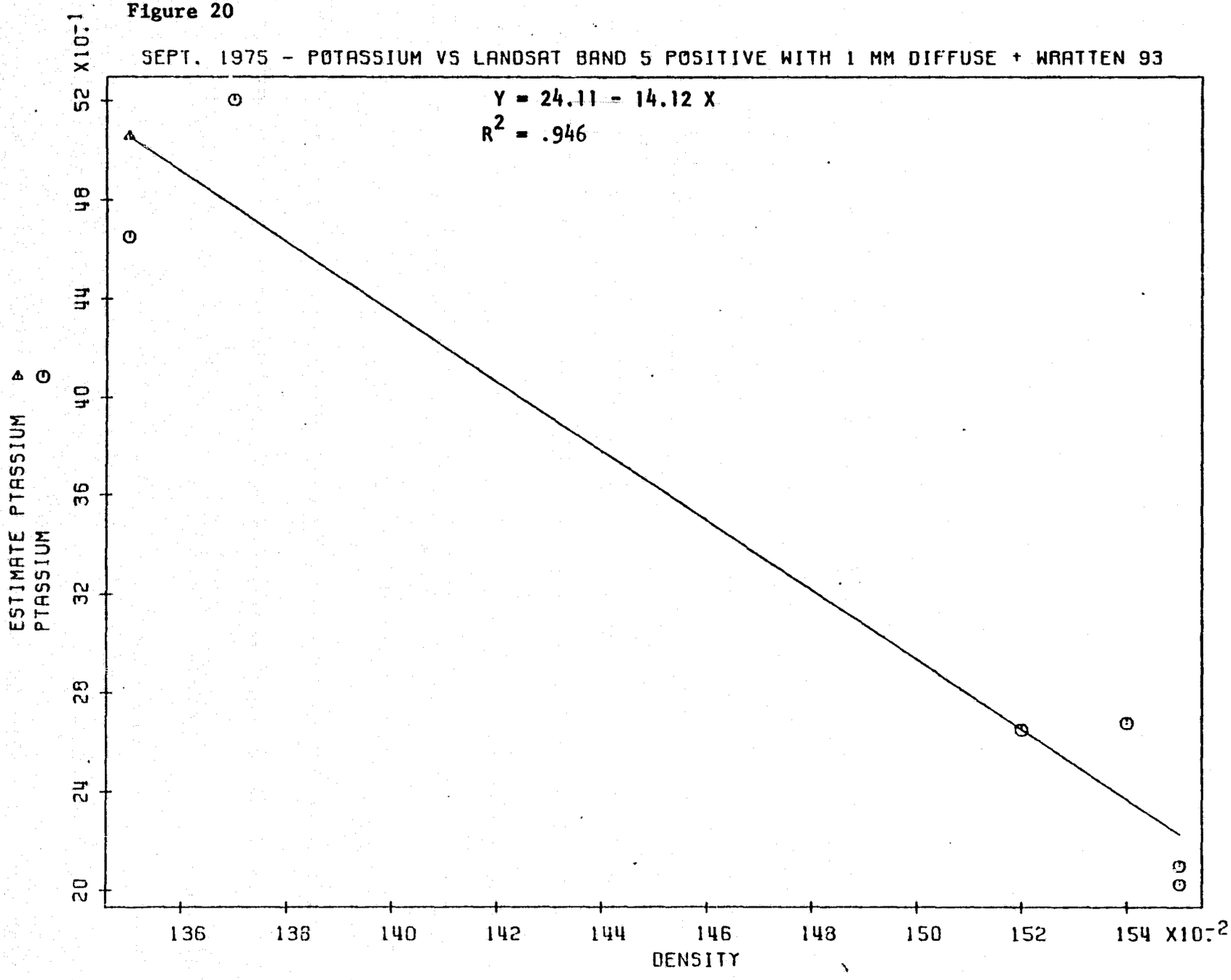
SEPT. 1975 - POTASSIUM VS LANDSAT BAND 5 POSITIVE WITH 1 MM DIFFUSE + WRATTEN 93
Y = 24.11 - 14.12 X
R2 = .946
ESTIMATE PTASSIUM
PTASSIUM
52 X10-1
48
44
40
36
32
28
24
20
136
138
140
142
144
146
148
150
152
154 X10-2
DENSITY

Figure 21

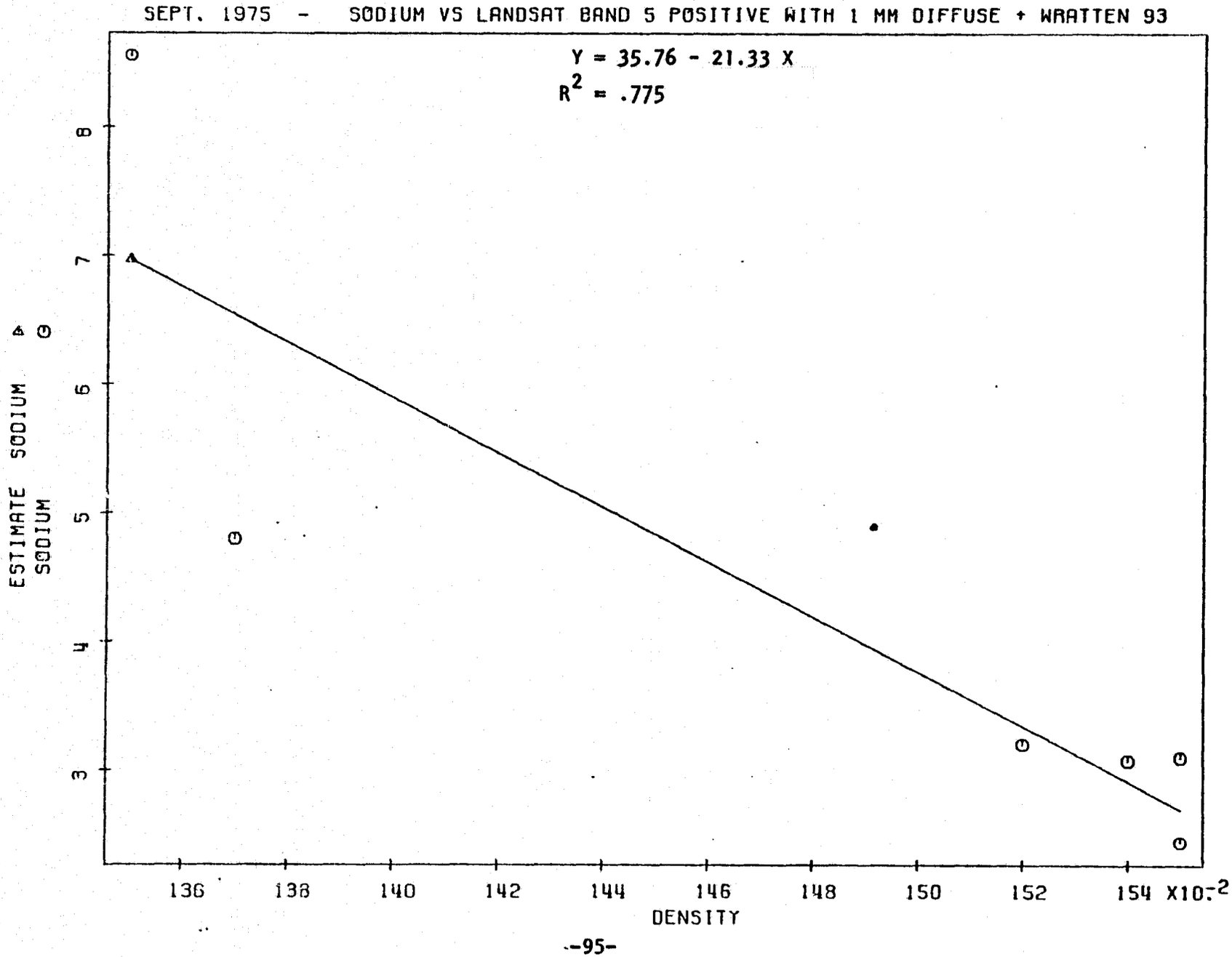
SEPT. 1975 - SODIUM VS LANDSAT BAND 5 POSITIVE WITH 1 MM DIFFUSE + WRATTEN 93
Y = 35.76 - 21.33 X
R2 = .775
ESTIMATE SODIUM
SODIUM
8
7
6
5
4
3
136
138
140
142
144
146
148
150
152
154 X10-2
DENSITY

Figure 22

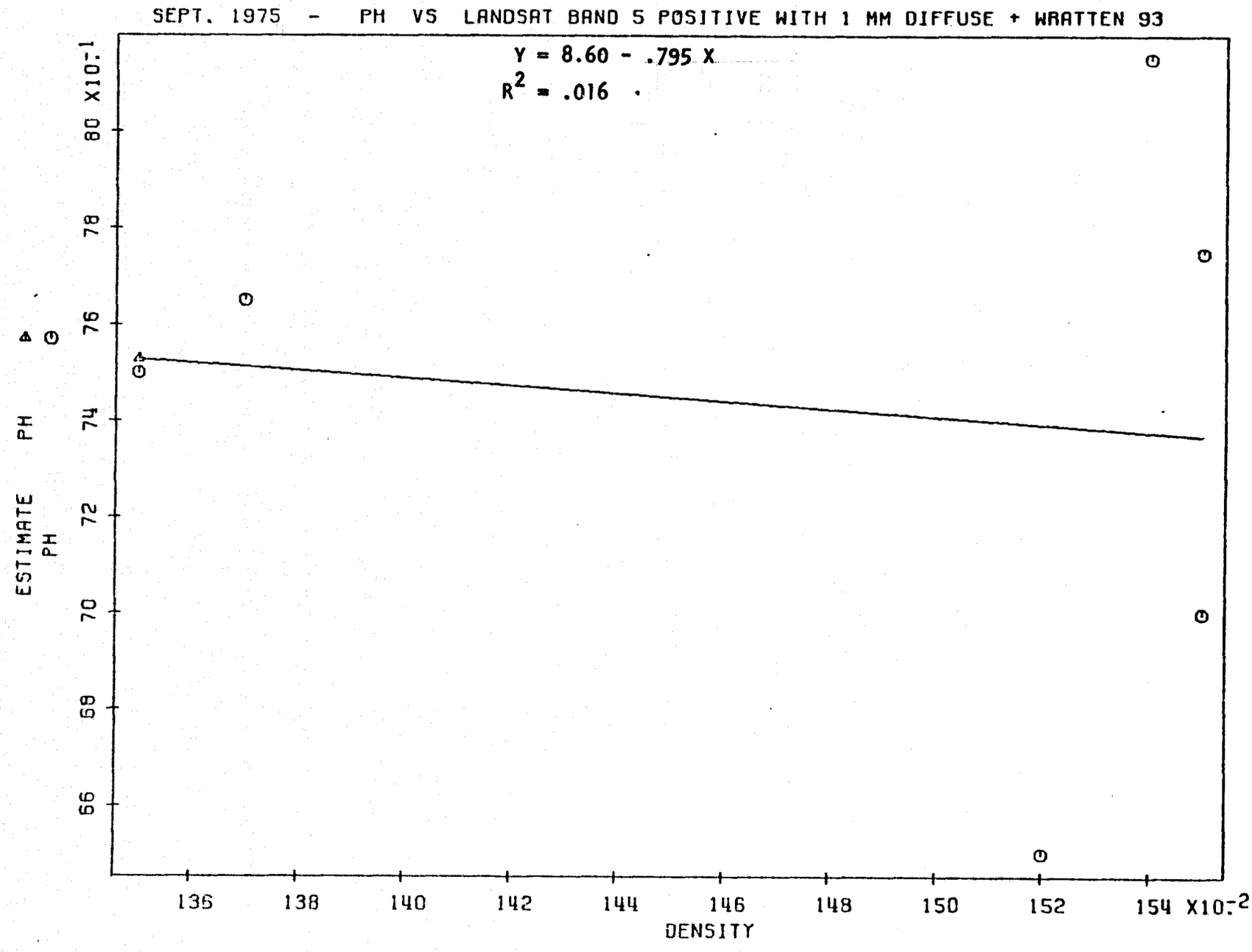
SEPT. 1975 - PH VS LANDSAT BAND 5 POSITIVE WITH 1 MM DIFFUSE + WRATTEN 93
Y = 8.60 - .795 X
R^2 = .016
ESTIMATE PH
80 X10-1
78
76
74
72
70
68
66
136
138
140
142
144
146
148
150
152
154 X10-2
DENSITY

Linear regression analysis shows calcium, magnesium, and specific conductivity (R^2=0.997, 0.973, and 0.971 respectively) to be most highly correlated with densitometric values. Hydrogen ion concentration (pH) still appears to be the least correlated water quality parameter, having an R^2 of only 0.016.

Table 25 shows the percent disturbed ground for each of the study watersheds. Forest openings due to roads, slides, or surface mining activities are included in the disturbed ground component of the watersheds. Figures 23-30 show percent disturbed ground - water quality correlations for April and September water quality data.

Sulfate and magnesium concentrations showed the highest correlations with percent disturbed ground (R^2=0.946, 0.925) of the April water quality figures, while JTU and calcium concentrations correlate best (R^2=0.923, 0.913) in the September figures. Hydrogen ion concentration (pH) continues to show the lowest correlations with R^2 values of 0.195 and 0.044 for April and September, respectively.

Differences in the water quality parameters between April and September samples may be accounted for, in part, by differences in precipitation and resultant flow rates for the time periods. April samples were taken during a period when precipitation rates were above normal. Stream flow from the watersheds was normal or above normal during this time, also.

September samples were taken during the summer after a two month period when virtually no precipitation was recorded on the watersheds. Flow

Table 25. Percentage Disturbance of Study Watersheds

Watershed	% Disturbed Ground
Falling Rock Branch	0.0
Jenny Fork	1.4
Field Branch	4.8
Little Millseat Branch	8.5
Mullins Fork	44.3
Miller Branch	49.2

Figure 23

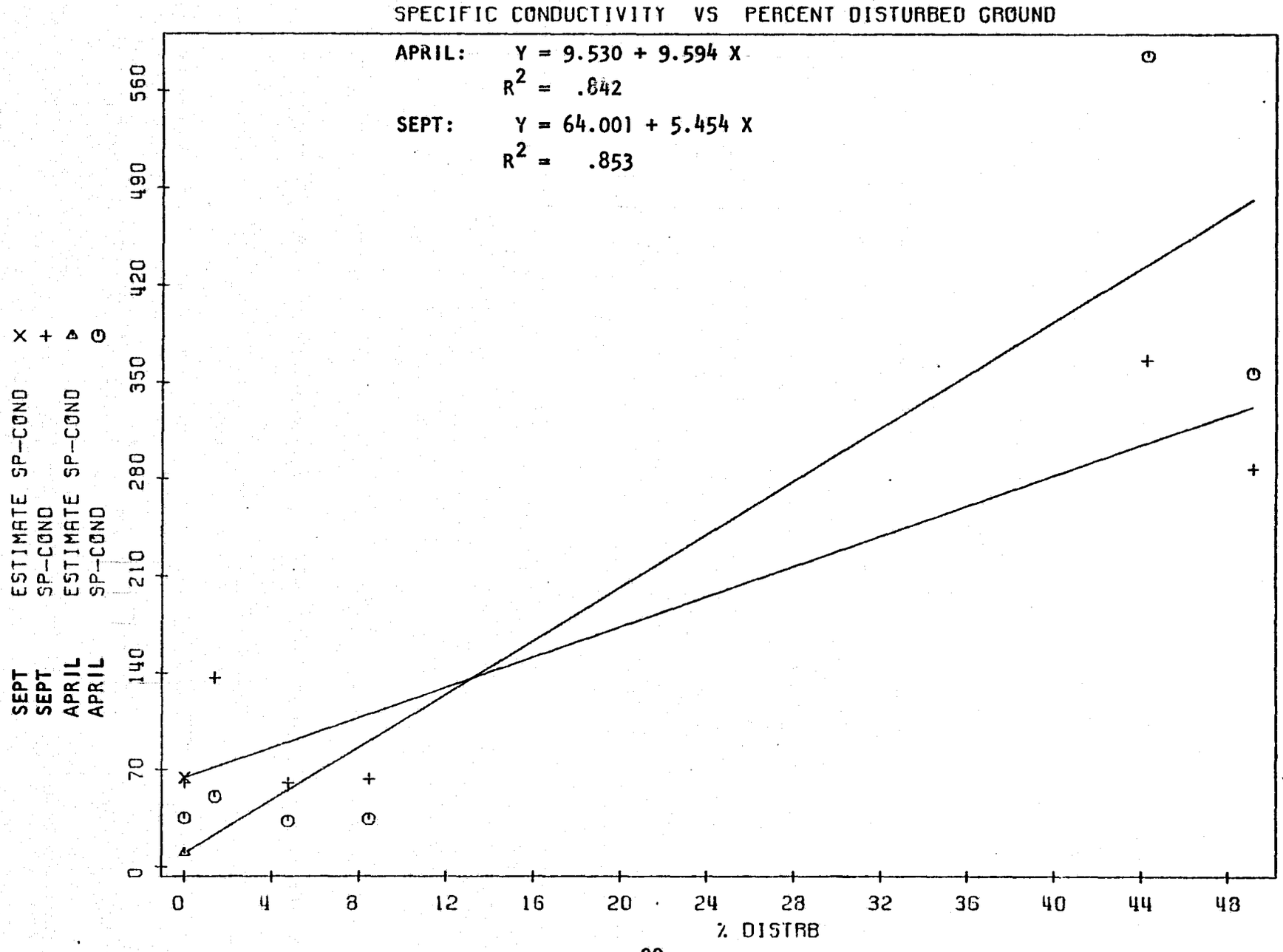
SPECIFIC CONDUCTIVITY VS PERCENT DISTURBED GROUND
APRIL: Y = 9.530 + 9.594 X
R2 = .842
SEPT: Y = 64.001 + 5.454 X
R2 = .853
SEPT ESTIMATE SP-COND X
SEPT SP-COND +
APRIL ESTIMATE SP-COND Δ
APRIL SP-COND ⊖
0
70
140
210
280
350
420
490
560
0
4
8
12
16
20
24
28
32
36
40
44
48
% DISTRB

Figure 24

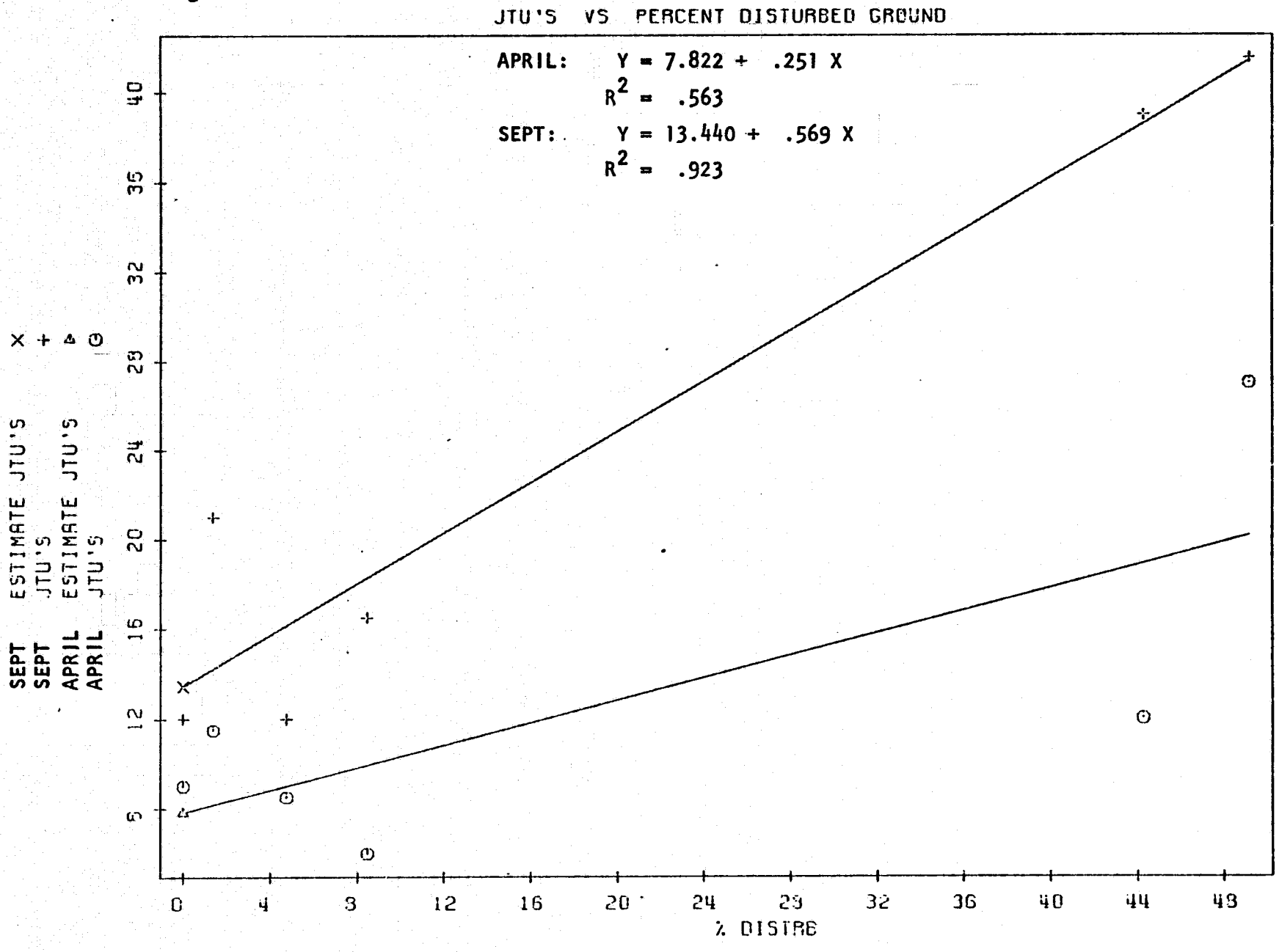
JTU'S VS PERCENT DISTURBED GROUND
APRIL: Y = 7.822 + .251 X
R2 = .563
SEPT: Y = 13.440 + .569 X
R2 = .923
SEPT ESTIMATE JTU'S X
SEPT JTU'S +
APRIL ESTIMATE JTU'S Δ
APRIL JTU'S ⊙
5
12
16
20
24
29
32
35
40
0
4
8
12
16
20
24
29
32
36
40
44
48
% DISTRB

Figure 25

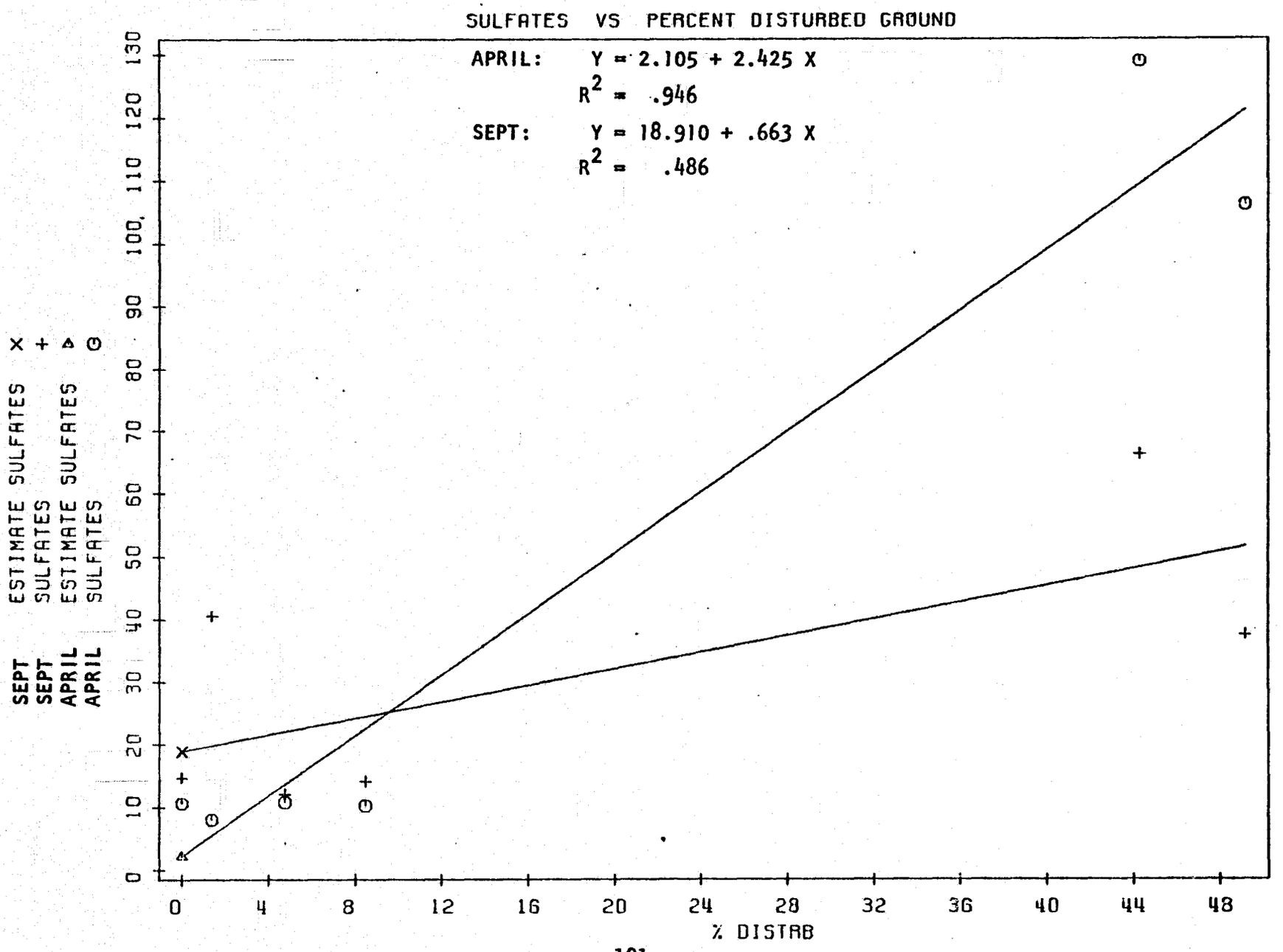
SULFATES VS PERCENT DISTURBED GROUND
APRIL: Y = 2.105 + 2.425 X
R2 = .946
SEPT: Y = 18.910 + .663 X
R2 = .486
SEPT ESTIMATE SULFATES ×
SEPT SULFATES +
APRIL ESTIMATE SULFATES △
APRIL SULFATES ⊙
0 10 20 30 40 50 60 70 80 90 100 110 120 130
0 4 8 12 16 20 24 28 32 36 40 44 48
% DISTRB

Figure 26

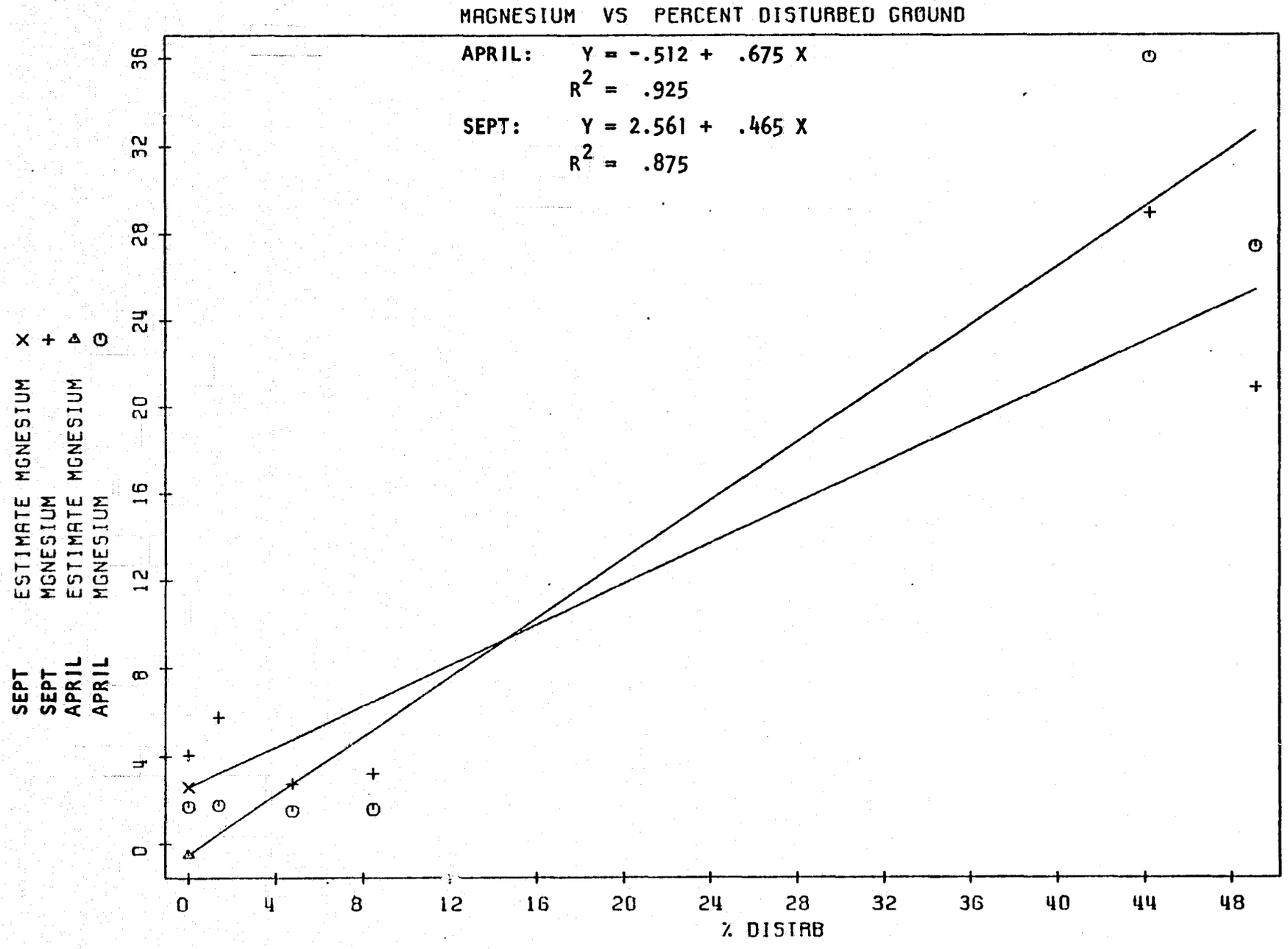
MAGNESIUM VS PERCENT DISTURBED GROUND
APRIL: Y = -.512 + .675 X
R2 = .925
SEPT: Y = 2.561 + .465 X
R2 = .875
SEPT ESTIMATE MGNESIUM X
SEPT MGNESIUM +
APRIL ESTIMATE MGNESIUM Δ
APRIL MGNESIUM ⊙
0 4 8 12 16 20 24 28 32 36
0 4 8 12 16 20 24 28 32 36 40 44 48
% DISTRB

Figure 27

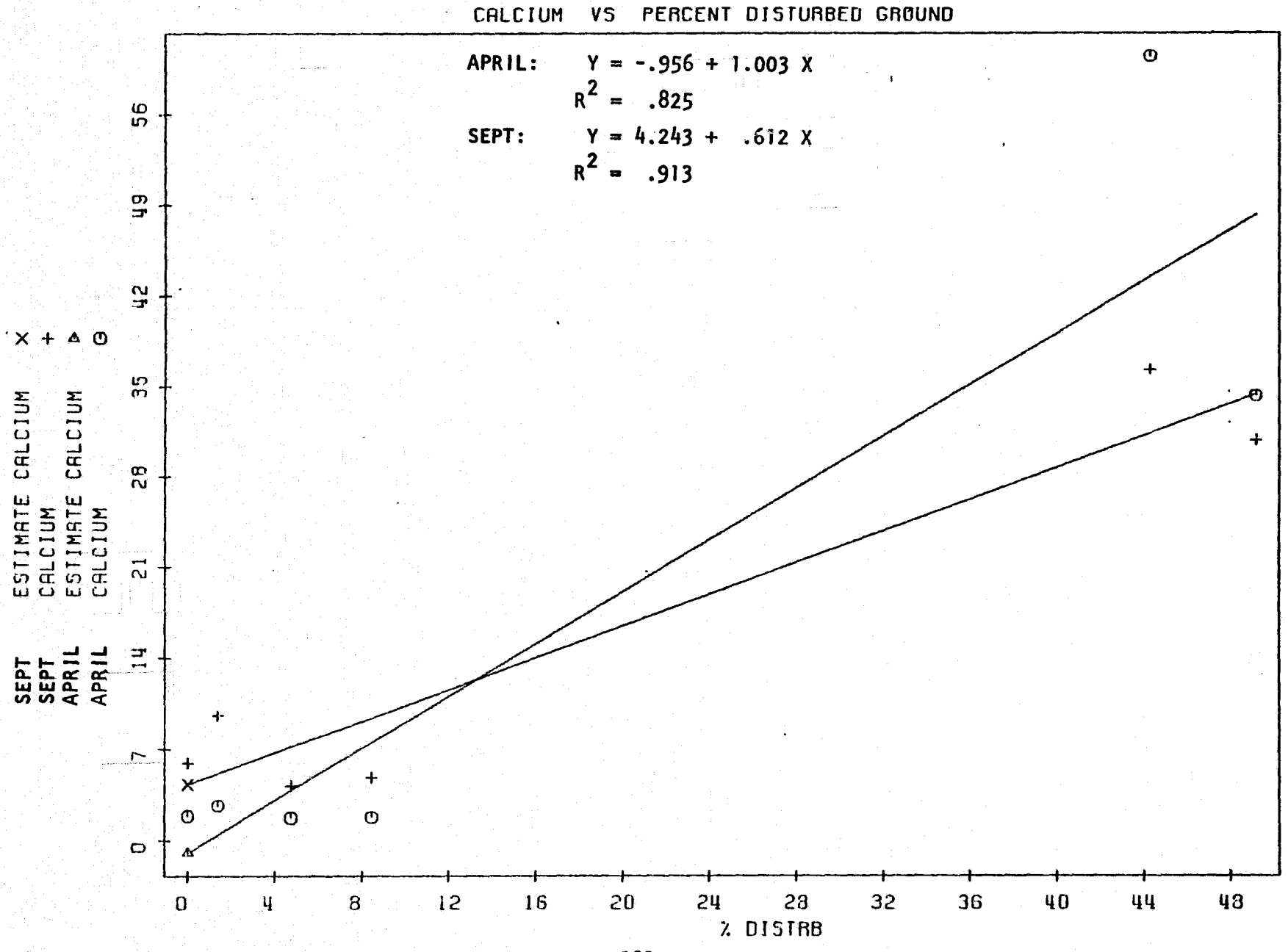
CALCIUM VS PERCENT DISTURBED GROUND
APRIL: Y = -.956 + 1.003 X
R2 = .825
SEPT: Y = 4.243 + .612 X
R2 = .913
X + Δ ⊙
SEPT ESTIMATE CALCIUM
SEPT CALCIUM
APRIL ESTIMATE CALCIUM
APRIL CALCIUM
0 7 14 21 28 35 42 49 56
0 4 8 12 16 20 24 28 32 36 40 44 48
% DISTRB

Figure 28

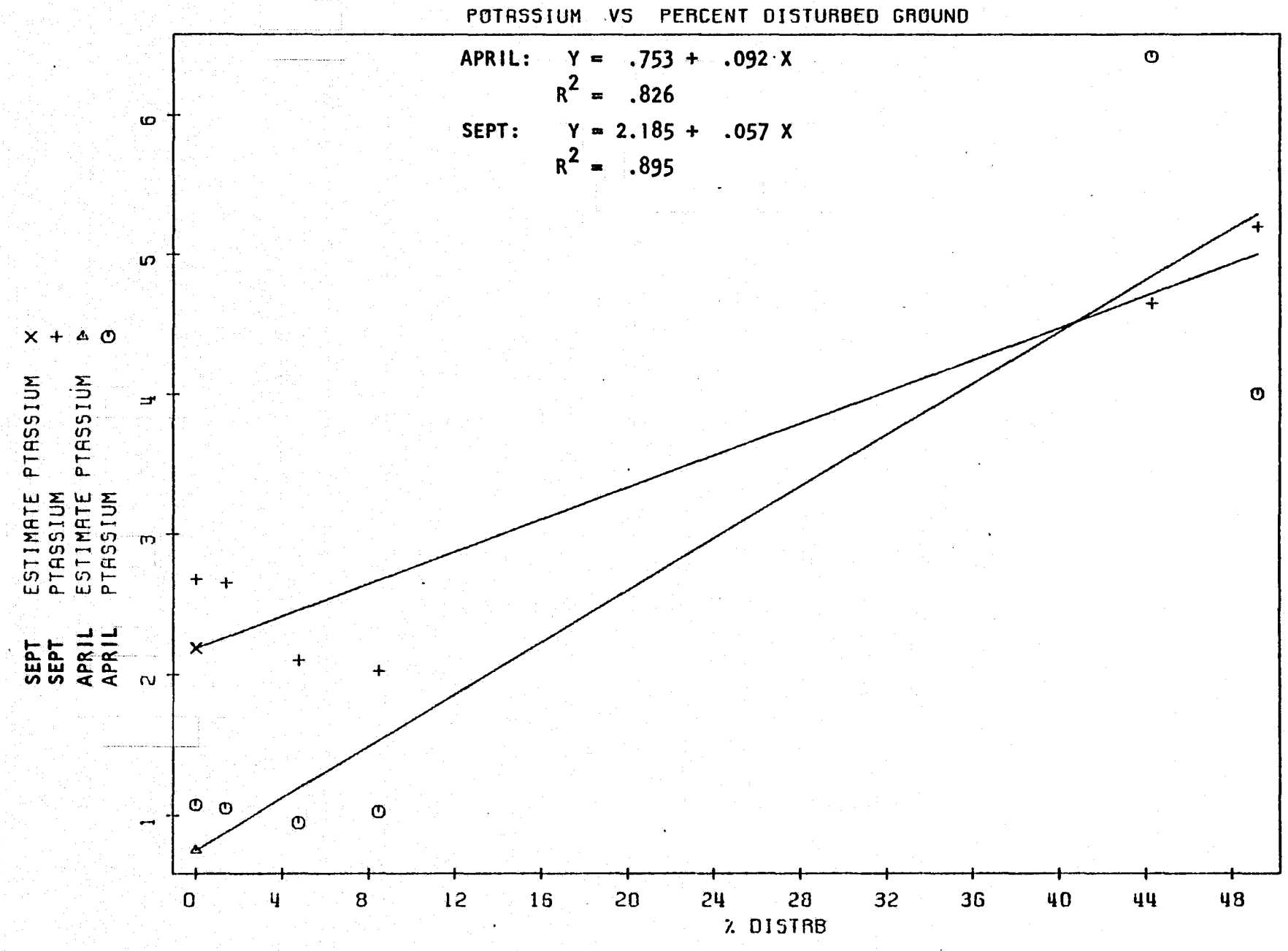
POTASSIUM VS PERCENT DISTURBED GROUND
APRIL: Y = .753 + .092 X
R2 = .826
SEPT: Y = 2.185 + .057 X
R2 = .895
SEPT ESTIMATE PTASSIUM X
SEPT PTASSIUM +
APRIL ESTIMATE PTASSIUM Δ
APRIL PTASSIUM O
1
2
3
4
5
6
0
4
8
12
16
20
24
28
32
36
40
44
48
% DISTRB

Figure 29

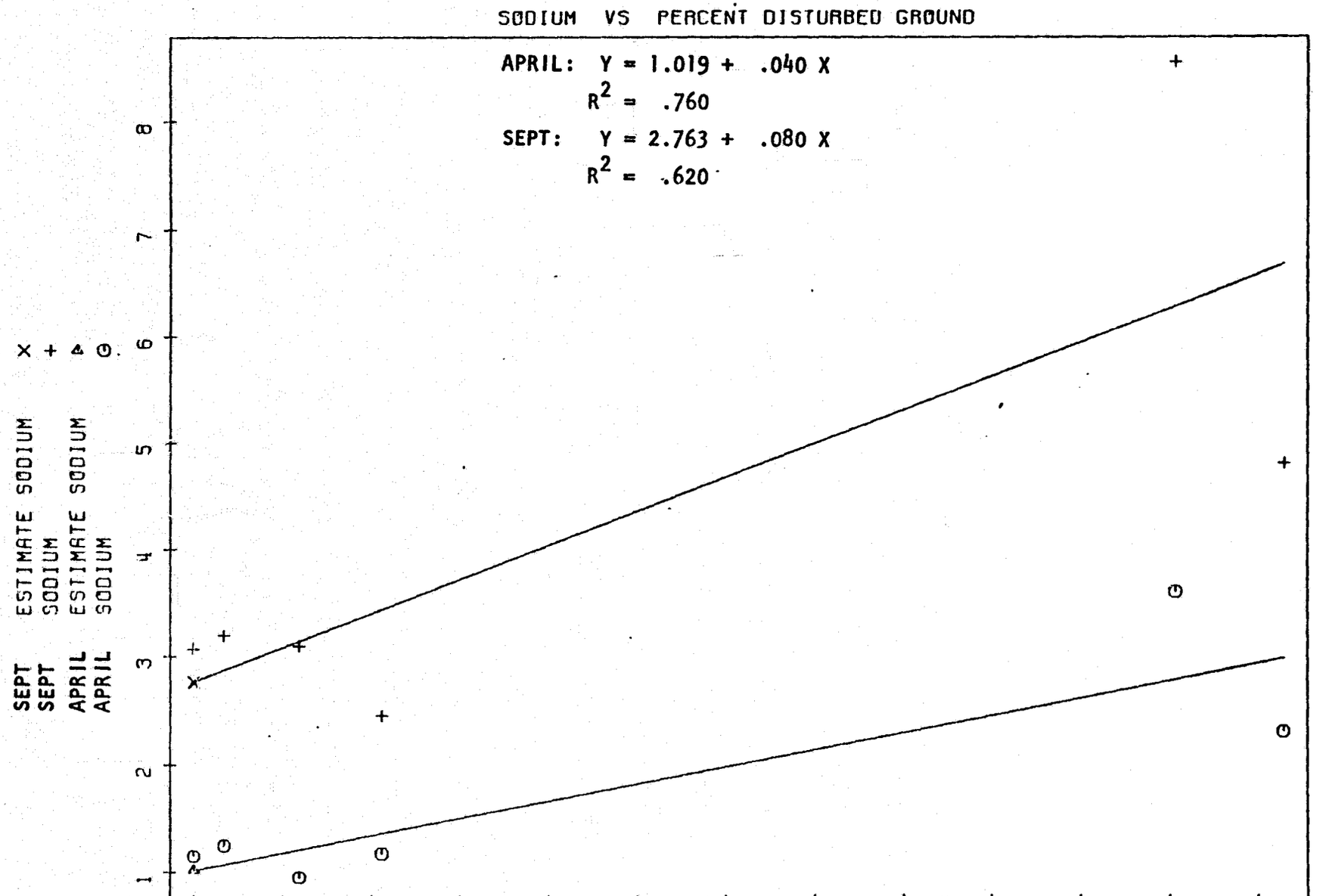
SODIUM VS PERCENT DISTURBED GROUND
APRIL: Y = 1.019 + .040 X
R2 = .760
SEPT: Y = 2.763 + .080 X
R2 = .620
SEPT ESTIMATE SODIUM
SEPT SODIUM
APRIL ESTIMATE SODIUM
APRIL SODIUM
1
2
3
4
5
6
7
8
0
4
8
12
16
20
24
28
32
36
40
44
48
% DISTRB

Figure 30

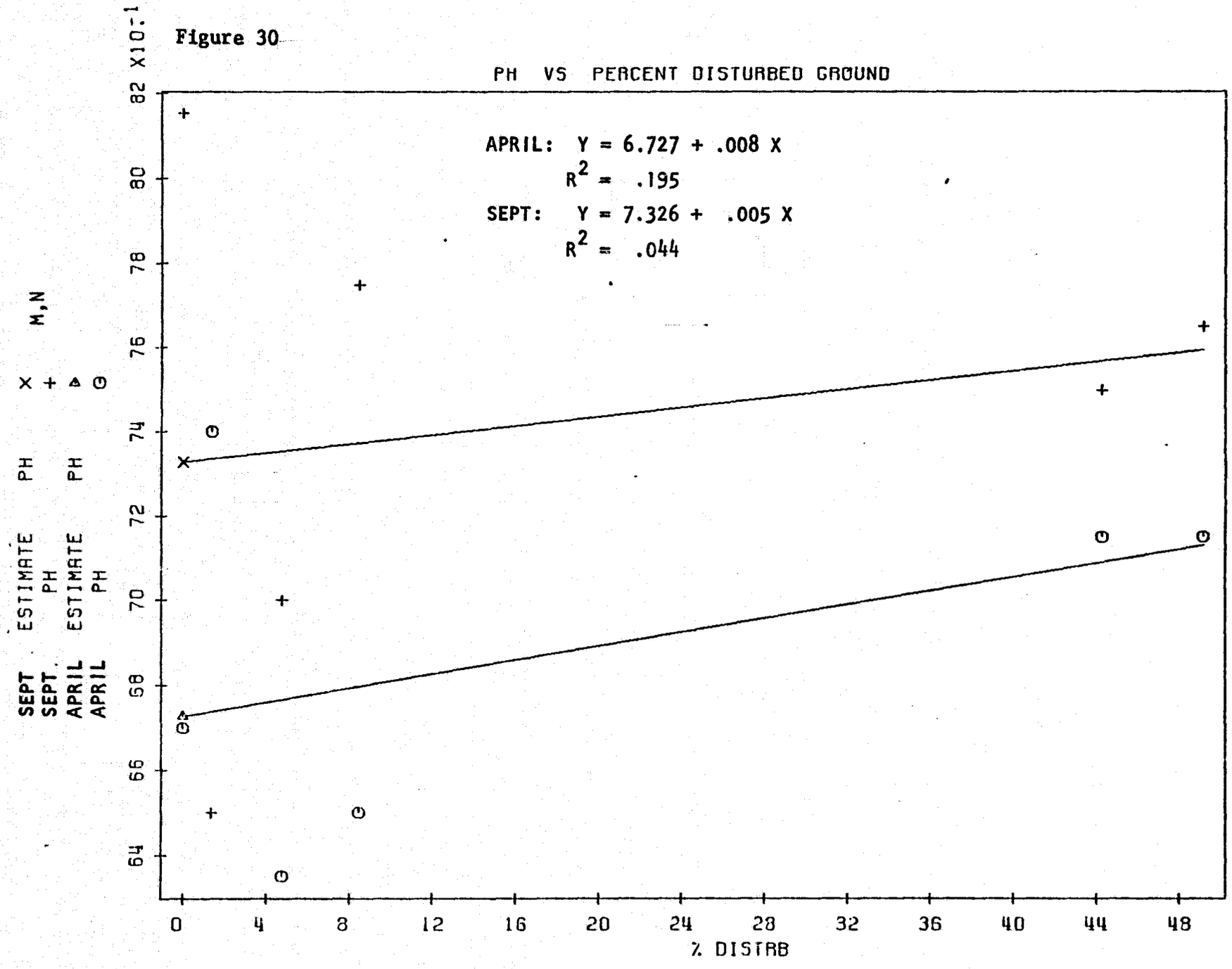
PH VS PERCENT DISTURBED GROUND
APRIL: Y = 6.727 + .008 X
R2 = .195
SEPT: Y = 7.326 + .005 X
R2 = .044
82 X10-1
80
78
76
74
72
70
68
66
64
0
4
8
12
16
20
24
28
32
36
40
44
48
% DISTRB
M,N
X + Δ ⊖
SEPT ESTIMATE PH
SEPT PH
APRIL ESTIMATE PH
APRIL PH

over the weirs for each watershed was minimal and in most cases nonexistent at this time.

Higher September values for the wholly forested watersheds may be due to low flow conditions which might have prevented the dilution of minerals present in the stream. Higher concentrations of these minerals would then result. Generally lower September values for the partially surface mined watersheds indicate that minerals were not being transported from the unstabilized mined areas into the stream, as was probably occurring during the rainy spring season.

The apparent high correlation between some of the parameters and densitometric values and disturbed ground percentages may be misleading. The various water quality parameters studied are quite highly correlated to each other. Thus, when one parameter is highly correlated, most of the others will appear similarly correlated.

A second factor that affects the reliability of correlation results is the lack of data in the middle ranges of the variables studied. With no mid-range data to include in the analyses, the relationship between any water quality parameter and densitometric or disturbed area values cannot be qualified. Correlations portrayed are linear regression equations of the relationships. Whether or not the linear regression equations are valid portrayals of these relationships is open to question.

Similarly, if a wide range of land uses or land cover had been included in the project study area, correlations might have been extendable to a

wider area within the Cumberland Plateau region of eastern Kentucky. Correlations devised from this study cannot presently be confidently extended to other areas.

Densitometry-Fertilization

Discernment of effects of the late April fertilization of Field Branch was not possible with densitometric analysis of Landsat imagery using techniques employed in this study. The size of this watershed - 41 hectares - made discrimination highly improbable, and imprecise placement of Landsat transparencies under the densitometer further limited analysis efforts.

Densitometric data of color infrared imagery from April and September, 1975 aircraft overflights was also analyzed for possible correlation with fertilization effects. The only available imagery of pre- and post-fertilization conditions was the April and September aircraft overflight imagery. Since the April multispectral coverage was incomplete, correlation efforts were limited to the color infrared imagery from these overflights.

April and September densitometric values of the wholly forested study watersheds were compared. The percent change of Field Branch values was compared to the percent change of the other three forested study watersheds taken as a composite. Initial results indicated that Field Branch values changed less from April to September than did the other watersheds. Examination of available aperture-filter combinations revealed Field Branch change ranged from 13-51 percent less than the other three watersheds.

When compared against just two of the other forested watersheds, Little Millseat Branch and Falling Rock Branch, differences ranged from 20-66 percent. Jenny Fork appeared to change more than Field Branch, but significantly less than Little Millseat Branch or Falling Rock Branch. Reasons for these differences were not readily apparent.

Initial results indicated potential for densitometric discrimination of fertilization effects. Further analysis was required to determine if differences were caused by fertilization effects or by basic differences in appearance of the watersheds on the pre-fertilization April imagery. Differences in densitometric data from the April imagery appeared to have caused the change differences among the watersheds. Using the green spectral response filter, which produced the greatest apparent differences, Field Branch April values averaged 0.79 and September values 1.66. Comparable averages for the composite of the other three watersheds were 0.65 for April and 1.68 for September. Other aperture-filter combinations were analyzed, with similar results.

Differences between pre- and post-fertilization densitometric values appeared to be due to pre-fertilization differences among watersheds and not to changes caused by fertilization. Detection of forest fertilization effects through densitometric analysis of pre- and post-application imagery does not appear to be feasible, based on the results of our study. Whether analysis of imagery taken at roughly the same time of year both before and after fertilization would offer better discrimination potential is open to conjecture.

Cost-Effective Analysis

Manual Densitometry-Aerial Photography

The utility of any analysis system must eventually consider relative costs associated with the levels of discrimination potential. The densitometric sampling system utilized with aircraft imagery was to secure one density reading per acre for each film-aperture-filter combination. No attempt was made to determine whether more or less intensive density point sampling would have provided significantly different discrimination potential. To standardize the analysis, a cost per acre will be determined for the best systems for multidate and single date sampling.

The system that best identified the eight recognized land cover categories utilized the density signatures obtained from the spring and fall color infrared transparencies when all four filters were utilized on the TD528 with the one (1) mm diffuse aperture. Approximately 2000 density values of this type can be registered and transferred to a computer coding sheet per day.

Since two dates and all four filters are required, we can only take 250 density signatures per date. The sampling intensity of one reading per acre for each date-aperture-filter combination thus allows an investigator to secure 250 acres of density signatures per man day or 31.25 acres per hour. With an hourly rate of $6.00 per hour for the interpreter the resultant cost of data point recording is equal to 19.2 cents per acre.

Approximately 100 data point cards can be transferred from computer coding forms to cards per hour. Key punch costs are $5.00 per hour for an effective rate of 5 cents per acre. Computer programming, analysis and interpretation amounts to an additional 5 cents per acre.

The 1:24,000 color infrared photography used in this study had a 9" x 9" format. Each image thus covered 7438 acres. The useable effective area was a 6" x 6" square in the center of each photo which included an area of 3306 acres. The imagery was taken to average 60 percent forward overlap and 30 percent sidelap. At a cost of $10.00 per frame with overlap in effective area, imagery costs amount to $28.00 per 3306 acres or 0.8 cents per acre. Additionally one hour is allowed to trim and attach transparencies to frames and ready forms for recording at a rate of $6.00 per hour or 0.2 cents per acre. The above results in a cost of 30.2 cents per acre to achieve a land classification system that gave an estimated overall error rate of 5.9 percent when considering the eight land cover groups.

The best April predictive system utilized only color infrared imagery taken with the one (1) mm diffuse aperture utilizing the TD528. With only one season of photography required, the sampling area was increased to 500 acres per day. This reduced the cost of data point recording to 9.6 cents per acre. Data transfer costs drop to 3 cents per acre and computer analysis costs remain constant at 5 cents per acre. Imagery costs are reduced to half or 0.4 cent per acre and preparation to 0.1 cent per acre. This analysis resulted in a cost per acre of 18.1 cents for a system that gave an estimated error rate of 11.9 percent.

The best September system utilized only color infrared imagery also but required the utilization of two different apertures and two filters in combination with each aperture. The requirement of utilizing two apertures reduces the number of data points recorded per day to 1500. This results in a reduction of acres sampled to 375 per day. Data point transfer costs increased to 12.8 cents per acre. Data transfer and computer analysis costs remain constant at 8 cents per acre. Imagery costs and preparation also remain at 0.5 cent per acre. This system thus resulted in a cost of 21.3 cents per acre for an estimated 12.7 percent error rate for the eight land cover classifications.

Manual Densitometer - Satellite Imagery

The study watersheds were either categorized as forested or partially surface mined for satellite imagery classification. One (1) mm aperture density signatures were secured from each imagery band from each watershed for a single date. Such signatures would differentiate the two watershed groups if the image was of satisfactory quality and sun angles were high enough to allow the greater reflectance of the surface mined areas to appear on the imagery. Single band density signatures were also capable of identifying such broad vegetative categories. Basically, such analysis is possible if a difference can be seen on the imagery. If visual contrasts are not apparent, density signatures are not likely to be discriminatory. Cost-effectiveness determinations are not meaningful for spot densitometer-satellite imagery sampling systems with this type of classification.

Color Additive Interpretation

Cost-effective analysis for color additive viewing, whether it be aircraft or satellite imagery, is not feasible. Such analysis is inexpensive and very effective; however, effectiveness is not quantifiable since the interpreter judges what looks best to him. Some insight might be gained by inspecting the results outlined in the section on color additive viewing and applying an individual's needs to the following cost data.

Color additive analysis requires that you have a viewer capable of accepting multispectral photography and satellite imagery chips. Such an instrument will cost approximately $10,000. Multispectral photography cost will vary according to scale and availability. Satellite imagery chips presently cost $8 per film positive and $10 per film negative for 1:3,369,000 scale transparencies. Film positive and negative transparencies at the scale of 1:1,000,000 scale cost $10 each.

If the desired combinations are known and the correct chips are in the holder, it will require approximately 15 minutes to generate the desired color composite. The time required to change chips and re-register images for a new rendition will vary from 20 to 30 minutes.

RECOMMENDATIONS

Uses

Satellite imagery

Remote sensing has potential for providing effective survey techniques to monitor land use and land use change at reasonable cost. Of the techniques and instrumentation evaluated in this study, color additive viewing of Landsat multispectral transparencies appears to offer the greatest potential for use by state and federal agencies. Use of a color additive viewer with satellite transparencies is recommended as a possible tool for agencies who need long term land use information in the categories described below.

Various combinations of Landsat bands, transparencies, filters, and dates of imaging can offer significant utility in natural resource monitoring and evaluation efforts. Surface mining activity and changes over time can be monitored quite effectively through color additive analysis of repetitive satellite coverage. Forest fire mapping can also be accomplished through analysis of repetitive Landsat imagery coverage. Other large scale land uses and/or land use changes, such as large area logging or farming, are similarly distinguishable through color additive analysis of Landsat transparencies. Geologic mapping is also facilitated by the use of color enhanced satellite imagery to note land forms and other geologic structures previously unrecognized.

The objection to use of Landsat imagery and imagery products most frequently expressed by persons in state and federal agencies queried as part

of this project was lag time - often 6 weeks or longer - between date of imaging and date of imagery availability to users. To the mine reclamation agency that requires efficient and rapid detection of illegal surface mining activity, lag time associated with satellite imagery eliminates its use from consideration. To the agency concerned with enforcement of water quality standards, satellite imagery may aid in proving cases against polluters but it will not provide information useful to timely elimination of a pollution problem. Increased use of Landsat imagery and imagery products can and will occur in Kentucky, but near real time availability must be achieved if full potential is to be realized.

Objections to imagery scale and resolution were also voiced by potential users of Landsat imagery and imagery products. Many persons were impressed with Landsat imagery clarity until scale of this imagery was mentioned. Scales of 1:3,369,000 and 1:1,000,000 are too small for many potential imagery users to efficiently or realistically use, and enlargement of this imagery produces clarity and resolution problems.

Increased imagery resolution, which will become available with the successful orbiting of Landsat C, may remove some objections. Objections to satellite imagery resolution and scale, raised by persons unfamiliar with the information capabilities of satellite imagery systems, may be eliminated by increased publicity and gradual infusion of satellite technology into the user community.

Quantification of observed land uses or land use changes is not readily achieved with Landsat transparencies, since even large land areas appear

relatively small. Even very small image measurement errors translate into large land area errors when using satellite imagery. Some feeling for the magnitude of this problem may be gained with the realization that a circle one millimeter in diameter on 1:1,000,000 imagery encompasses a land area of 78 hectares (194 acres).

Densitometry of satellite imagery, utilizing manual spot densitometers which are not equipped to allow precise referencing and repositioning of imagery, appears to have very limited utility. Slight repositioning errors can cause significant changes in density readings which may significantly influence consequent data correlations and interpretations. Densitometer aperture sizes would have to be significantly smaller than one millimeter, even with precision referencing and repositioning capacities, for useful densitometry of satellite imagery.

Aircraft Imagery

Color additive viewing of aircraft multispectral imagery appears to have some utility in land use discrimination. Multidate color additive analysis of aircraft multispectral imagery could have significant potential for land use change classification. Change notation potential is dependent on color additive viewer capacity for scale adjustment, as imagery from successive overflights is likely to differ significantly in scale.

Color additive analysis of multispectral aircraft imagery also has potential utility for vegetation discrimination. Color enhancement of single date-multiband combinations can produce composites in which distinctions among species of species groups are highlighted. Plant communities would

probably be classified more successfully through multidate-single band or multidate-multiband color composite generation. Multidate composite generation would incorporate differences in phenological development among plant communities into resulting composites. Plant communities having changed at different rates should likely appear different in multidate aircraft composites, just as large areas of land use change appear different in multidate composites of satellite imagery.

Color additive analysis of multidate aircraft multispectral imagery may have greater vegetation discrimination potential than either single date color composite generation or single date color infrared imagery. Although equipment limitations prevented multidate color additive analysis of aircraft multispectral imagery in this study, published work of other researchers indicate that multidate analyses, which allow incorporation of temporal change, generally yield better classifications than single date analyses.

Comparison of single date color enhancement of aircraft multispectral imagery to single date color infrared imagery, as to vegetation discrimination potential, does not readily yield definitive answers. Color infrared imagery utility for vegetation surveys has been clearly established. Similar utility of multispectral imagery has not been as definitively established.

Selection of proper imagery to use in a given situation should take into account costs of acquisition and use. Costs associated with color imagery processing are higher than similar costs with black and white imagery.

Effective area per film image is higher with normal 9" x 9" format color infrared imagery than with four band multispectral imagery at the same scale. More flight lines and images per flight line will be necessary to provide equivalent four band multispectral coverage of a given area than would be required with conventional 9" x 9" imagery. Utility of resultant imagery and imagery products and cost per unit should be considered in any imagery acquisition decision.

Results indicate that values derived from manual spot densitometry of multitemporal 1:24,000 color infrared aircraft imagery can classify, with a good degree of accuracy, areas within the Cumberland Plateau of eastern Kentucky as small as one hectare into one of the eight ground cover types defined in this study. When differentiation between Undisturbed and Disturbed Forest areas is the sole criterion of interest, classification results are highly accurate if based upon imagery taken during foliated ground cover conditions.

Densitometry of multi-seasonal imagery leads to considerably better classification results than similar analysis of single date imagery for the eight project cover types. Transparencies from prefoliated conditions provide better separation of conifers and hardwoods than those from foliated conditions. Evidence also indicates the one millimeter aperture to be the best of the apertures available to project investigators for classification of the most specific interpretation level.

Rugged topography makes field surveys difficult and time-consuming. Analysis methodology described herein may prove helpful in monitoring reclamation

of mined areas and forest damage due to mining, logging, fire, and other potentially destructive events.

BIBLIOGRAPHY

Baumgardner, M.F. and J.A. Henderson, Jr. 1973. Mapping Soils, Crops and Rangelands by Machine Analysis of Multi-Temporal ERTS-1 Data. Laboratory for Applications of Remote Sensing Information Note 121173, Purdue University.

Braun, E.L. 1972. Deciduous Forests of North America. Hafner Publishing Company, New York, N.Y.

Cipra, J.E., P.H. Swain, J.H. Gill, M.F. Baumgardner and S.J. Kristof. 1972. Definition of Spectrally Separable Classes for Soil Survey Research. Laboratory for Applications of Remote Sensing Print 100372, Purdue University.

Coggeshall, M.E. and R.M. Hoffer. 1973. Basic Forest Cover Mapping using Digitized Remote Sensor Data and ADP Techniques. Laboratory for Applications of Remote Sensing Information Note 030573, Purdue University.

Dixon, W.J. 1975. BMDP Biomedical Computer Programs. University of California Press, Los Angeles. pp. 411-414.

Driscoll, R.S., J.N. Reppert and R.C. Heller. 1974. Microdensitometry to Identify Plant Communities and Components on Color Infrared Aerial Photos. Journal of Range Management 27:66-70.

Graves, D.H. and M.C. Hammetter. 1975. Densitometer and Color Additive Viewing of Remotely Sensed Imagery. In Proc., 1975 Winter Meeting - Kentucky-Tennessee Section, Society of American Foresters, Lexington, Kentucky.

Hutchins, R.B., R.L. Blevins, J.D. Hill and E.H. White. 1975. The Influence of Soils and Microclimate on Vegetation of Forested Slopes in Eastern Kentucky. Soil Science 121(4):234-240.

Jennrich, R.I. 1976. Stepwise Discriminant Analysis. In Statistical Methods for Digital Computers. ed., Enslein, K., A. Ralston and H.S. Wilf, Wiley, New York, N.Y.

Jones, A.D. 1976. Photographic Data Extraction from Landsat Images. Photogrammetric Engineering and Remote Sensing. 42(11):1423-1426.

Lachenbruch, P.A. 1965. Estimation of Error Rates in Discriminant Analysis. Ph.D. Dissertation (unpublished) University of California, Los Angeles.

Lachenbruch, P.A. 1968. On Expected Probabilities of Misclassification in Discriminant Analysis, Necessary Sample Size, and a Relation with the Multiple Correlation Coefficient. Biometrics 24:823-834.

Lachenbruch, P.A. and M.R. Mickey. 1968. Estimation of Error Rates in Discriminant Analysis. Technometrics 10:1-11.

BIBLIOGRAPHY (cont)

Lawrence, R.D. and J.H. Herzog. 1975. Geology and Forestry Classification from ERTS-1 Digital Data. Photogrammetric Engineering and Remote Sensing 41(10):1241-1251.

Nichols, J.D., ed. 1974. ERTS-1 Data as an Aid to Wildland Resource Management in Northern California. Series 16, Issue 62. Spaces Sciences Laboratory, University of California, Berkeley. pp. 55-63.

Rao, C.R. 1972. Linear Statistical Inference and Its Applications. Wiley, New York, N.Y. pp. 574-582.

Siegal, B.S. and M.J. Abrams. 1976. Geologic Mapping Using Landsat Data. Photogrammetric Engineering and Remote Sensing 42(3):325-337.

Steiner, D. 1970. Time Dimension for Crop Surveys from Space. Photogrammetric Engineering 36:187-194.

Steiner, D. and H. Maurer. 1969. The Use of Stereo Height as a Discriminating Variable for Crop Classification on Aerial Photographs. Photogrammetria 24:223-241.

Todd, W.J., P.W. Mausel and M.F. Baumgardner. 1973. Urban Land Use Monitoring from Computer-Implemented Processing of Airborne Multispectral Sensor Data. Laboratory for Applications of Remote Sensing Information Note 061873, Purdue University.

Todd, W.J., P.W. Mausel and K. Wenner. 1973. Preparation of Urban Land Use Inventories by Machine-Processing of ERTS MSS Data. In Proc., Symposium on Significant Results Obtained from the Earth Resources Technology Satellite-1. Goddard Space Flight Center, New Carrollton, Maryland. pp. 1031-1039.

Welby, C.W. 1976. Landsat-1 Imagery for Geologic Evaluation. Photogrammetric Engineering and Remote Sensing 42(11):1411-1419.

Wiegand, C.L., R.W. Leamer and D.A. Weber. 1975. Pattern Recognition of Soils and Crops from Space. Photogrammetric Engineering and Remote Sensing 41(4):471-478.

Appendix A

WATERSHED = LITTLE MILLSEAT

TYPE	BASAL AREA PER HECTARE	(ACRE)	STANDARD ERROR OF BASAL AREA		NUMBER OF TREES PER HECTARE	(ACRE)	STANDARD ERROR OF NUMBER OF TREES		VOLUME PER HECTARE	(ACRE)	HECTARES	ACRES
1	14.5	(63.2)	1.0	(4.2)	3822.0	(1546.8)	885.9	(358.5)	122.3	(1747.5)	6.09	15.05
2	21.3	(92.9)	1.7	(7.3)	1709.9	(692.0)	584.6	(236.6)	222.3	(3176.7)	5.42	13.40
3	24.8	(107.9)	1.3	(5.8)	1720.1	(696.1)	543.2	(219.8)	262.0	(3744.5)	4.38	10.82
4	19.5	(85.1)	0.9	(4.0)	3630.0	(1469.1)	543.0	(219.7)	191.0	(2729.5)	14.56	35.98
5	12.2	(53.2)	1.3	(5.6)	388.3	(157.1)	162.9	(65.9)	136.0	(1943.7)	3.04	7.52
6	14.0	(61.0)	1.6	(6.9)	5028.5	(2035.0)	1202.8	(486.7)	95.5	(1364.5)	7.14	17.64
7	18.5	(80.8)	0.9	(3.7)	3459.7	(1400.1)	760.7	(307.8)	119.8	(1712.0)	9.80	24.22
8	15.9	(69.3)	1.7	(7.3)	5148.6	(2083.6)	1269.6	(513.8)	141.2	(2017.4)	4.66	11.52
9	15.6	(67.9)	3.1	(13.6)	4752.7	(1923.4)	1638.2	(663.0)	142.0	(2028.9)	2.76	6.82
10	19.4	(84.6)	1.1	(4.7)	2142.8	(867.2)	658.4	(266.5)	199.8	(2856.0)	4.28	10.58
11	17.2	(75.0)	2.0	(8.7)	2388.2	(966.5)	737.3	(298.4)	174.8	(2498.3)	4.66	11.52
12	15.3	(66.7)	1.0	(4.3)	2530.1	(1023.9)	688.8	(278.8)	134.5	(1922.2)	9.04	22.34
13	20.8	(90.5)	2.1	(9.0)	4385.1	(1774.6)	851.9	(344.8)	149.6	(2137.9)	2.57	6.35
14	21.8	(95.0)	2.3	(10.2)	2214.5	(896.2)	848.3	(343.3)	185.2	(2646.5)	1.71	4.23
	17.8	(77.5)	0.4	(1.6)	3236.1	(1309.6)	236.1	(95.5)	159.6	(2280.6)	80.13	197.99

* UNITS FOR BASAL AREA ARE SQUARE METERS (SQUARE FEET)
$ UNITS FOR VOLUME ARE CUBIC METERS (CUBIC FEET)

WATERSHED = FALLING ROCK

TYPE	BASAL AREA PER HECTARE	(ACRE)	STANDARD ERROR OF BASAL AREA		NUMBER OF TREES PER HECTARE	(ACRE)	STANDARD ERROR OF NUMBER OF TREES		VOLUME PER HECTARE	(ACRE)	HECTARES	ACRES
1	20.1	(87.6)	1.3	(5.6)	1875.1	(758.9)	408.9	(165.5)	189.4	(2706.6)	17.45	43.11
2	18.6	(81.2)	0.9	(3.7)	1934.0	(782.7)	434.5	(175.9)	183.3	(2620.2)	6.11	15.11
3	21.2	(92.4)	1.5	(6.6)	2086.9	(844.5)	361.0	(146.1)	179.8	(2569.9)	3.42	8.44
4	25.0	(108.9)	1.3	(5.7)	2980.6	(1206.2)	1328.1	(537.5)	277.1	(3960.3)	3.51	8.67
5	20.0	(87.1)	1.4	(6.0)	3184.0	(1288.6)	1442.1	(583.6)	171.4	(2448.8)	4.23	10.44
6	23.0	(100.0)	2.5	(11.1)	2641.3	(1068.9)	731.6	(296.1)	216.9	(3099.8)	3.69	9.11
7	21.0	(91.6)	1.5	(6.5)	3576.5	(1447.4)	1021.9	(413.6)	174.9	(2499.2)	6.65	16.44
9	19.5	(84.9)	1.1	(4.7)	2171.8	(878.9)	676.3	(273.7)	196.6	(2809.5)	3.33	8.22
10	22.6	(98.3)	1.5	(6.7)	5113.8	(2069.5)	1429.6	(578.6)	203.3	(2905.9)	6.39	15.78
12	20.7	(90.3)	2.0	(8.7)	1242.6	(502.9)	290.4	(117.5)	202.0	(2887.3)	2.16	5.33
13	29.9	(130.4)	2.5	(11.0)	8122.9	(3287.3)	1776.8	(719.1)	211.9	(3028.6)	2.07	5.11
14	15.2	(66.0)	1.1	(4.7)	2941.0	(1190.2)	871.4	(352.7)	130.8	(1869.8)	6.84	16.89
15	20.3	(88.4)	1.4	(5.9)	2514.0	(1017.4)	593.1	(240.0)	176.4	(2520.8)	6.03	14.89
16	18.5	(80.6)	1.3	(5.6)	1430.4	(578.9)	333.3	(134.9)	155.0	(2215.0)	6.30	15.56
17	25.2	(109.9)	1.8	(8.0)	1343.9	(543.9)	236.9	(95.9)	239.2	(3418.8)	2.88	7.11
18	18.9	(82.2)	1.1	(4.9)	4644.6	(1879.6)	1111.8	(450.0)	141.4	(2020.5)	3.87	9.56
19	21.8	(9[illegible]0)	2.0	(8.6)	4531.0	(1833.7)	848.9	(343.5)	163.2	(2332.6)	1.71	4.22
20	19.2	(83.7)	1.5	(6.7)	3256.2	(1317.8)	688.7	(278.7)	169.7	(2425.7)	3.96	9.78
21	20.7	(90.1)	1.6	(6.8)	2688.3	(1087.9)	1327.9	(537.4)	199.1	(2844.8)	2.52	6.22
	20.4	(89.1)	0.4	(1.7)	2814.5	(1139.0)	205.7	(83.2)	184.2	(2632.6)	93.08	229.99

* UNITS FOR BASAL AREA ARE SQUARE METERS (SQUARE FEET)
$ UNITS FOR VOLUME ARE CUBIC METERS (CUBIC FEET)

WATERSHED = FIELD BRANCH

TYPE	BASAL AREA PER HECTARE	(ACRE)	STANDARD ERROR OF BASAL AREA	(ACRE)	NUMBER OF TREES PER HECTARE	(ACRE)	STANDARD ERROR OF NUMBER OF TREES	(ACRE)	VOLUME PER HECTARE	(ACRE)	HECTARES	ACRES
1	16.4	(71.3)	1.9	(8.3)	1306.7	(528.8)	282.2	(114.2)	162.6	(2324.1)	3.95	9.76
2	20.5	(89.1)	1.4	(6.2)	2330.1	(943.0)	524.9	(212.4)	181.2	(2590.0)	6.37	15.74
3	20.5	(89.1)	1.9	(8.3)	1290.9	(522.4)	337.4	(136.5)	200.9	(2870.9)	1.89	4.66
4	14.8	(64.3)	1.1	(5.0)	2054.5	(831.4)	654.8	(265.0)	134.6	(1923.2)	2.69	6.65
5	12.4	(54.0)	1.0	(4.3)	3604.9	(1458.9)	1084.8	(439.0)	94.6	(1352.1)	4.58	11.31
6	8.9	(38.6)	1.8	(7.9)	1717.5	(695.0)	844.1	(341.6)	67.2	(961.0)	2.69	6.65
7	17.4	(75.9)	2.4	(10.4)	1255.2	(508.0)	375.1	(151.8)	161.5	(2307.9)	1.89	4.66
8	17.3	(75.2)	1.9	(8.4)	6339.9	(2565.7)	2220.2	(898.5)	109.6	(1566.3)	3.14	7.76
9	16.6	(72.3)	0.9	(3.8)	2475.0	(1001.6)	762.2	(308.5)	160.2	(2290.2)	5.38	13.30
10	19.5	(85.1)	1.4	(6.1)	1209.5	(489.5)	235.0	(95.1)	195.5	(2794.0)	3.77	9.31
11	13.2	(57.6)	1.5	(6.4)	2059.2	(833.3)	576.4	(233.3)	129.2	(1846.2)	4.13	10.20
	16.3	(70.9)	0.5	(2.0)	2415.3	(977.4)	268.6	(108.7)	146.6	(2095.1)	40.47	100.00

* UNITS FOR BASAL AREA ARE SQUARE METERS (SQUARE FEET)
$ UNITS FOR VOLUME ARE CUBIC METERS (CUBIC FEET)

WATERSHED = JENNY FORK

TYPE	BASAL AREA PER HECTARE	(ACRE)	STANDARD ERROR OF BASAL AREA		NUMBER OF TREES PER HECTARE	(ACRE)	STANDARD ERROR OF NUMBER OF TREES		VOLUME PER HECTARE	(ACRE)	HECTARES	ACRES
1	25.0	(108.9)	2.9	(12.8)	4616.9	(1868.4)	1939.4	(784.9)	206.7	(2954.7)	1.24	3.07
2	21.8	(94.8)	1.8	(7.7)	2101.9	(850.6)	778.6	(315.1)	210.5	(3008.5)	2.01	4.96
3	9.1	(39.6)	2.6	(11.3)	3497.9	(1415.6)	2890.5	(1169.8)	66.5	(949.8)	2.29	5.67
4	19.8	(86.3)	1.4	(6.0)	2443.9	(989.0)	835.6	(338.2)	175.0	(2501.2)	2.58	6.38
5	17.7	(77.0)	1.0	(4.3)	1590.3	(643.6)	447.3	(181.0)	179.2	(2561.4)	7.74	19.13
6	20.5	(89.1)	1.5	(6.5)	2144.0	(867.6)	882.1	(357.0)	205.2	(2933.3)	2.29	5.67
7	17.7	(77.2)	2.3	(10.1)	4971.0	(2011.7)	1425.4	(576.9)	122.8	(1755.0)	1.63	4.02
8	19.5	(84.9)	2.2	(9.6)	2166.9	(876.9)	1404.5	(568.4)	189.9	(2714.5)	1.34	3.31
9	21.6	(94.0)	1.7	(7.6)	5439.3	(2201.3)	1846.4	(747.2)	160.9	(2298.9)	2.20	5.43
10	20.5	(89.1)	1.6	(6.9)	3569.4	(1444.5)	1251.4	(506.4)	191.0	(2729.0)	3.82	9.45
11	23.5	(102.3)	3.0	(13.2)	4024.3	(1628.6)	450.8	(182.5)	162.9	(2328.4)	1.24	3.07
12	16.8	(73.0)	2.1	(9.0)	3472.1	(1405.1)	961.4	(389.1)	123.8	(1769.9)	2.68	6.61
13	20.9	(91.1)	2.6	(11.5)	1679.1	(679.5)	617.0	(249.7)	215.8	(3084.3)	2.20	5.43
14	23.0	(100.1)	1.8	(7.8)	1345.1	(544.3)	498.7	(201.8)	252.7	(3611.5)	3.44	8.50
15	21.6	(94.0)	1.4	(6.1)	1259.5	(509.7)	720.9	(291.7)	222.9	(3185.5)	2.20	5.43
16	20.6	(89.6)	1.2	(5.3)	2007.5	(812.4)	574.4	(232.4)	209.3	(2991.1)	7.94	19.61
17	19.5	(84.8)	1.0	(4.1)	2076.7	(840.4)	564.7	(228.5)	219.1	(3131.1)	6.12	15.12
18	15.5	(67.3)	2.1	(9.1)	2470.6	(999.8)	1370.8	(554.8)	151.9	(2170.8)	2.10	5.20
19	18.5	(80.6)	1.9	(8.2)	1752.8	(709.3)	765.4	(309.8)	179.8	(2569.6)	2.68	6.61
20	18.0	(78.2)	1.7	(7.6)	1321.2	(534.7)	675.9	(273.5)	196.8	(2812.3)	3.63	8.98
21	17.1	(74.6)	1.0	(4.5)	3383.6	(1369.3)	984.6	(398.5)	156.4	(2235.4)	5.64	13.94
22	17.5	(76.2)	1.3	(5.8)	3804.2	(1539.5)	1175.3	(475.6)	128.4	(1834.5)	4.88	12.05
23	16.9	(73.7)	1.4	(6.2)	682.3	(276.1)	110.2	(44.6)	165.9	(2370.4)	3.54	8.74
24	2.9	(12.7)	1.4	(6.0)	1957.3	(792.1)	1916.7	(775.7)	18.8	(269.0)	3.54	8.74
25	21.7	(94.4)	1.1	(4.6)	1824.4	(738.3)	462.4	(187.1)	203.5	(2909.0)	6.02	14.88
26	19.0	(82.9)	2.3	(10.1)	2921.2	(1182.2)	643.4	(260.4)	148.0	(2115.8)	2.58	6.38
27	19.6	(81.2)	1.7	(7.3)	489.0	(197.9)	75.2	(30.5)	197.4	(2820.7)	1.53	3.78
28	19.4	(84.4)	1.8	(8.0)	834.5	(337.7)	206.7	(83.6)	201.3	(2877.2)	6.69	16.53
29	21.6	(94.0)	1.8	(7.7)	679.0	(274.8)	160.4	(64.9)	241.4	(3450.2)	4.01	9.92
30	21.3	(92.9)	2.2	(9.5)	1915.1	(775.0)	558.8	(226.1)	218.7	(3124.8)	5.26	12.99
31	18.9	(82.5)	1.7	(7.5)	255.6	(103.4)	46.9	(19.0)	202.2	(2889.5)	2.20	5.43
32	20.9	(91.1)	1.7	(7.3)	517.9	(209.6)	131.5	(53.2)	233.6	(3338.6)	6.88	17.01
33	16.5	(71.8)	2.5	(11.0)	661.8	(267.8)	191.0	(77.3)	167.9	(2399.8)	2.01	4.96
	18.9	(82.3)	0.3	(1.3)	2039.2	(825.3)	153.7	(62.2)	185.0	(2643.8)	116.17	287.06

* UNITS FOR BASAL AREA ARE SQUARE METERS (SQUARE FEET)
$ UNITS FOR VOLUME ARE CUBIC METERS (CUBIC FEET)

REPRODUCIBILITY OF THE
ORIGINAL PAGE IS POOR

WATERSHED = MILLER BRANCH

TYPE	BASAL AREA PER HECTARE	(ACRE)	STANDARD ERROR OF BASAL AREA		NUMBER OF TREES PER HECTARE	(ACRE)	STANDARD ERROR OF NUMBER OF TREES		VOLUME PER HECTARE	(ACRE)	HECTARES	ACRES
1	15.1	(65.6)	1.8	(7.9)	859.5	(347.8)	628.3	(254.3)	144.1	(2059.8)	2.98	7.36
2	10.9	(47.5)	2.2	(9.6)	8765.8	(3547.5)	1303.5	(527.5)	55.1	(787.3)	2.31	5.70
3	12.5	(54.4)	1.3	(5.8)	3247.7	(1314.3)	1336.9	(541.0)	107.0	(1529.2)	4.71	11.64
4	0.0		0.0		0.0		0.0		0.0		1.15	2.85
5	5.1	(22.3)	1.1	(4.7)	4572.9	(1850.6)	1174.6	(475.3)	14.8	(211.6)	12.59	31.11
6	16.5	(71.8)	3.0	(13.0)	6694.6	(2709.3)	1891.1	(765.3)	125.9	(1798.9)	5.77	14.25
7	0.0		0.0		0.0		0.0		0.0		1.83	4.51
8	0.0		0.0		0.0		0.0		0.0		6.63	16.39
9	16.5	(71.8)	3.8	(16.4)	529.1	(214.1)	307.8	(124.6)	152.7	(2182.6)	1.06	2.61
10	15.3	(66.5)	3.1	(13.4)	2721.9	(1101.5)	999.5	(404.5)	137.9	(1970.4)	2.79	6.89
11	14.3	(62.1)	1.6	(7.1)	1219.3	(493.4)	544.8	(220.5)	148.1	(2117.0)	5.00	12.35
12	0.0		0.0		0.0		0.0		0.0		3.27	8.08
13	0.0		0.0		0.0		0.0		0.0		3.56	8.79
14	17.7	(77.2)	1.5	(6.6)	428.1	(173.3)	47.8	(19.3)	183.2	(2618.3)	1.83	4.51
15	0.0		0.0		0.0		0.0		0.0		7.02	17.34
16	18.2	(79.2)	2.0	(8.8)	2986.2	(1208.5)	1128.7	(456.8)	142.4	(2035.6)	3.36	8.31
17	18.7	(81.7)	2.3	(9.9)	622.0	(251.7)	203.8	(82.5)	202.8	(2898.7)	3.46	8.55
18	19.8	(86.1)	2.5	(10.8)	2237.7	(905.6)	888.1	(359.4)	198.7	(2840.2)	3.94	9.74
19	14.2	(61.9)	3.3	(14.2)	4516.5	(1827.8)	1346.2	(544.8)	98.0	(1400.5)	1.44	3.56
20	0.0		0.0		0.0		0.0		0.0		0.77	1.90
21	9.1	(39.6)	0.0	(0.0)	4860.1	(1966.8)	2532.5	(1024.9)	69.9	(998.9)	1.44	3.56
	9.0	(39.1)	0.4	(1.8)	2390.5	(967.4)	275.7	(111.6)	75.4	(1077.9)	76.89	190.00

* UNITS FOR BASAL AREA ARE SQUARE METERS (SQUARE FEET)
$ UNITS FOR VOLUME ARE CUBIC METERS (CUBIC FEET)

WATERSHED = MULLINS FORK

TYPE	BASAL AREA PER HECTARE	(ACRE)	STANDARD ERROR OF BASAL AREA		NUMBER OF TREES PER HECTARE	(ACRE)	STANDARD ERROR OF NUMBER OF TREES		VOLUME PER HECTARE	(ACRE)	HECTARES	ACRES
1	0.0		0.0		0.0		0.0		0.0		1.59	3.92
2	22.9	(99.5)	1.3	(5.5)	5007.9	(2026.7)	955.3	(386.6)	209.1	(2987.8)	7.44	18.38
3	17.4	(75.9)	1.4	(6.0)	2609.8	(1056.2)	827.3	(334.8)	152.6	(2180.4)	4.17	10.30
4	19.3	(84.1)	1.1	(5.0)	11778.6	(4766.7)	4786.2	(1937.0)	108.0	(1543.1)	1.49	3.68
5	19.7	(85.6)	1.0	(4.3)	1756.2	(710.7)	488.8	(197.8)	214.7	(3067.8)	8.43	20.84
6	24.4	(106.4)	1.9	(8.5)	14279.8	(5779.0)	2544.0	(1029.5)	133.8	(1912.1)	1.39	3.43
7	17.4	(75.6)	1.7	(7.6)	5251.2	(2125.1)	1551.0	(627.7)	142.3	(2033.4)	3.27	8.09
8	0.0		0.0		0.0		0.0		0.0		1.69	4.17
9	13.6	(59.4)	2.8	(12.3)	4149.9	(1679.4)	724.2	(293.1)	121.3	(1733.4)	2.38	5.88
10	0.0		0.0		0.0		0.0		0.0		6.75	16.67
11	12.3	(53.5)	0.9	(4.0)	4445.2	(1799.0)	1359.0	(550.0)	75.2	(1074.3)	3.27	8.09
12	0.0		0.0		0.0		0.0		0.0		6.75	16.67
13	13.6	(59.4)	1.7	(7.5)	2942.1	(1190.6)	1230.0	(497.8)	114.3	(1633.0)	1.78	4.41
14	8.4	(36.8)	1.9	(8.3)	3482.3	(1409.3)	2667.6	(1079.5)	68.7	(982.0)	2.28	5.64
15	13.0	(56.4)	2.1	(9.2)	1574.4	(637.1)	681.3	(275.7)	126.5	(1807.7)	3.77	9.31
16	14.6	(63.6)	2.5	(10.8)	3489.6	(1412.2)	1277.8	(517.1)	125.2	(1789.4)	3.08	7.60
17	17.5	(76.4)	3.2	(14.0)	1933.2	(782.4)	906.5	(366.9)	152.3	(2176.8)	2.78	6.86
18	20.2	(88.0)	1.7	(7.5)	766.5	(310.2)	141.2	(57.2)	194.4	(2777.9)	3.37	8.33
19	0.8	(3.3)	0.6	(2.5)	1214.8	(491.6)	888.7	(359.7)	1.6	(22.2)	15.57	38.48
20	14.9	(65.1)	1.6	(7.1)	4759.3	(1926.1)	1367.5	(553.4)	118.2	(1689.7)	3.17	7.84
21	19.0	(82.7)	1.3	(5.9)	3285.6	(1329.7)	835.1	(337.9)	177.7	(2540.0)	6.55	16.18
22	18.0	(78.4)	1.2	(5.1)	2915.9	(1180.1)	879.1	(355.8)	161.7	(2310.8)	4.46	11.03
23	16.7	(72.7)	0.7	(3.1)	1770.0	(716.3)	360.8	(146.0)	173.1	(2474.4)	13.19	32.60
24	4.5	(19.8)	2.1	(9.0)	4555.4	(1843.5)	2560.0	(1036.0)	12.5	(178.6)	2.68	6.62
25	0.0		0.0		0.0		0.0		0.0		1.89	4.66
26	0.0		0.0		0.0		0.0		0.0		9.72	24.02
27	0.0		0.0		0.0		0.0		0.0		9.43	23.29
	10.2	(44.5)	0.2	(1.0)	2144.9	(868.0)	183.1	(74.1)	92.6	(1323.1)	132.33	326.99

* UNITS FOR BASAL AREA ARE SQUARE METERS (SQUARE FEET)
$ UNITS FOR VOLUME ARE CUBIC METERS (CUBIC FEET)

Appendix B LANDSAT Imagery - Mean Densities and Standard Deviations* for 2 Watershed Groups

April 12, 1975 Description	Undisturbed Forest	Approximately 50% Disturbed
P-MS4-1d-Visual	1.2775 (.222)	1.145 (.071)
P-MS4-1d-Wratten #18A	1.2450 (.238)	1.110 (.000)
P-MS4-1d-Wratten #93	1.2550 (.238)	1.130 (.000)
P-MS4-1d-Wratten #96	1.2600 (.183)	1.125 (.071)
P-MS4-1p-Visual	1.7450 (.289)	1.610 (.141)
P-MS4-1p-Wratten #18A	1.8550 (.289)	1.715 (.071)
P-MS4-1p-Wratten #93	1.7550 (.289)	1.615 (.071)
P-MS4-1p-Wratten #96	1.7850 (.289)	1.640 (.141)
P-MS5-1d-Visual	1.2325 (.287)	1.090 (.141)
P-MS5-1d-Wratten #18A	1.2050 (.332)	1.065 (.212)
P-MS5-1d-Wratten #93	1.2150 (.332)	1.080 (.141)
P-MS5-1d-Wratten #96	1.2150 (.332)	1.080 (.141)
P-MS5-1p-Visual	1.6725 (.222)	1.515 (.071)
P-MS5-1p-Wratten #18A	1.7800 (.258)	1.610 (.141)
P-MS5-1p-Wratten #93	1.6875 (.275)	1.530 (.000)
P-MS5-1p-Wratten #96	1.7100 (.258)	1.545 (.071)
P-MS6-1d-Visual	1.0550 (.265)	0.910 (.141)
P-MS6-1d-Wratten #18A	1.0350 (.265)	0.900 (.141)
P-MS6-1d-Wratten #93	1.0525 (.250)	0.910 (.141)
P-MS6-1d-Wratten #96	1.0450 (.265)	0.910 (.141)
P-MS6-1p-Visual	1.4725 (.330)	1.315 (.071)
P-MS6-1p-Wratten #18A	1.5525 (.411)	1.385 (.071)
P-MS6-1p-Wratten #93	1.4725 (.330)	1.325 (.071)
P-MS6-1p-Wratten #96	1.4900 (.337)	1.335 (.071)
P-MS7-1d-Visual	1.0250 (.192)	0.925 (.071)
P-MS7-1d-Wratten #18A	1.0050 (.192)	0.905 (.071)
P-MS7-1d-Wratten #93	1.0150 (.192)	0.915 (.071)
P-MS7-1d-Wratten #96	1.0125 (.171)	0.915 (.071)
P-MS7-1p-Visual	1.4400 (.271)	1.330 (.000)
P-MS7-1p-Wratten #18A	1.5275 (.320)	1.410 (.000)
P-MS7-1p-Wratten #93	1.4400 (.271)	1.335 (.071)
P-MS7-1p-Wratten #96	1.4575 (.320)	1.345 (.071)

Description	Undisturbed Forest	Approximately 50% Disturbed
N-MS4-1d-Visual	0.9325 (.150)	1.080 (.141)
N-MS4-1d-Wratten #18A	0.9375 (.171)	1.080 (.141)
N-MS4-1d-Wratten #93	0.9225 (.150)	1.065 (.212)
N-MS4-1d-Wratten #96	0.9275 (.171)	1.065 (.212)
N-MS4-1p-Visual	1.3150 (.058)	1.495 (.071)
N-MS4-1p-Wratten #18A	1.4100 (.082)	1.615 (.071)
N-MS4-1p-Wratten #93	1.3175 (.050)	1.500 (.141)
N-MS4-1p-Wratten #96	1.3300 (.000)	1.520 (.141)
N-MS5-1d-Visual	1.0750 (.192)	1.205 (.212)
N-MS5-1d-Wratten #18A	1.0725 (.171)	1.205 (.212)
N-MS5-1d-Wratten #93	1.0675 (.189)	1.195 (.212)
N-MS5-1d-Wratten #96	1.0625 (.171)	1.190 (.141)
N-MS5-1p-Visual	1.4975 (.236)	1.625 (.071)
N-MS5-1p-Wratten #18A	1.6175 (.275)	1.760 (.000)
N-MS5-1p-Wratten #93	1.4975 (.236)	1.630 (.000)
N-MS5-1p-Wratten #96	1.5150 (.265)	1.650 (.000)
N-MS6-1d-Visual	1.1225 (.126)	1.250 (.141)
N-MS6-1d-Wratten #18A	1.1225 (.126)	1.250 (.141)
N-MS6-1d-Wratten #93	1.1100 (.082)	1.235 (.071)
N-MS6-1d-Wratten #96	1.1100 (.082)	1.240 (.141)
N-MS6-1p-Visual	1.5450 (.192)	1.695 (.212)
N-MS6-1p-Wratten #18A	1.6750 (.265)	1.835 (.354)
N-MS6-1p-Wratten #93	1.5475 (.222)	1.695 (.212)
N-MS6-1p-Wratten #96	1.5675 (.222)	1.720 (.283)
N-MS7-1d-Visual	1.1475 (.236)	1.215 (.071)
N-MS7-1d-Wratten #18A	1.1425 (.287)	1.210 (.141)
N-MS7-1d-Wratten #93	1.1300 (.245)	1.195 (.071)
N-MS7-1d-Wratten #96	1.1325 (.287)	1.200 (.141)
N-MS7-1p-Visual	1.5700 (.316)	1.680 (.141)
N-MS7-1p-Wratten #18A	1.6975 (.310)	1.810 (.141)
N-MS7-1p-Wratten #93	1.5725 (.299)	1.680 (.141)
N-MS7-1p-Wratten #96	1.6200 (.744)	1.710 (.141)

September 3, 1975

Description	Undisturbed Forest	Approximately 50% Disturbed
P-MS4-ld-Visual	1.4475 (.050)	1.405 (.071)
P-MS4-ld-Wratten #18A	1.4175 (.050)	1.375 (.071)
P-MS4-ld-Wratten #93	1.4250 (.058)	1.385 (.071)
P-MS4-ld-Wratten #96	1.4375 (.050)	1.390 (.000)
P-MS4-lp-Visual	1.9675 (.050)	1.895 (.212)
P-MS4-lp-Wratten #18A	2.0925 (.096)	2.010 (.141)
P-MS4-lp-Wratten #93	1.9875 (.050)	1.900 (.141)
P-MS4-lp-Wratten #96	2.0075 (.050)	1.920 (.141)
P-MS5-ld-Visual	1.5575 (.126)	1.385 (.071)
P-MS5-ld-Wratten #18A	1.5175 (.126)	1.355 (.071)
P-MS5-ld-Wratten #93	1.5400 (.141)	1.360 (.141)
P-MS5-ld-Wratten #96	1.5500 (.141)	1.360 (.141)
P-MS5-lp-Visual	2.1000 (.141)	1.890 (.141)
P-MS5-lp-Wratten #93	2.2275 (.096)	1.995 (.212)
P-MS5-lp-Wratten #93	2.1100 (.141)	1.890 (.141)
P-MS5-lp-Wratten #96	2.1300 (.141)	1.910 (.141)
P-MS6-ld-Visual	0.9125 (.263)	0.885 (.071)
P-MS6-ld-Wratten #18A	0.9000 (.216)	0.875 (.071)
P-MS6-ld-Wratten #93	0.9075 (.250)	0.880 (.141)
P-MS6-ld-Wratten #96	0.9100 (.216)	0.885 (.071)
P-MS6-lp-Visual	1.2925 (.222)	1.285 (.071)
P-MS6-lp-Wratten #18A	1.3525 (.171)	1.350 (.000)
P-MS6-lp-Wratten #93	1.2950 (.173)	1.280 (.000)
P-MS6-lp-Wratten #96	1.3050 (.173)	1.290 (.000)
P-MS7-ld-Visual	0.8650 (.100)	0.970 (.141)
P-MS7-ld-Wratten #18A	0.8550 (.100)	0.960 (.141)
P-MS7-ld-Wratten #93	0.8575 (.126)	0.970 (.141)
P-MS7-ld-Wratten #96	0.8625 (.150)	0.970 (.141)
P-MS7-lp-Visual	1.2175 (.206)	1.355 (.212)
P-MS7-lp-Wratten #18A	1.2825 (.222)	1.415 (.354)
P-MS7-lp-Wratten #93	1.2350 (.192)	1.360 (.283)
P-MS7-lp-Wratten #96	1.2450 (.192)	1.365 (.354)

Description	Undisturbed Forest	Approximately 50% Disturbed
N-MS4-1d-Visual	0.8525 (.206)	0.950 (.141)
N-MS4-1d-Wratten #18A	0.8625 (.206)	0.955 (.212)
N-MS4-1d-Wratten #93	0.8450 (.208)	0.940 (.141)
N-MS4-1d-Wratten #96	0.8525 (.206)	0.940 (.141)
N-MS4-1p-Visual	1.2225 (.050)	1.395 (.071)
N-MS4-1p-Wratten #18A	1.3200 (.082)	1.505 (.071)
N-MS4-1p-Wratten #93	1.2375 (.096)	1.405 (.071)
N-MS4-1p-Wratten #96	1.2500 (.082)	1.415 (.071)
N-MS5-1d-Visual	0.7500 (.082)	0.890 (.283)
N-MS5-1d-Wratten #18A	0.7625 (.096)	0.895 (.212)
N-MS5-1d-Wratten #93	0.7400 (.082)	0.885 (.212)
N-MS5-1d-Wratten #96	0.7425 (.096)	0.885 (.212)
N-MS5-1p-Visual	1.0750 (.058)	1.305 (.071)
N-MS5-1p-Wratten #18A	1.1625 (.096)	1.395 (.071)
N-MS5-1p-Wratten #93	1.0900 (.082)	1.310 (.000)
N-MS5-1p-Wratten #96	1.1050 (.058)	1.325 (.071)
N-MS6-1d-Visual	1.2425 (.150)	1.205 (.071)
N-MS6-1d-Wratten #18A	1.2475 (.150)	1.205 (.071)
N-MS6-1d-Wratten #93	1.2275 (.150)	1.185 (.071)
N-MS6-1d-Wratten #96	1.2300 (.116)	1.190 (.000)
N-MS6-1p-Visual	1.7125 (.126)	1.680 (.141)
N-MS6-1p-Wratten #18A	1.8550 (.100)	1.825 (.212)
N-MS6-1p-Wratten #93	1.7125 (.126)	1.685 (.212)
N-MS6-1p-Wratten #96	1.7425 (.126)	1.710 (.141)
N-MS7-1d-Visual	1.3400 (.082)	1.225 (.212)
N-MS7-1d-Wratten #18A	1.3425 (.096)	1.225 (.212)
N-MS7-1d-Wratten #93	1.3225 (.096)	1.205 (.212)
N-MS7-1d-Wratten #96	1.3300 (.082)	1.205 (.212)
N-MS7-1p-Visual	1.8500 (.082)	1.730 (.141)
N-MS7-1p-Wratten #18A	2.0000 (.082)	1.865 (.071)
N-MS7-1p-Wratten #93	1.8575 (.050)	1.735 (.071)
N-MS7-1p-Wratten #96	1.8875 (.050)	1.765 (.071)

* Standard Deviations in parentheses have been multiplied by 10

Appendix C

Group = Coniferous-Deciduous

April 1975 Densitometry Data

Description		Mean	Standard Deviation
Average	CIR-1d-Combination	0.805	0.110
Average	CIR-2d-Combination	0.775	0.065
Average	CIR-1d-Wratten #18A	1.078	0.052
Average	CIR-1d-Wratten #96	0.797	0.066
Average	CIR-1d-Wratten #93	0.701	0.072
Average	CIR-1d-Visual	0.798	0.056
Average	CIR-1p-Wratten #18A	1.165	0.058
Average	CIR-1p-Wratten #96	0.881	0.079
Average	CIR-1p-Wratten #93	0.767	0.086
Average	CIR-1p-Visual	0.857	0.063
Average	CIR-3d-Wratten #18A	1.044	0.057
Average	CIR-3d-Wratten #96	0.772	0.079
Average	CIR-3d-Wratten #93	0.671	0.079
Average	CIR-3d-Visual	0.768	0.062
C. V.	CIR-1d-Combination	11.046	2.654
C. V.	CIR-2d-Combination	11.750	3.462
C. V.	CIR-1d-Wratten #18A	7.128	1.567
C. V.	CIR-1d-Wratten #96	10.113	4.402
C. V.	CIR-1d-Wratten #93	11.681	5.390
C. V.	CIR-1d-Visual	9.832	3.414
C. V.	CIR-1p-Wratten #18A	8.005	1.851
C. V.	CIR-1p-Wratten #96	12 696	3.509
C. V.	CIR-1p-Wratten #93	14.552	5.021
C. V.	CIR-1p-Visual	12.793	4.117
C. V.	CIR-3d-Wratten #18A	6.647	0.175
C. V.	CIR-3d-Wratten #96	9.971	1.410
C. V.	CIR-3d-Wratten #93	11.487	1.896
C. V.	CIR-3d-Visual	9.663	0.536
Ratio	CIR-1d-#18A/CIR-1d-#96	1.355	0.051
Ratio	CIR-1d-#93/CIR-1d-Visual	0.877	0.029
Ratio	CIR-1p-#18A/CIR-1p-#96	1.325	0.058
Ratio	CIR-1p-#93/CIR-1p-Visual	0.894	0.036
Ratio	CIR-3d-#18A/CIR-3d-#96	1.357	0.065
Ratio	CIR-3d-#93/CIR-3d-Visual	0.872	0.031

Group = Deciduous-Hemlock

Description		Mean	Standard Deviation
Average	CIR-1d-Combination	1.002	0.063
Average	CIR-2d-Combination	0.902	0.098
Average	CIR-1d-Wratten #18A	1.250	0.094
Average	CIR-1d-Wratten #96	0.976	0.085
Average	CIR-1d-Wratten #93	0.882	0.072
Average	CIR-1d-Visual	0.993	0.080
Average	CIR-1p-Wratten #18A	1.303	0.135
Average	CIR-1p-Wratten #96	1.016	0.133
Average	CIR-1p-Wratten #93	0.902	0.134
Average	CIR-1p-Visual	1.017	0.138
Average	CIR-3d-Wratten #18A	1.208	0.125
Average	CIR-3d-Wratten #96	0.927	0.114
Average	CIR-3d-Wratten #93	0.821	0.111
Average	CIR-3d-Visual	0.945	0.115
C. V.	CIR-1d-Combination	20.632	5.165
C. V.	CIR-2d-Combination	18.930	2.709
C. V.	CIR-1d-Wratten #18A	12.176	2.716
C. V.	CIR-1d-Wratten #96	19.848	3.286
C. V.	CIR-1d-Wratten #93	24.014	2.654
C. V.	CIR-1d-Visual	19.143	3.307
C. V.	CIR-1p-Wratten #18A	14.925	0.588
C. V.	CIR-1p-Wratten #96	22.600	2.378
C. V.	CIR-1p-Wratten #93	26.312	3.431
C. V.	CIR-1p-Visual	22.760	1.713
C. V.	CIR-3d-Wratten #18A	11.012	1.963
C. V.	CIR-3d-Wratten #96	16.422	0.797
C. V.	CIR-3d-Wratten #93	19.390	0.205
C. V.	CIR-3d-Visual	16.323	1.427
Ratio	CIR-1d-#18A/CIR-1d-#96	1.282	0.015
Ratio	CIR-1d-#93/CIR-1d-Visual	0.888	0.004
Ratio	CIR-1p-#18A/CIR-1p-#96	1.286	0.041
Ratio	CIR-1p-#93/CIR-1p-Visual	0.886	0.013
Ratio	CIR-3d-#18A/CIR-3d-#96	1.306	0.031
Ratio	CIR-3d-#93/CIR-3d-Visual	0.868	0.012

Group = Deciduous

Description		Mean	Standard Deviation
Average	CIR-1d-Combination	0.828	0.187
Average	CIR-2d-Combination	0.824	0.182
Average	CIR-1d-Wratten #18A	1.140	0.190
Average	CIR-1d-Wratten #96	0.796	0.173
Average	CIR-1d-Wratten #93	0.683	0.161
Average	CIR-1d-Visual	0.830	0.180
Average	CIR-1p-Wratten #18A	1.239	0.198
Average	CIR-1p-Wratten #96	0.894	0.186
Average	CIR-1p-Wratten #93	0.761	0.175
Average	CIR-1p-Visual	0.902	0.195
Average	CIR-3d-Wratten #18A	1.134	0.195
Average	CIR-3d-Wratten #96	0.810	0.176
Average	CIR-3d-Wratten #93	0.693	0.165
Average	CIR-3d-Visual	0.834	0.184
C. V.	CIR-1d-Combination	10.709	5.659
C. V.	CIR-2d-Combination	9.663	5.068
C. V.	CIR-1d-Wratten #18A	8.079	4.006
C. V.	CIR-1d-Wratten #96	10.987	5.264
C. V.	CIR-1d-Wratten #93	11.977	5.732
C. V.	CIR-1d-Visual	10.821	5.185
C. V.	CIR-1p-Wratten #18A	7.499	3.822
C. V.	CIR-1p-Wratten #96	10.073	4.990
C. V.	CIR-1p-Wratten #93	11.141	5.445
C. V.	CIR-1p-Visual	10.523	5.130
C. V.	CIR-3d-Wratten #18A	5.621	3.488
C. V.	CIR-3d-Wratten #96	7.425	4.426
C. V.	CIR-3d-Wratten #93	8.221	4.770
C. V.	CIR-3d-Visual	7.491	4.474
Ratio	CIR-1d-#18A/CIR-1d-#96	1.449	0.075
Ratio	CIR-1d-#93/CIR-1d-Visual	0.820	0.022
Ratio	CIR-1p-#18A/CIR-1p-#96	1.400	0.066
Ratio	CIR-1p-#93/CIR-1p-Visual	0.843	0.018
Ratio	CIR-3d-#18A/CIR-3d-#96	1.413	0.064
Ratio	CIR-3d-#93/CIR-3d-Visual	0.828	0.019

Group = Dense Grass 1

Description		Mean	Standard Deviation
Average	CIR-1d-Combination	0.713	0.298
Average	CIR-2d-Combination	0.690	0.299
Average	CIR-1d-Wratten #18A	0.947	0.261
Average	CIR-1d-Wratten #96	0.668	0.300
Average	CIR-1d-Wratten #93	0.601	0.302
Average	CIR-1d-Visual	0.695	0.265
Average	CIR-1p-Wratten #18A	1.036	0.280
Average	CIR-1p-Wratten #96	0.762	0.338
Average	CIR-1p-Wratten #93	0.676	0.352
Average	CIR-1p-Visual	0.752	0.307
Average	CIR-3d-Wratten #18A	0.971	0.284
Average	CIR-3d-Wratten #96	0.711	0.317
Average	CIR-3d-Wratten #93	0.636	0.323
Average	CIR-3d-Visual	0.719	0.299
C. V.	CIR-1d-Combination	14.470	10.116
C. V.	CIR-2d-Combination	7.421	6.722
C. V.	CIR-1d-Wratten #18A	5.931	3.621
C. V.	CIR-1d-Wratten #96	8.865	3.744
C. V.	CIR-1d-Wratten #93	9.091	2.705
C. V.	CIR-1d-Visual	7.916	3.771
C. V.	CIR-1p-Wratten #18A	7.671	4.144
C. V.	CIR-1p-Wratten #96	10.302	4.613
C. V.	CIR-1p-Wratten #93	11.186	3.955
C. V.	CIR-1p-Visual	10.778	6.002
C. V.	CIR-3d-Wratten #18A	3.726	2.696
C. V.	CIR-3d-Wratten #96	5.347	2.766
C. V.	CIR-3d-Wratten #93	5.754	2.649
C. V.	CIR-3d-Visual	5.219	4.322
Ratio	CIR-1d-#18A/CIR-1d-#96	1.496	0.240
Ratio	CIR-1d-#93/CIR-1d-Visual	0.843	0.102
Ratio	CIR-1p-#18A/CIR-1p-#96	1.432	0.226
Ratio	CIR-1p-#93/CIR-1p-Visual	0.876	0.102
Ratio	CIR-3d-#18A/CIR-3d-#96	1.443	0.234
Ratio	CIR-3d-#93/CIR-3d-Visual	0.871	0.097

Group = Dense Grass 2

Description		Mean	Standard Deviation
Average	CIR-1d-Combination	0.586	0.141
Average	CIR-2d-Combination	0.556	0.125
Average	CIR-1d-Wratten #18A	0.833	0.165
Average	CIR-1d-Wratten #96	0.519	0.127
Average	CIR-1d-Wratten #93	0.450	0.104
Average	CIR-1d-Visual	0.581	0.137
Average	CIR-1p-Wratten #18A	0.892	0.171
Average	CIR-1p-Wratten #96	0.577	0.132
Average	CIR-1p-Wratten #93	0.486	0.115
Average	CIR-1p-Visual	0.593	0.150
Average	CIR-3d-Wratten #18A	0.816	0.147
Average	CIR-3d-Wratten #96	0.525	0.118
Average	CIR-3d-Wratten #93	0.450	0.010
Average	CIR-3d-Visual	0.561	0.130
C. V.	CIR-1d-Combination	15.445	4.898
C. V.	CIR-2d-Combination	13.024	5.383
C. V.	CIR-1d-Wratten #18A	12.759	2.101
C. V.	CIR-1d-Wratten #96	16.384	2.937
C. V.	CIR-1d-Wratten #93	14.717	4.069
C. V.	CIR-1d-Visual	14.340	2.914
C. V.	CIR-1p-Wratten #18A	10.275	2.376
C. V.	CIR-1p-Wratten #96	12.201	3.369
C. V.	CIR-1p-Wratten #93	11.876	3.673
C. V.	CIR-1p-Visual	13.390	3.458
C. V.	CIR-3d-Wratten #18A	9.043	2.670
C. V.	CIR-3d-Wratten #96	10.915	3.704
C. V.	CIR-3d-Wratten #93	10.704	3.742
C. V.	CIR-3d-Visual	11.301	3.546
Ratio	CIR-1d-#18A/CIR-1d-#96	1.618	0.066
Ratio	CIR-1d-#93/CIR-1d-Visual	0.775	0.014
Ratio	CIR-1p-#18A/CIR-1p-#96	1.555	0.051
Ratio	CIR-1p-#93/CIR-1p-Visual	0.823	0.022
Ratio	CIR-3d-#18A/CIR-3d-#96	1.565	0.062
Ratio	CIR-3d-#93/CIR-3d-Visual	0.804	0.024

Group = Sparse Grass 1

Description		Mean	Standard Deviation
Average	CIR-1d-Combination	0.457	0.204
Average	CIR-2d-Combination	0.473	0.221
Average	CIR-1d-Wratten #18A	0.719	0.229
Average	CIR-1d-Wratten #96	0.451	0.200
Average	CIR-1d-Wratten #93	0.404	0.170
Average	CIR-1d-Visual	0.496	0.194
Average	CIR-1p-Wratten #18A	0.795	0.248
Average	CIR-1p-Wratten #96	0.525	0.225
Average	CIR-1p-Wratten #93	0.449	0.202
Average	CIR-1p-Visual	0.523	0.229
Average	CIR-3d-Wratten #18A	0.722	0.258
Average	CIR-3d-Wratten #96	0.469	0.233
Average	CIR-3d-Wratten #93	0.410	0.208
Average	CIR-3d-Visual	0.487	0.238
C. V.	CIR-1d-Combination	16.126	2.661
C. V.	CIR-2d-Combination	14.210	3.387
C. V.	CIR-1d-Wratten #18A	10.140	1.184
C. V.	CIR-1d-Wratten #96	13.685	1.337
C. V.	CIR-1d-Wratten #93	13.237	2.577
C. V.	CIR-1d-Visual	14.074	1.944
C. V.	CIR-1p-Wratten #18A	7.175	3.352
C. V.	CIR-1p-Wratten #96	9.456	4.754
C. V.	CIR-1p-Wratten #93	10.386	4.712
C. V.	CIR-1p-Visual	10.664	5.985
C. V.	CIR-3d-Wratten #18A	7.785	0.959
C. V.	CIR-3d-Wratten #96	9.489	0.544
C. V.	CIR-3d-Wratten #93	10.149	0.978
C. V.	CIR-3d-Visual	11.889	2.879
Ratio	CIR-1d-#18A/CIR-1d-#96	1.648	0.159
Ratio	CIR-1d-#93/CIR-1d-Visual	0.810	0.027
Ratio	CIR-1p-#18A/CIR-1p-#96	1.560	0.139
Ratio	CIR-1p-#93/CIR-1p-Visual	0.856	0.023
Ratio	CIR-3d-#18A/CIR-3d-#96	1.603	0.169
Ratio	CIR-3d-#93/CIR-3d-Visual	0.839	0.028

Group = Sparse Grass 2

Description		Mean	Standard Deviation
Average	CIR-1d-Combination	0.548	0.145
Average	CIR-2d-Combination	0.554	0.112
Average	CIR-1d-Wratten #18A	0.811	0.129
Average	CIR-1d-Wratten #96	0.476	0.080
Average	CIR-1d-Wratten #93	0.418	0.076
Average	CIR-1d-Visual	0.576	0.122
Average	CIR-1p-Wratten #18A	0.850	0.156
Average	CIR-1p-Wratten #96	0.518	0.090
Average	CIR-1p-Wratten #93	0.440	0.091
Average	CIR-1p-Visual	0.574	0.161
Average	CIR-3d-Wratten #18A	0.808	0.132
Average	CIR-3d-Wratten #96	0.501	0.079
Average	CIR-3d-Wratten #93	0.432	0.074
Average	CIR-3d-Visual	0.568	0.145
C. V.	CIR-1d-Combination	23.468	18.612
C. V.	CIR-2d-Combination	23.818	23.183
C. V.	CIR-1d-Wratten #18A	10.423	4.706
C. V.	CIR-1d-Wratten #96	13.330	5.055
C. V.	CIR-1d-Wratten #93	10.950	3.500
C. V.	CIR-1d-Visual	14.181	8.518
C. V.	CIR-1p-Wratten #18A	16.018	9.836
C. V.	CIR-1p-Wratten #96	18.943	10.509
C. V.	CIR-1p-Wratten #93	20.086	11.570
C. V.	CIR-1p-Visual	23.937	18.413
C. V.	CIR-3d-Wratten #18A	8.817	5.728
C. V.	CIR-3d-Wratten #96	11.726	8.205
C. V.	CIR-3d-Wratten #93	12.338	8.975
C. V.	CIR-3d-Visual	12.579	10.191
Ratio	CIR-1d-#18A/CIR-1d-#96	1.703	0.016
Ratio	CIR-1d-#93/CIR-1d-Visual	0.729	0.023
Ratio	CIR-1p-#18A/CIR-1p-#96	1.638	0.016
Ratio	CIR-1p-#93/CIR-1p-Visual	0.774	0.058
Ratio	CIR-3d-#18A/CIR-3d-#96	1.613	0.009
Ratio	CIR-3d-#93/CIR-3d-Visual	0.770	0.067

Group = Black Locust-Grass

Description		Mean	Standard Deviation
Average	CIR-1d-Combination	0.535	0.083
Average	CIR-2d-Combination	0.510	0.051
Average	CIR-1d-Wratten #18A	0.782	0.069
Average	CIR-1d-Wratten #96	0.483	0.050
Average	CIR-1d-Wratten #93	0.418	0.039
Average	CIR-1d-Visual	0.528	0.052
Average	CIR-1p-Wratten #18A	0.889	0.100
Average	CIR-1p-Wratten #96	0.580	0.072
Average	CIR-1p-Wratten #93	0.486	0.057
Average	CIR-1p-Visual	0.580	0.085
Average	CIR-3d-Wratten #18A	0.778	0.071
Average	CIR-3d-Wratten #96	0.499	0.049
Average	CIR-3d-Wratten #93	0.425	0.041
Average	CIR-3d-Visual	0.522	0.066
C. V.	CIR-1d-Combination	13.970	3.277
C. V.	CIR-2d-Combination	12.357	1.180
C. V.	CIR-1d-Wratten #18A	10.987	2.409
C. V.	CIR-1d-Wratten #96	13.962	2.742
C. V.	CIR-1d-Wratten #93	12.058	2.841
C. V.	CIR-1d-Visual	12.419	3.178
C. V.	CIR-1p-Wratten #18A	10.769	2.184
C. V.	CIR-1p-Wratten #96	12.943	2.675
C. V.	CIR-1p-Wratten #93	13.184	3.028
C. V.	CIR-1p-Visual	13.744	3.138
C. V.	CIR-3d-Wratten #18A	8.790	1.659
C. V.	CIR-3d-Wratten #96	10.603	2.150
C. V.	CIR-3d-Wratten #93	10.411	2.627
C. V.	CIR-3d-Visual	11.588	2.954
Ratio	CIR-1d-#18A/CIR-1d-#96	1.621	0.026
Ratio	CIR-1d-#93/CIR-1d-Visual	0.792	0.014
Ratio	CIR-1p-#18A/CIR-1p-#96	1.535	0.024
Ratio	CIR-1p-#93/CIR-1p-Visual	0.841	0.027
Ratio	CIR-3d-#18A/CIR-3d-#96	1.561	0.017
Ratio	CIR-3d-#93/CIR-3d-Visual	0.816	0.027

September 1975 Group = Coniferous-Deciduous

Description		Mean	Standard Deviation
Average	CIR-1d-Wratten #18A	1.027	0.061
Average	CIR-1d-Wratten #96	1.185	0.079
Average	CIR-1d-Wratten #93	1.495	0.075
Average	CIR-1d-Visual	1.084	0.072
Average	CIR-3d-Wratten #18A	1.018	0.068
Average	CIR-3d-Wratten #96	1.248	0.081
Average	CIR-3d-Wratten #93	1.545	0.074
Average	CIR-3d-Visual	1.120	0.078
Average	MS2-3d-Wratten #18A	0.653	0.018
Average	MS2-3d-Wratten #96	0.609	0.024
Average	MS2-3d-Wratten #93	0.605	0.020
Average	MS2-3d-Visual	0.602	0.025
Average	MS3-3d-Wratten #18A	1.043	0.025
Average	MS3-3d-Wratten #96	1.023	0.028
Average	MS3-3d-Wratten #93	1.017	0.028
Average	MS3-3d-Visual	1.010	0.031
Average	MS4-3d-Wratten #18A	0.655	0.037
Average	MS4-3d-Wratten #96	0.614	0.044
Average	MS4-3d-Wratten #93	0.609	0.041
Average	MS4-3d-Visual	0.603	0.043
C. V.	CIR-1d-Wratten #18A	2.052	0.781
C. V.	CIR-1d-Wratten #96	2.572	0.916
C. V.	CIR-1d-Wratten #93	2.807	0.531
C. V.	CIR-1d-Visual	2.682	0.705
C. V.	CIR-3d-Wratten #18A	1.114	0.202
C. V.	CIR-3d-Wratten #96	1.263	0.224
C. V.	CIR-3d-Wratten #93	1.364	0.162
C. V.	CIR-3d-Visual	1.306	0.169
C. V.	MS2-3d-Wratten #18A	2.076	0.955
C. V.	MS2-3d-Wratten #96	2.319	1.324
C. V.	MS2-3d-Wratten #93	2.510	1.150
C. V.	MS2-3d-Visual	2.356	1.022
C. V.	MS3-3d-Wratten #18A	1.805	1.278
C. V.	MS3-3d-Wratten #96	1.644	1.224
C. V.	MS3-3d-Wratten #93	1.913	1.247
C. V.	MS3-3d-Visual	1.729	1.166

September 1975 Group = Coniferous-Deciduous

Description		Mean	Standard Deviation
C. V.	MS4-3d-Wratten #18A	1.892	1.661
C. V.	MS4-3d-Wratten #96	2.256	2.149
C. V.	MS4-3d-Wratten #93	1.857	2.116
C. V.	MS4-3d-Visual	2.245	2.101
Ratio	CIR-1d-#18A/CIR-1d-#96	0.867	0.012
Ratio	CIR-1d-#93/CIR-1d-Visual	1.381	0.034
Ratio	CIR-3d-#18A/CIR-3d-#96	0.815	0.002
Ratio	CIR-3d-#93/CIR-3d-Visual	1.381	0.035
Ratio	MS2-3d-#18A/MS3-3d-#18A	0.626	0.004
Ratio	MS2-3d-#18A/MS4-3d-#18A	0.998	0.031
Ratio	MS3-3d-#18A/MS4-3d-#18A	1.595	0.053
Ratio	MS2-3d-#96/MS3-3d-#96	0.595	0.009
Ratio	MS2-3d-#96/MS4-3d-#96	0.994	0.039
Ratio	MS3-3d-#96/MS4-3d-#96	1.670	0.075
Ratio	MS2-3d-#93/MS3-3d-#93	0.594	0.005
Ratio	MS2-3d-#93/MS4-3d-#93	0.995	0.036
Ratio	MS3-3d-#93/MS4-3d-#93	1.674	0.067
Ratio	MS2-3d-Visual/MS3-3d-Visual	0.596	0.008
Ratio	MS2-3d-Visual/MS4-3d-Visual	1.000	0.034
Ratio	MS3-3d-Visual/MS4-3d-Visual	1.678	0.068

April and
September 1975

% Increase CIR-1d-Wratten #18A	-4.403	10.446
% Increase CIR-1d-Wratten #96	49.843	22.618
% Increase CIR-1d-Wratten #93	115.550	33.113
% Increase CIR-1d-Visual	36.630	18.471
% Increase CIR-3d-Wratten #18A	-2.107	11.764
% Increase CIR-3d-Wratten #96	63.440	26.468
% Increase CIR-3d-Wratten #93	133.230	37.251
% Increase CIR-3d-Visual	46.917	21.030

September 1975 Group = Deciduous-Hemlock

Description		Mean	Standard Deviation
Average	CIR-1d-Wratten #18A	1.137	0.020
Average	CIR-1d-Wratten #96	1.339	0.023
Average	CIR-1d-Wratten #93	1.671	0.041
Average	CIR-1d-Visual	1.214	0.033
Average	CIR-3d-Wratten #18A	1.139	0.026
Average	CIR-3d-Wratten #96	1.408	0.021
Average	CIR-3d-Wratten #93	1.725	0.024
Average	CIR-3d-Visual	1.261	0.028
Average	MS2-3d-Wratten #18A	0.718	0.027
Average	MS2-3d-Wratten #96	0.680	0.028
Average	MS2-3d-Wratten #93	0.675	0.026
Average	MS2-3d-Visual	0.671	0.028
Average	MS-3d-Wratten #18A	1.145	0.030
Average	MS3-3d-Wratten #96	1.119	0.025
Average	MS3-3d-Wratten #93	1.118	0.026
Average	MS3-3d-Visual	1.113	0.024
Average	MS4-3d-Wratten #18A	0.745	0.034
Average	MS4-3d-Wratten #96	0.706	0.033
Average	MS4-3d-Wratten #93	0.702	0.032
Average	MS4-3d-Visual	0.698	0.029
C. V.	CIR-1d-Wratten #18A	4.412	1.235
C. V.	CIR-1d-Wratten #96	4.422	0.970
C. V.	CIR-1d-Wratten #93	3.668	0.459
C. V.	CIR-1d-Visual	4.836	1.459
C. V.	CIR-3d-Wratten #18A	3.182	0.647
C. V.	CIR-3d-Wratten #96	2.974	0.845
C. V.	CIR-3d-Wratten #93	2.682	0.541
C. V.	CIR-3d-Visual	3.399	0.718
C. V.	MS2-3d-Wratten #18A	3.335	1.826
C. V.	MS2-3d-Wratten #96	3.858	2.122
C. V.	MS2-3d-Wratten #93	3.643	2.068
C. V.	MS2-3d-Visual	3.864	2.083
C. V.	MS3-3d-Wratten #18A	3.186	1.920
C. V.	MS3-3d-Wratten #96	3.018	1.939
C. V.	MS3-3d-Wratten #93	3.177	2.102

September 1975 — Group = Deciduous-Hemlock

Description		Mean	Standard Deviation
C. V.	MS3-3d-Visual	3.275	2.141
C. V.	MS4-3d-Wratten #18A	4.523	3.424
C. V.	MS4-3d-Wratten #96	5.198	3.893
C. V.	MS4-3d-Wratten #93	4.994	3.768
C. V.	MS4-3d-Visual	5.036	3.918
Ratio	CIR-1d-#18A/CIR-1d-#96	0.849	0.003
Ratio	CIR-1d-#93/CIR-1d-Visual	1.377	0.018
Ratio	CIR-3d-#18A/CIR-3d-#96	0.809	0.009
Ratio	CIR-3d-#93/CIR-3d-Visual	1.368	0.022
Ratio	MS2-3d-#18A/MS3-3d-#18A	0.627	0.018
Ratio	MS2-3d-#18A/MS4-3d-#18A	0.965	0.025
Ratio	MS3-3d-#18A/MS4-3d-#18A	1.538	0.033
Ratio	MS2-3d-#96/MS3-3d-#96	0.608	0.021
Ratio	MS2-3d-#96/MS4-3d-#96	0.965	0.030
Ratio	MS3-3d-#96/MS4-3d-#96	1.588	0.042
Ratio	MS2-3d-#93/MS3-3d-#93	0.603	0.022
Ratio	MS2-3d-#93/MS4-3d-#93	0.962	0.030
Ratio	MS3-3d-#93/MS4-3d-#93	1.595	0.042
Ratio	MS3-3d-Visual/MS4-3d-Visual	0.602	0.022
Ratio	MS2-3d-Visual/MS3-3d-Visual	0.962	0.032
Ratio	MS3-3d-Visual/MS4-3d-Visual	1.597	0.034

April and
September 1975

% Increase CIR-1d-Wratten #18A	-8.637	8.168
% Increase CIR-1d-Wratten #96	37.977	13.534
% Increase CIR-1d-Wratten #93	90.260	16.043
% Increase CIR-1d-Visual	22.817	11.626
% Increase CIR-3d-Wratten #18A	-4.967	10.858
% Increase CIR-3d-Wratten #96	53.470	18.285
% Increase CIR-3d-Wratten #93	112.397	24.871
% Increase CIR-3d-Visual	34.763	15.554

September 1975 Group = Deciduous

Description		Mean	Standard Deviation
Average	CIR-1d-Wratten #18A	1.133	0.112
Average	CIR-1d-Wratten #96	1.331	0.140
Average	CIR-1d-Wratten #93	1.661	0.147
Average	CIR-1d-Visual	1.200	0.128
Average	CIR-3d-Wratten #18A	1.128	0.112
Average	CIR-3d-Wratten #96	1.394	0.139
Average	CIR-3d-Wratten #93	1.707	0.149
Average	CIR-3d-Visual	1.242	0.127
Average	MS2-3d-Wratten #18A	0.728	0.083
Average	MS2-3d-Wratten #96	0.690	0.089
Average	MS2-3d-Wratten #93	0.684	0.086
Average	MS2-3d-Visual	0.680	0.087
Average	MS3-3d-Wratten #18A	1.153	0.128
Average	MS3-3d-Wratten #96	1.124	0.124
Average	MS3-3d-Wratten #93	1.122	0.125
Average	MS3-3d-Visual	1.120	0.129
Average	MS4-3d-Wratten #18A	0.707	0.079
Average	MS4-3d-Wratten #96	0.667	0.084
Average	MS4-3d-Wratten #93	0.661	0.082
Average	MS4-3d-Visual	0.656	0.084
C. V.	CIR-1d-Wratten #18A	3.073	1.332
C. V.	CIR-1d-Wratten #96	3.244	1.437
C. V.	CIR-1d-Wratten #93	2.874	1.278
C. V.	CIR-1d-Visual	3.440	1.539
C. V.	CIR-3d-Wratten #18A	2.112	1.204
C. V.	CIR-3d-Wratten #96	2.193	1.310
C. V.	CIR-3d-Wratten #93	2.052	1.275
C. V.	CIR-3d-Visual	2.244	1.266
C. V.	MS2-3d-Wratten #18A	2.593	2.337
C. V.	MS2-3d-Wratten #96	2.899	2.613
C. V.	MS2-3d-Wratten #93	2.887	2.608
C. V.	MS2-3d-Visual	2.948	2.614
C. V.	MS3-3d-Wratten #18A	2.616	2.147
C. V.	MS3-3d-Wratten #96	2.632	2.090
C. V.	MS3-3d-Wratten #93	2.651	2.126

September 1975 — Group = Deciduous

Description		Mean	Standard Deviation
C. V.	MS3-3d-Visual	2.702	2.188
C. V.	MS4-3d-Wratten #18A	3.106	1.710
C. V.	MS4-3d-Wratten #96	3.490	1.960
C. V.	MS4-3d-Wratten #93	3.432	1.948
C. V.	MS4-3d-Visual	3.506	1.954
Ratio	CIR-1d-#18A/CIR-1d-#96	0.852	0.012
Ratio	CIR-1d-#93/CIR-1d-Visual	1.388	0.046
Ratio	CIR-3d-#18A/CIR-3d-#96	0.809	0.010
Ratio	CIR-3d-#93/CIR-3d-Visual	1.378	0.042
Ratio	MS2-3d-#18A/MS-3d-#18A	0.632	0.018
Ratio	MS2-3d-#18A/MS4-3d-#18A	1.035	0.094
Ratio	MS3-3d-#18A/MS4-3d-#18A	1.638	0.141
Ratio	MS2-3d-#96/MS3-3d-#96	0.613	0.021
Ratio	MS2-3d-#96/MS4-3d-#96	1.040	0.106
Ratio	MS3-3d-#96/MS4-3d-#96	1.697	0.160
Ratio	MS2-3d-#93/MS3-3d-#93	0.609	0.020
Ratio	MS2-3d-#93/MS4-3d-#93	1.041	0.105
Ratio	MS3-3d-#93/MS4-3d-#93	1.708	0.161
Ratio	MS2-3d-Visual/MS3-3d-Visual	0.607	0.020
Ratio	MS2-3d-Visual/MS4-3d-Visual	1.043	0.109
Ratio	MS3-3d-Visual/MS4-3d-Visual	1.717	0.169

April and
September 1975

% Increase CIR-1d-Wratten #18A	1.186	13.473
% Increase CIR-1d-Wratten #96	72.974	30.979
% Increase CIR-1d-Wratten #93	153.608	49.042
% Increase CIR-1d-Visual	49.124	24.565
% Increase CIR-3d-Wratten #18A	1.427	14.087
% Increase CIR-3d-Wratten #96	78.102	32.083
% Increase CIR-3d-Wratten #93	156.858	49.578
% Increase CIR-3d-Visual	53.769	26.095

September 1975 Group = Dense Grass 1

Description		Mean	Standard Deviation
Average	CIR-1d-Wratten #18A	1.034	0.172
Average	CIR-1d-Wratten #96	1.093	0.250
Average	CIR-1d-Wratten #93	1.303	0.303
Average	CIR-1d-Visual	1.065	0.220
Average	CIR-3d-Wratten #18A	1.042	0.154
Average	CIR-3d-Wratten #96	1.173	0.234
Average	CIR-3d-Wratten #93	1.364	0.279
Average	CIR-3d-Visual	1.123	0.199
Average	MS2-3d-Wratten #18A	0.633	0.117
Average	MS2-3d-Wratten #96	0.593	0.118
Average	MS2-3d-Wratten #93	0.591	0.121
Average	MS2-3d-Visual	0.582	0.123
Average	MS3-3d-Wratten #18A	0.937	0.244
Average	MS3-3d-Wratten #96	0.904	0.249
Average	MS3-3d-Wratten #93	0.898	0.249
Average	MS3-3d-Visual	0.896	0.253
Average	MS4-3d-Wratten #18A	0.822	0.137
Average	MS4-3d-Wratten #96	0.791	0.144
Average	MS4-3d-Wratten #93	0.783	0.143
Average	MS4-3d-Visual	0.778	0.142
C. V.	CIR-1d-Wratten #18A	5.828	3.200
C. V.	CIR-1d-Wratten #96	8.443	5.345
C. V.	CIR-1d-Wratten #93	8.894	5.829
C. V.	CIR-1s-Visual	7.694	4.898
C. V.	CIR-3d-Wratten #18A	3.887	2.498
C. V.	CIR-3d-Wratten #96	5.187	3.668
C. V.	CIR-3d-Wratten #93	5.694	4.120
C. V.	CIR-3d-Visual	4.704	3.704
C. V.	MS2-3d-Wratten #18A	5.726	3.462
C. V.	MS2-3d-Wratten #96	6.170	3.634
C. V.	MS2-3d-Wratten #93	6.194	3.873
C. V.	MS2-3d-Visual	6.317	3.909
C. V.	MS3-3d-Wratten #18A	5.744	4.160
C. V.	MS3-3d-Wratten #96	6.040	4.649
C. V.	MS3-3d-Wratten #93	6.047	4.623

September 1975 — Group = Dense Grass 1

Description		Mean	Standard Deviation
C. V.	MS3-3d-Visual	6.397	4.929
C. V.	MS4-3d-Wratten #18A	5.189	1.747
C. V.	MS4-3d-Wratten #96	5.699	1.959
C. V.	MS4-3d-Wratten #93	5.866	1.897
C. V.	MS4-3d-Visual	5.740	1.993
Ratio	CIR-1d-#18A/CIR-1d-#96	0.957	0.068
Ratio	CIR-1d-#93/CIR-1d-Visual	1.219	0.067
Ratio	CIR-3d-#18A/CIR-3d-#96	0.896	0.057
Ratio	CIR-3d-#93/CIR-3d-Visual	1.210	0.060
Ratio	MS2-3d-#18A/MS3-3d-#18A	0.687	0.063
Ratio	MS2-3d-#18A/MS4-3d-#18A	0.780	0.155
Ratio	MS3-3d-#18A/MS4-3d-#18A	1.154	0.313
Ratio	MS2-3d-#96/MS3-3d-#96	0.669	0.063
Ratio	MS2-3d-#96/MS4-3d-#96	0.762	0.161
Ratio	MS3-3d-#96/MS4-3d-#96	1.159	0.329
Ratio	MS2-3d-#93/MS3-3d-#93	0.670	0.060
Ratio	MS2-3d-#93/MS4-3d-#93	0.766	0.165
Ratio	MS3-3d-#93/MS4-3d-#93	1.164	0.337
Ratio	MS2-3d-Visual/MS3-3d-Visual	0.662	0.057
Ratio	MS2-3d-Visual/MS4-3d-Visual	0.761	0.168
Ratio	MS3-3d-Visual/MS4-3d-Visual	1.169	0.341

April and
September 1975

% Increase CIR-1d-Wratten #18A	15.400	31.754
% Increase CIR-1d-Wratten #96	87.880	73.970
% Increase CIR-1d-Wratten #93	155.108	104.146
% Increase CIR-1d-Visual	69.428	58.794
% Increase CIR-3d-Wratten #18A	14.910	35.511
% Increase CIR-3d-Wratten #96	93.315	85.248
% Increase CIR-3d-Wratten #93	158.597	116.799
% Increase CIR-3d-Visual	80.628	78.478

September 1975 Group = Dense Grass 2

Description		Mean	Standard Deviation
Average	CIR-1d-Wratten #18A	0.987	0.151
Average	CIR-1d-Wratten #96	1.031	0.208
Average	CIR-1d-Wratten #93	1.234	0.241
Average	CIR-1d-Visual	1.016	0.194
Average	CIR-3d-Wratten #18A	0.978	0.167
Average	CIR-3d-Wratten #96	1.088	0.228
Average	CIR-3d-Wratten #93	1.270	0.258
Average	CIR-3d-Visual	1.048	0.216
Average	MS2-3d-Wratten #18A	0.565	0.107
Average	MS2-3d-Wratten #96	0.523	0.108
Average	MS2-3d-Wratten #93	0.519	0.107
Average	MS2-3d-Visual	0.509	0.110
Average	MS3-3d-Wratten #18A	0.829	0.179
Average	MS3-3d-Wratten #96	0.794	0.184
Average	MS3-3d-Wratten #93	0.790	0.184
Average	MS3-3d-Visual	0.784	0.187
Average	MS4-3d-Wratten #18A	0.810	0.050
Average	MS4-3d-Wratten #96	0.778	0.053
Average	MS4-3d-Wratten #93	0.771	0.052
Average	MS4-3d-Visual	0.768	0.053
C. V.	CIR-1d-Wratten #18A	6.851	3.371
C. V.	CIR-1d-Wratten #96	9.774	4.791
C. V.	CIR-1d-Wratten #93	10.173	4.477
C. V.	CIR-1d-Visual	8.278	4.094
C. V.	CIR-3d-Wratten #18A	5.046	2.501
C. V.	CIR-3d-Wratten #96	6.885	3.484
C. V.	CIR-3d-Wratten #93	7.058	3.343
C. V.	CIR-3d-Visual	6.043	2.990
C. V.	MS2-3d-Wratten #18A	4.895	1.280
C. V.	MS2-3d-Wratten #96	5.442	1.565
C. V.	MS2-3d-Wratten #93	5.402	1.423
C. V.	MS2-3d-Visual	5.690	1.347
C. V.	MS3-3d-Wratten #18A	6.610	2.648
C. V.	MS3-3d-Wratten #96	7.023	2.192
C. V.	MS3-3d-Wratten #93	7.001	2.410

September 1975 — Group = Dense Grass 2

Description		Mean	Standard Deviation
C. V.	MS3-3d-Visual	7.104	2.554
C. V.	MS4-3d-Wratten #18A	6.296	1.798
C. V.	MS4-3d-Wratten #96	6.925	1.924
C. V.	MS4-3d-Wratten #93	6.838	2.167
C. V.	MS4-3d-Visual	6.926	1.944
Ratio	CIR-1d-#18A/CIR-1d-#96	0.965	0.054
Ratio	CIR-1d-#93/CIR-1d-Visual	1.215	0.040
Ratio	CIR-3d-#18A/CIR-3d-#96	0.905	0.044
Ratio	CIR-3d-#93/CIR-3d-Visual	1.213	0.034
Ratio	MS2-3d-#18A/MS3-3d-#18A	0.684	0.019
Ratio	MS2-3d-#18A/MS4-3d-#18A	0.700	0.140
Ratio	MS3-3d-#18A/MS4-3d-#18A	1.027	0.224
Ratio	MS2-3d-#18A/MS3-3d-#18A	0.661	0.019
Ratio	MS2-3d-#96/MS4-3d-#96	0.675	0.146
Ratio	MS3-3d-#96/MS4-3d-#96	1.025	0.239
Ratio	MS2-3d-#96/MS3-3d-#96	0.660	0.019
Ratio	MS2-3d-#93/MS4-3d-#93	0.676	0.146
Ratio	MS3-3d-#93/MS4-3d-#93	1.028	0.241
Ratio	MS2-3d-Visual/MS3-3d-Visual	0.651	0.016
Ratio	MS2-3d-Visual/MS4-3d-Visual	0.666	0.149
Ratio	MS3-3d-Visual/MS4-3d-Visual	1.026	0.245

April and
September 1975

% Increase CIR-1d-Wratten #18A	19.235	7.546
% Increase CIR-1d-Wratten #96	100.515	21.220
% Increase CIR-1d-Wratten #93	176.720	32.937
% Increase CIR-1d-Visual	76.222	14.139
% Increase CIR-3d-Wratten #18A	20.260	10.917
% Increase CIR-3d-Wratten #96	109.005	31.362
% Increase CIR-3d-Wratten #93	184.832	43.962
% Increase CIR-3d-Visual	88.162	22.916

September 1975 Group = Sparse Grass 1

Description		Mean	Standard Deviation
Average	CIR-1d-Wratten #18A	0.836	0.059
Average	CIR-1d-Wratten #96	0.794	0.088
Average	CIR-1d-Wratten #93	0.944	0.104
Average	CIR-1d-Visual	0.826	0.073
Average	CIR-3d-Wratten #18A	0.790	0.060
Average	CIR-3d-Wratten #96	0.793	0.087
Average	CIR-3d-Wratten #93	0.919	0.099
Average	CIR-3d-Visual	0.804	0.080
Average	MS2-3d-Wratten #18A	0.504	0.069
Average	MS2-3d-Wratten #96	0.461	0.066
Average	MS2-3d-Wratten #93	0.457	0.069
Average	MS2-3d-Visual	0.449	0.069
Average	MS3-3d-Wratten #18A	0.686	0.103
Average	MS3-3d-Wratten #96	0.648	0.108
Average	MS3-3d-Wratten #93	0.643	0.105
Average	MS3-3d-Visual	0.639	0.107
Average	MS4-3d-Wratten #18A	0.932	0.041
Average	MS4-3d-Wratten #96	0.908	0.040
Average	MS4-3d-Wratten #93	0.900	0.043
Average	MS4-3d-Visual	0.893	0.043
C. V.	CIR-1d-Wratten #18A	11.131	3.712
C. V.	CIR-1d-Wratten #96	16.274	5.198
C. V.	CIR-1d-Wratten #93	16.112	4.930
C. V.	CIR-1d-Visual	14.470	5.197
C. V.	CIR-3d-Wratten #18A	6.527	2.164
C. V.	CIR-3d-Wratten #96	8.785	3.260
C. V.	CIR-3d-Wratten #93	8.840	3.016
C. V.	CIR-3d-Visual	8.417	3.045
C. V.	MS2-3d-Wratten #18A	9.512	6.086
C. V.	MS2-3d-Wratten #96	10.454	6.744
C. V.	MS2-3d-Wratten #93	10.698	7.016
C. V.	MS2-3d-Visual	11.104	7.292
C. V.	MS3-3d-Wratten #18A	10.165	5.673
C. V.	MS3-3d-Wratten #96	11.463	6.286
C. V.	MS3-3d-Wratten #93	11.090	6.150

September 1975 — Group = Sparse Grass 1

Description		Mean	Standard Deviation
C. V.	MS3-3d-Visual	11.525	6.276
C. V.	MS4-3d-Wratten #18A	3.778	2.838
C. V.	MS4-3d-Wratten #96	4.138	2.906
C. V.	MS4-3d-Wratten #93	4.391	2.897
C. V.	MS4-3d-Visual	4.044	3.050
Ratio	CIR-1d-#18A/CIR-1d-#96	1.057	0.039
Ratio	CIR-1d-#93/CIR-1d-Visual	1.141	0.025
Ratio	CIR-3d-#18A/CIR-3d-#96	0.999	0.032
Ratio	CIR-3d-#93/CIR-3d-Visual	1.142	0.010
Ratio	MS2-3d-#18A/MS3-3d-#18A	0.736	0.012
Ratio	MS2-3d-#18A/MS4-3d-#18A	0.539	0.050
Ratio	MS3-3d-#18A/MS4-3d-#18A	0.734	0.078
Ratio	MS2-3d-#96/MS3-3d-#96	0.712	0.020
Ratio	MS2-3d-#96/MS4-3d-#96	0.506	0.051
Ratio	MS3-3d-#96/MS4-3d-#96	0.711	0.088
Ratio	MS2-3d-#93/MS3-3d-#93	0.713	0.014
Ratio	MS2-3d-#93/MS4-3d-#93	0.507	0.053
Ratio	MS3-3d-#93/MS4-3d-#93	0.712	0.083
Ratio	MS2-3d-Visual/MS3-3d-Visual	0.704	0.016
Ratio	MS2-3d-Visual/MS4-3d-Visual	0.501	0.054
Ratio	MS3-3d-Visual/MS4-3d-Visual	0.712	0.085

April and
September 1975

% Increase CIR-1d-Wratten #18A	25.605	26.756
% Increase CIR-1d-Wratten #96	102.798	56.242
% Increase CIR-1d-Wratten #93	167.205	72.634
% Increase CIR-1d-Visual	84.562	45.964
% Increase CIR-3d-Wratten #18A	23.100	32.132
% Increase CIR-3d-Wratten #96	107.160	70.576
% Increase CIR-3d-Wratten #93	176.715	97.563
% Increase CIR-3d-Visual	97.982	66.120

September 1975 Group = Sparse Grass 2

Description		Mean	Standard Deviation
Average	CIR-1d-Wratten #18A	0.903	0.174
Average	CIR-1d-Wratten #96	0.843	0.181
Average	CIR-1d-Wratten #93	0.991	0.214
Average	CIR-1d-Visual	0.910	0.240
Average	CIR-3d-Wratten #18A	0.941	0.093
Average	CIR-3d-Wratten #96	0.966	0.079
Average	CIR-3d-Wratten #93	1.102	0.095
Average	CIR-3d-Visual	0.998	0.153
Average	MS2-3d-Wratten #18A	0.612	0.097
Average	MS2-3d-Wratten #96	0.574	0.100
Average	MS2-3d-Wratten #93	0.568	0.095
Average	MS2-3d-Visual	0.564	0.107
Average	MS3-3d-Wratten #18A	0.832	0.074
Average	MS3-3d-Wratten #96	0.804	0.087
Average	MS3-3d-Wratten #93	0.792	0.082
Average	MS3-3d-Visual	0.790	0.078
Average	MS4-3d-Wratten #18A	0.854	0.139
Average	MS4-3d-Wratten #96	0.824	0.147
Average	MS4-3d-Wratten #93	0.814	0.148
Average	MS4-3d-Visual	0.813	0.146
C. V.	CIR-1d-Wratten #18A	12.993	12.448
C. V.	CIR-1d-Wratten #96	18.353	17.362
C. V.	CIR-1d-Wratten #93	18.770	18.743
C. V.	CIR-1d-Visual	18.809	19.267
C. V.	CIR-3d-Wratten #18A	5.847	4.337
C. V.	CIR-3d-Wratten #96	7.201	5.202
C. V.	CIR-3d-Wratten #93	7.636	5.597
C. V.	CIR-3d-Visual	7.976	6.676
C. V.	MS2-3d-Wratten #18A	2.595	0.758
C. V.	MS2-3d-Wratten #96	3.314	0.083
C. V.	MS2-3d-Wratten #93	3.550	0.343
C. V.	MS2-3d-Visual	3.143	1.351
C. V.	MS3-3d-Wratten #18A	5.924	1.850
C. V.	MS3-3d-Wratten #96	6.193	1.706
C. V.	MS3-3d-Wratten #93	6.561	2.535

September 1975 Group = Sparse Grass 2

Description		Mean	Standard Deviation
Average	CIR-1d-Wratten #18A	0.903	0.174
Average	CIR-1d-Wratten #96	0.843	0.181
Average	CIR-1d-Wratten #93	0.991	0.214
Average	CIR-1d-Visual	0.910	0.240
Average	CIR-3d-Wratten #18A	0.941	0.093
Average	CIR-3d-Wratten #96	0.966	0.079
Average	CIR-3d-Wratten #93	1.102	0.095
Average	CIR-3d-Visual	0.998	0.153
Average	MS2-3d-Wratten #18A	0.612	0.097
Average	MS2-3d-Wratten #96	0.574	0.100
Average	MS2-3d-Wratten #93	0.568	0.095
Average	MS2-3d-Visual	0.564	0.107
Average	MS3-3d-Wratten #18A	0.832	0.074
Average	MS3-3d-Wratten #96	0.804	0.087
Average	MS3-3d-Wratten #93	0.792	0.082
Average	MS3-3d-Visual	0.790	0.078
Average	MS4-3d-Wratten #18A	0.854	0.139
Average	MS4-3d-Wratten #96	0.824	0.147
Average	MS4-3d-Wratten #93	0.814	0.148
Average	MS4-3d-Visual	0.813	0.146
C. V.	CIR-1d-Wratten #18A	12.993	12.448
C. V.	CIR-1d-Wratten #96	18.353	17.362
C. V.	CIR-1d-Wratten #93	18.770	18.743
C. V.	CIR-1d-Visual	18.809	19.267
C. V.	CIR-3d-Wratten #18A	5.847	4.337
C. V.	CIR-3d-Wratten #96	7.201	5.202
C. V.	CIR-3d-Wratten #93	7.636	5.597
C. V.	CIR-3d-Visual	7.976	6.676
C. V.	MS2-3d-Wratten #18A	2.595	0.758
C. V.	MS2-3d-Wratten #96	3.314	0.083
C. V.	MS2-3d-Wratten #93	3.550	0.343
C. V.	MS2-3d-Visual	3.143	1.351
C. V.	MS3-3d-Wratten #18A	5.924	1.850
C. V.	MS3-3d-Wratten #96	6.193	1.706
C. V.	MS3-3d-Wratten #93	6.561	2.535

September 1975 — Group = Sparse Grass 2

Description		Mean	Standard Deviation
C. V.	MS3-3d-Visual	6.171	1.984
C. V.	MS4-3d-Wratten #18A	2.546	0.333
C. V.	MS4-3d-Wratten #96	3.022	1.226
C. V.	MS4-3d-Wratten #93	3.169	1.096
C. V.	MS4-3d-Visual	3.282	0.936
Ratio	CIR-1d-#18A/CIR-1d-#96	1.074	0.024
Ratio	CIR-1d-#93/CIR/1d-Visual	1.096	0.055
Ratio	CIR-3d-#18A/CIR-3d-#96	0.973	0.017
Ratio	CIR-3d-#93/CIR-3d-Visual	1.100	0.075
Ratio	MS2-3d-#18A/MS3-3d-#18A	0.732	0.051
Ratio	MS2-3d-#18A/MS4-3d-#18A	0.736	0.234
Ratio	MS3-3d-#18A/MS4-3d-#18A	0.996	0.250
Ratio	MS2-3d-#96/MS3-3d-#96	0.712	0.047
Ratio	MS2-3d-#96/MS4-3d-#96	0.719	0.249
Ratio	MS3-3d-#96/MS4-3d-#96	1.000	0.284
Ratio	MS2-3d-#93/MS3-3d-#93	0.715	0.046
Ratio	MS2-3d-#93/MS4-3d-#93	0.720	0.247
Ratio	MS3-3d-#93/MS4-3d-#93	0.998	0.282
Ratio	MS2-3d-Visual/MS3-3d-Visual	0.711	0.065
Ratio	MS2-3d-Visual/MS4-3d-Visual	0.717	0.261
Ratio	MS3-3d-Visual/MS4-3d-Visual	0.996	0.275

April and
September 1975

% Increase CIR-1d-Wratten #18A	11.040	3.832
% Increase CIR-1d-Wratten #96	76.210	8.443
% Increase CIR-1d-Wratten #93	136.045	8.351
% Increase CIR-1d-Visual	57.080	8.570
% Increase CIR-3d-Wratten #18A	17.010	7.594
% Increase CIR-3d-Wratten #96	93.985	14.856
% Increase CIR-3d-Wratten #93	156.950	21.807
% Increase CIR-3d-Visual	78.235	18.618

September 1975 Group = Black Locust-Grass

Description		Mean	Standard Deviation
Average	CIR-1d-Wratten #18A	1.059	0.076
Average	CIR-1d-Wratten #96	1.132	0.101
Average	CIR-1d-Wratten #93	1.353	0.115
Average	CIR-1d-Visual	1.100	0.097
Average	CIR-3d-Wratten #18A	1.041	0.075
Average	CIR-3d-Wratten #96	1.171	0.096
Average	CIR-3d-Wratten #93	1.370	0.107
Average	CIR-3d-Visual	1.125	0.097
Average	MS2-3d-Wratten #18A	0.631	0.111
Average	MS2-3d-Wratten #96	0.589	0.116
Average	MS2-3d-Wratten #93	0.583	0.113
Average	MS2-3d-Visual	0.577	0.116
Average	MS3-3d-Wratten #18A	0.921	0.183
Average	MS3-3d-Wratten #96	0.893	0.186
Average	MS3-3d-Wratten #93	0.886	0.188
Average	MS3-3d-Visual	0.885	0.194
Average	MS4-3d-Wratten #18A	0.806	0.090
Average	MS4-3d-Wratten #96	0.773	0.098
Average	MS4-3d-Wratten #93	0.765	0.094
Average	MS4-3d-Visual	0.762	0.094
C. V.	CIR-1d-Wratten #18A	5.768	1.827
C. V.	CIR-1d-Wratten #96	8.094	1.938
C. V.	CIR-1d-Wratten #93	8.400	1.754
C. V.	CIR-1d-Visual	7.200	2.171
C. V.	CIR-3d-Wratten #18A	4.390	1.550
C. V.	CIR-3d-Wratten #96	5.032	1.994
C. V.	CIR-3d-Wratten #93	4.855	2.008
C. V.	CIR-3d-Visual	4.963	2.020
C. V.	MS2-3d-Wratten #18A	5.028	2.345
C. V.	MS2-3d-Wratten #96	5.409	2.914
C. V.	MS2-3d-Wratten #93	5.493	2.774
C. V.	MS2-3d-Visual	5.744	2.863
C. V.	MS3-3d-Wratten #18A	5.393	1.680
C. V.	MS3-3d-Wratten #96	5.951	2.025
C. V.	MS3-3d-Wratten #93	5.763	1.988

September 1975 — Group = Black Locust-Grass

Description		Mean	Standard Deviation
C. V.	MS3-3d-Visual	6.020	2.028
C. V.	MS4-3d-Wratten #18A	3.690	1.218
C. V.	MS4-3d-Wratten #96	4.150	1.650
C. V.	MS4-3d-Wratten #93	4.122	1.391
C. V.	MS4-3d-Visual	4.105	1.561
Ratio	CIR-1d-#18A/CIR-1d-#96	0.937	0.018
Ratio	CIR-1d-#93/CIR-1d-Visual	1.230	0.010
Ratio	CIR-3d-#18A/CIR-3d-#96	0.890	0.011
Ratio	CIR-3d-#93/CIR-3d-Visual	1.219	0.016
Ratio	MS2-3d-#18A/MS3-3d-#18A	0.686	0.018
Ratio	MS2-3d-#18A/MS4-3d-#18A	0.780	0.071
Ratio	MS3-3d-#18A/MS4-3d-#18A	1.138	0.115
Ratio	MS2-3d-#96/MS3-3d-#96	0.660	0.008
Ratio	MS2-3d-#96/MS4-3d-#96	0.759	0.076
Ratio	MS3-3d-#96/MS4-3d-#96	1.151	0.122
Ratio	MS2-3d-#93/MS3-3d-#93	0.660	0.013
Ratio	MS2-3d-#93/MS4-3d-#93	0.760	0.075
Ratio	MS3-3d-#93/MS4-3d-#93	1.153	0.124
Ratio	MS2-3d-Visual/MS3-3d-Visual	0.654	0.013
Ratio	MS2-3d-Visual/MS4-3d-Visual	0.754	0.078
Ratio	MS3-3d-Visual/MS4-3d-Visual	1.154	0.132

April and
September 1975

% Increase CIR-1d-Wratten #18A	35.557	2.612
% Increase CIR-1d-Wratten #96	134.567	6.658
% Increase CIR-1d-Wratten #93	223.953	11.442
% Increase CIR-1d-Visual	108.423	3.368
% Increase CIR-3d-Wratten #18A	33.997	4.138
% Increase CIR-3d-Wratten #96	135.107	4.956
% Increase CIR-3d-Wratten #93	222.517	6.829
% Increase CIR-3d-Visual	116.160	11.167

Appendix D

Multidisciplinary Meetings/Symposiums Attended

Personnel	Meeting	Location	Date
Wittwer, Hammetter	Ky. Bureau of Highways small drainage survey	Frankfort, Ky.	Dec., 1974
Graves, Wittwer, Shilling, Hammetter	Southeastern Remote Sensing Symposium	Athens, Ga.	Jan., 1975
Hammetter	Symposium on Machine Processing of Remotely Sensed Data, LARS	Lafayette, Ind.	June, 1975
Coltharp, Wittwer, Hammetter	Northeast Forest Soils Conference	Slade, Ky.	Aug., 1975
Faculty	Governor's Conference on Forestry	Lexington, Ky.	Oct., 1975
Graves*, Hammetter	Workshop for Environmental Applications of MSS Imagery	Ft. Belvoir, Va.	Nov., 1975
Faculty, Graves*	Ky.-Tenn. Section Meeting SAF	Lexington, Ky.	Dec., 1975
Coltharp*, Graves*, Hammetter*	NASA Seminar	Huntsville, Ala.	Jan., 1976
Hammetter*	92nd Annual Meeting ASP	Washington, D.C.	Feb., 1976
Hammetter*	Seminar on Remote Sensing Applications in Ky.	Lexington, Ky.	March, 1976
Hammetter*	SCS Workshop	Lexington, Ky.	March, 1976
Hammetter	Cooperative planning meeting with Office of Planning & Research	Frankfort, Ky.	March, 1976
Hammetter	Strip Mine Reclamation Seminar	Slade, Ky.	April, 1976
Coltharp, Hammetter	EPA/EPIC Tour and Meeting	Warrenton, Pa.	June, 1976
Hammetter, Wittwer	East Kentucky Chapter Meeting-SAF	Portsmouth, Ohio	July, 1976
Faculty	Ky.-Tenn. Section Meeting SAF	Cadiz, Ky.	July, 1976
Graves, Hammetter	Technology Transfer Meeting with NASA, other UK officials	Lexington, Ky.	July, 1976

Multidisciplinary Meetings/Symposiums Attended(cont'd)

Personnel	Meeting	Location	Date
Hammetter	Ecosystem Classification Meeting	Richmond, Ky.	Aug., 1976
Graves, Hammetter	National SAF Meeting - Remote Sensing Working Group	New Orleans, La.	Oct., 1976
Graves*	10th Annual Kentucky Land Surveyors Conference	Louisville, Ky.	Feb., 1977
Project personnel	Meeting with NASA to discuss project implications	Huntsville, Ala.	Feb., 1977
Project personnel**	Joint Seminar with SCS, other environmental agencies	Lexington, Ky.	

*Speaker **Planned Meeting

REMOTE SENSING SEMINAR ATTENDEES

Mr. James Kennamer
Mr. Harold Jolley
Mr. Archie D. Weeks
Soil Conservation Service
333 Waller Avenue
Lexington, KY 40505

Dr. Willem Meijer
School of Biological Sciences
216 Funkhouser
University of Kentucky
Lexington, KY 40506

Mr. Fred Schuhmann
Strip Mine Reclamation
6th Floor
Capital Plaza Tower
Frankfort, KY 40601

Mr. Willis Vogel
U.S. Forest Service
204 Center Street
Berea, KY 40403

Dr. Gerald Nordin
Department of Entomology
S 225 J Agri. Science North
University of Kentucky
Lexington, KY 40506

Mr. Darrell West
Environmental Sciences Division
Oak Ridge National Laboratory
Building 3017
Oak Ridge, TENN 37830

Dr. Robert Honea
Energy Division
Oak Ridge National Laboratory
Oak Ridge, TENN 37830

Dr. William Adams
Department of Geography
Eastern Kentucky University
Richmond, KY 40475

Mr. Ernie Spisz
Mr. Ed Maslowski
Ms Joyce T. Dooley
NASA
Lewis Research Center
21000 Brook Park Road
Cleveland, Ohio 44135

Mr. J.R. Farson, Jr.
Division of Conservation
1121 Louisville Road
Frankfort, KY 40601

Dr. Alan Randall
Agricultural Economics
710 Agri. Science South
University of Kentucky
Lexington, KY 40506

Mr. Orlen Grunewald
Agricultural Economics
715 Agri. Science South
University of Kentucky
Lexington, KY 40506

Ms Barbara Columbia
Bluegrass Area Development District
160 East Reynolds Road
Lexington, KY 40503

Mr. Dave Lueck
Division of Air Pollution
Capital Plaza Tower
Frankfort, KY 40601

Dr. James E. Jones
IMMR
213 Bradley Hall
University of Kentucky
Lexington, KY 40506

Mr. Don Blome
IMMR
411 Bradley Hall
University of Kentucky
Lexington, KY 40506

Mr. Birney Fish
Office of Planning and Research
6th Floor
Capital Plaza Tower
Frankfort, KY 40601

Mr. Walter Martin
Mr. Paul Fitch
Division of Water Quality
Century Plaza
U.S. 127 South
Frankfort, KY 40601

Mr. Mahlon Hammetter
Department of Forestry
121 Thomas Poe Cooper Bldg.
University of Kentucky
Lexington, KY 40506